Malonyl- conjugates of isoflavones: Structure, Bioavailability and Chemical Modifications during Processing

A DISSERTATION
SUBMITTED TO THE FACULTY OF THE GRADUATE SCHOOL
OF THE UNIVERSITY OF MINNESOTA
BY

Vamsidhar Yerramsetty

IN PARTIAL FULFILLMENT OF THE REQUIREMENTS FOR
THE DEGREE OF DOCTORATE OF PHILOSOPHY

Baraem Ismail

SEPTEMBER 2013

ACKNOWLEDGEMENTS

I would like to thank my advisor, Dr. Baream Ismail, for allowing me the opportunity to conduct research for my degree in her laboratory, and for her guidance and encouragement. Thanks and gratitude are also expressed to:

My committee members: Dr. Mindy Kurzer for agreeing to be part of my Master's and Doctoral Committee(s). I sincerely thank her for sharing her experiences which I am sure will inspire me to pursue more adventours in life; Dr. Daniel Gallher, for his utmost patience in assisting me with the animal study that is an integral part of my PhD thesis project. His friendly attitude and his zeal to learn are some attributes I intend to inculcate in my personal and professional life; Dr. Ted Labuza, for assisting me with various queries during my PhD and Dr. Mirko Bunzel for assiting me with NMR studies.

Kevin Mathias (Past member – protein/phytochemical lab) for helping me getting started at the University of Minnesota; Timothy Hinze (Shimadzu Scientific), Thomas Krick, Dr. Loraine Anderson (Centre for Mass Spectrometry and Proteomics, U of M) for their kind assistance in teaching me the nuances of liquid chromatography/mass spectrometry techniques; Dr. Adrian Hegeman, Dr. Mikel Roe, Dr. Paul Boswell for assiting me with sysnthesis protocols and stable isotope dilution mass spectrometry; Dr. Jean Paul (Flavor chemistry laboratory, University of Minnesota) for his generous help for the past 5 years

Special friend(s) at the Food Science department, University of Minnesota: Bridget Mclatchey, Sravanthi Priya Mallapally, Edem Folly, Omer Celik, Kristina Sandvik, Josephine Charve, Smitha Raithore and all the great friends I made at the university.

Healthy Foods and Healthy Lives Instituite for their generous funding to conduct my research

My colleagues in the protein/phytochemical laboratory, and

Last but not the least, my family who supported me in all the adeventours I pursued and will support in the adventours I intend to pursue.

ABSTRACT

Soy isoflavones are often associated with prevention of cancer, cardiovascular diseases, osteoporosis, and postmenopausal symptoms. However, the demonstration of theses physiological effects is highly inconsistent. Not all soy foods deliver the same isoflavone-associated benefits. Inconsistency in isoflavone research is partly attributed to the inadequate profiling of isoflavones, lack of standardization of the source of isoflavones, and lack of standard analytical methods for profiling and quantifying isoflavones present in different soy matrices. We are convinced that inconsistent results are due to differences in the bioavailability of the different isoflavone forms consumed. Since isoflavones in soy foods differ in their forms (e.g. conjugated and non-conjugated), large differences may exist in their bioavailability. Therefore, it is crucial to adequately profile the administered isoflavones and study the effect of their conjugation on their bioavailability. Additionally, isomerization of different isoflavone forms occurs upon thermal processing. Complete structural elucidation of the isomers and determination of their thermal stability in soy systems are important for understanding their physiological relevance.

Therefore, the overall objective of this study was to determine effect of processing on the chemical modifications of isoflavones and to detect all biologically relevant forms, together with providing adequate and reliable bioavailability data for each of the most abundant isoflavone forms.

Isoflavones were extracted from soy grits and were separated and isolated using semi-preparative liquid chromatography. Identification of the different isoflavones forms and isomers was accomplished based on UV wave scan, mass spectrometry, and nuclear magnetic resonance (NMR) analysis. Effect of thermal processing on isomer stability was determined by subjecting soymilk to thermal treatment at 100°C for time intervals ranging from 1 to 60 min. A rapid analytical procedure was developed to quantify isoflavones in biological fluids using stable isotope dilution mass spectrometry (SID-LCMS). Two novel isotopically labeled (SIL) analogues of natural SERMs, genistein and daidzein were synthesized using a H/D exchange reaction mechanism. Computational

chemistry coupled with MS and NMR data confirmed the site and mechanism of deuteration. The developed method was sensitive, selective, precise and accurate. Bioavailability of malonylglucosides and their respective non-conjugated glucosides was determined in a model rat system. Rats were gavaged with an assigned isoflavone form. Blood and urine samples were collected at different time intervals. Different isoflavone metabolites in plasma were determined using the developed SID-LCMS method. Bioavailability was determined by calculating pharmokinetic parameters, assuming first order disposition kinetics.

NMR characterization of the malonylglucoside isomers revealed its structure to be 4”-*O*-malonylglucosides, suggesting a malonyl migration from the glucose-6-position to the glucose-4-position. The malonylgenistin isomer represented 6-9 % of the total calculated genistein content in soymilk heated at 100°C for various periods of time. Based on rat peak plasma and urine levels and area under the curve (AUC) of the aglycone post ingestion of the respective isoflavones, it was quite evident that the malonylglucosides were significantly ($P \leq 0.05$) less bioavailable than their non-conjugated counterparts.

The present work provided full elucidation of the chemical structure of malonylglucoside isomers. We demonstrated for the first time that the formation of the malonylisomers is governed by thermal processing time in a soymilk system. Disregarding the isomer formation upon heating can result in overestimation of loss in total isoflavone content and misinterpretation of the biological contributions. Additionally, this work provided a validated analytical SID-LC/MS method to detect natural and known synthetic selective estrogen receptor modulators (SERMs) in a single analytical assay. Finally, this work differentiated for the first time the bioavailability of malonylglucosides as compared to their non-conjugated counterparts. The observed differences explained to a significiant extent the controversy in isoflavone research. We believe that the results of this work will help streamline the experimental approach undertaken by various researchers to achieve consistent clinical conclusions and to optimize the processing parameters that result in the most bioavailable isoflavone profile, thus maximizing their health benefits.

TABLE OF CONTENTS

Page

LIST OF TABLES

LIST OF FIGURES

Figure Page

1. LITERATURE REVIEW

1.1. Introduction and objectives

Many epidemiological studies have linked lower rates of various diseases like breast cancer, type-II diabetes, obesity, cardiovascular disease and post-menopausal symptoms among Asian population to high soy consumption. Numerous clinical studies ensued over the past three decades, of which several have concluded that isoflavones are among the main components of soy that contribute to the aforementioned health benefits. While many studies attributed positive health benefits to isoflavones, there is some evidence suggesting no effects or adverse effects. Thus, there is no absolute consensus on the health benefits of isoflavones. Reasons behind inconsistent results might include variations in food matrix, inter-individual metabolism, gut microflora and administration of different isoflavone profiles during clinical studies. Of these factors, we believe that lack of accurate structural profiling of the ingested isoflavones and ignoring differences in their bioavailability significantly contribute to the inconsistency in clinical results.

The main isoflavones found in soybeans are genistein, daidzein and glycitein. Each of the isoflavones exists in four different forms, aglycone, non-conjugated β-glycoside, acetylglucoside and malonylglucoside. The isoflavone profile (i.e., the distribution of the different forms) in raw soybeans changes considerably upon processing. Structural interconversions among the various isoflavone forms are commonly noted upon processing. Coupled with interconversions, significant loss in the total isoflavone amount occurs under various processing conditions. The loss was mainly attributed to either leeching into waste stream or complete degradation. Recent studies have shown that loss in total isoflavones is not confined to complete degradation alone but may result in the formation of unidentified isoflavone derivatives of some biological relevance.

We have demonstrated for the first time the formation of isomeric forms upon heating malonylglucosides. These isomers were previously disregarded resulting in an overestimation of total degradation or loss. Because of their close structural resemblance to known isoflavones forms, the isomeric forms might be biologically relevant. Since

chemical structure plays an important role in determining isoflavone bioavailability, complete structural elucidation of the isomers, using powerful analytical tools such as nuclear magnetic resonance (NMR), is necessary in order to better predict their physiological relevance.

Additionally, we have demonstrated that the malonylglucoside isomers are thermally unstable and rapidly convert back to known isoflavone forms, namely malonylglucosides and their non-conjugated β-glucosides. However, in soy food systems the isomer conversion mechanism can be affected by the presence of soy protein, which was shown to have a protective effect against thermal degradation and interconversion of isoflavones. It is thus crucial to carry out a study in a real soy system (such as soymilk), to monitor the formation and conversion of the isomers in the presence of other soy components, mainly the protein. Determining chemical conversions in real soy systems, aids in understanding the effect of processing and the consequent interconversions on the bioavailability of isoflavones.

Despite their abundance in many soy foods, no attempt was made to determine the *in-vivo* bioavailability of malonylglucosides. We hypothesize that malonylglucosides are less bioavailable than non-conjugated β-glucosides. Since enzymatic assays are site specific, malonylation of glucose in malonylglucosides will affect their hydrolysis rate by β-glucosidases. The hydrolysis of glucosides by β-glucosidases into aglycones is a prerequisite for the absorption of isoflavones. It is, therefore, important to determine the effect of conjugation of isoflavones on their bioavailability.

The long term goal of this study is to determine the isoflavone chemical modifications that occur upon processing and to detect all biologically relevant forms, together with providing adequate and reliable bioavailability data for each of the most abundant isoflavone forms. Therefore, the specific objectives were:

Objective 1) Perform a complete structural elucidation of the malonylglucoside isomers following NMR analysis and monitor the level of malonylglucoside isomers in a complex food matrix (soymilk) subjected to various processing conditions

Objective 2) Development of a simple, fast and accurate method for the direct quantitation of isoflavones in rat plasma using stable isotope dilution mass spectrometry

Objective 3) Determine the effect of malonyl conjugation on isoflavone bioavailability in a model rat system

Results of this work will help streamline the experimental approach undertaken by various researchers to achieve consistent clinical conclusions and to optimize the processing parameters that result in the most bioavailable isoflavone profile, thus maximizing their health benefits.

1.2. Significance of soybeans

Soybean has been a popular food crop for many centuries. The extent of cultivation, use, and the economic and health benefits offered by soybean have distinguished it from many other food crops. Initially, soybean was cultivated in most parts of the world to exploit its intrinsic advantage of fixing nitrogen via soil bacteria. The roots nodules of soybean contain billions of Rhizobium bacteria which fixes nitrogen, thereby improving the quality of the soil (Angela et al., 1986). However, since soybean contains oil, its utilization extended to oil extraction and subsequent uses in the preparation of paints and varnishes (Johannes et al., 1995).

Until the 1970s, soybean was mainly used for oil extraction or as animal feed. However, the consumption of soybean markedly increased with the advent of Japanese traditional foods such as miso, tempeh and tofu into the United States market. Owing to many technological and engineering advances, a second generation of soy-products such as soymilk, soy cheese and soy frozen desserts are now available in the market. This resulted in a tremendous growth in the soy market from $300 million in 1992 to about $4 billion in 2007 (Data courtesy, Soy Foods Association of North America). Today about, 90% of the soybean consumed in the United States is in the form of various soy protein products, and a mere 10% of soybean is utilized as animal feed. This propelled the economy of soybean production, particularly in the United States. Today, in the United States, soybean is second only to corn in terms of farm value (USDA, Economic Research Service), and as of 2006, United States together with Brazil and Argentina account for about 80% of the world's total soybean production (Shurtleff and Aoyagi, 2007).

Another important contributing factor to the increase in soybean consumption in the United States can be attributed to the increase in the awareness among consumers of the many health benefits associated with soybeans (Lee et al., 2003). Each component of soybean has its own health advantage and hence can be used to promote soy-based products. The protein quality of soybeans is very high and is generally comparable to that of animal proteins. The only amino acids present in less abundance in soy protein are

methionine and tryptophan. Hence, food manufacturing companies often mix methionine and tryptophan rich corn protein with soy protein to yield a very high quality protein. From a nutritional standpoint, soy protein-based infant formulas are on par with milk-based infant formulas. Additionally, several studies indicated that soy protein rich diets reduce the total cholesterol level by about 30% (Kito et al., 1993). Taking into account the data from this and many other clinical studies, FDA approved a health claim stating that "Diets low in saturated fat and cholesterol that includes 25 grams of soy protein a day may reduce the risk of heart disease". Together with soy protein many researchers indicated that isoflavones are also among the main contributors to several health benefits.

1.3 Significance of isoflavones

1.3.1 Synthesis and role of isoflavones in the plant

Isoflavones are polyphenolic compounds that belong to a diverse group of plant secondary metabolites called flavonoids. Most of the flavonoids, including isoflavones, are synthesized in plants by the phenyl-propanoid pathway (Parr and Bolwell, 2000). Briefly, the pathway involves the amino acid phenylalanine that is produced via the shikimic acid pathway that undergoes various enzyme assisted modifications to convert to p-coumaroyl-CoA. Subsequently, the enzyme chalcone synthase catalyzes addition, condensation and cyclization of p-coumaroyl-CoA to either 2',4,4',6'-tetrahydroxychalcone (naringenin chalcone) or 2',4',4-trihydroxychalcone (isoliquiritigenin) (Hashim et al., 2002). In the final stages, the enzyme isoflavone synthase catalyzes the transformation of the two flavanones to isoflavones (Hakamatsuka et al., 1990). The catalytic reaction involves P450-catalyzed hydroxylation coupled with aryl migration (Hakamatsuka et al., 1990). The enzyme isoflavone synthase is specific to legumes, and few other species such as red clover, and thus is directly responsible for the predominant presence of isoflavones in the aforementioned plant species (Yu et al., 2000). In these plant species, isoflavones play the role of phytoalexins, i.e., they protect the plant against microbial infections and hence are part of the plant's defensive

mechanism (Dixon et al., 2008). Typically, plants enzymatically glycosylate isoflavones and store them in their inactive form as glucosides. Thus, there exist multiple chemical structures of isoflavones in nature.

1.3.2 Chemical structure and profile of isoflavones

The primary structure of isoflavones is a substituted 3-phenyl-chromen-4-one conjugated system, which resembles to a great extent the human estrogen structure (Figure 1 A). Based on the differences in the primary structure, soy isoflavones can be classified into three types, genistein, daidzein and glycitein. The structural difference between the three types is attributed to the functional group present at R1 and R2 positions (Figure 1B). Specifically, daidzein derivatives have both R1 and R2 as hydrogen atoms. In case of genistein derivatives, R1 is H and R2 is OH. Glycitein derivatives have a methoxy group at R1and a hydrogen atom at R2 position. Each type of isoflavone can exist in four different chemical forms, aglycone, non-conjugated β-glucoside, acetylglucoside, and malonylglucoside. The structural variation between each chemical form is due to the glycosylation and esterification patterns that the primary structure might undergo (Figure 1B).

Soybeans are the richest source of isoflavones (Coward et al., 1993). The majority of isoflavones in soybeans are confined to the hypocotyl region of the bean, where about 5% of the total isoflavone content is present in the aglycone form. The remaining 95% is comprised of the non-conjugated and the conjugated glucosides (Price and Fenwick, 1985). The total isoflavone content of raw soybeans depends on numerous factors such as crop variety, location, climate, cultivation practice, and storage conditions (Wang and Murphy, 1994a). Amongst different varieties, total isoflavone content in raw soybeans varies from 0.1 to 5 mg per gram of soybean (Coward et al., 1993).

Subsequent storage and processing conditions also affect the isoflavone content (Wang and Murphy, 1994b). Depending on the processing conditions employed, different soy-derived products vary in their total isoflavone content. Some examples include

tempeh (625 μg/g), bean paste (593 μg/g), miso (294 μg/g), and fermented bean curd (390 μg/g) (Murphy et al., 1999).

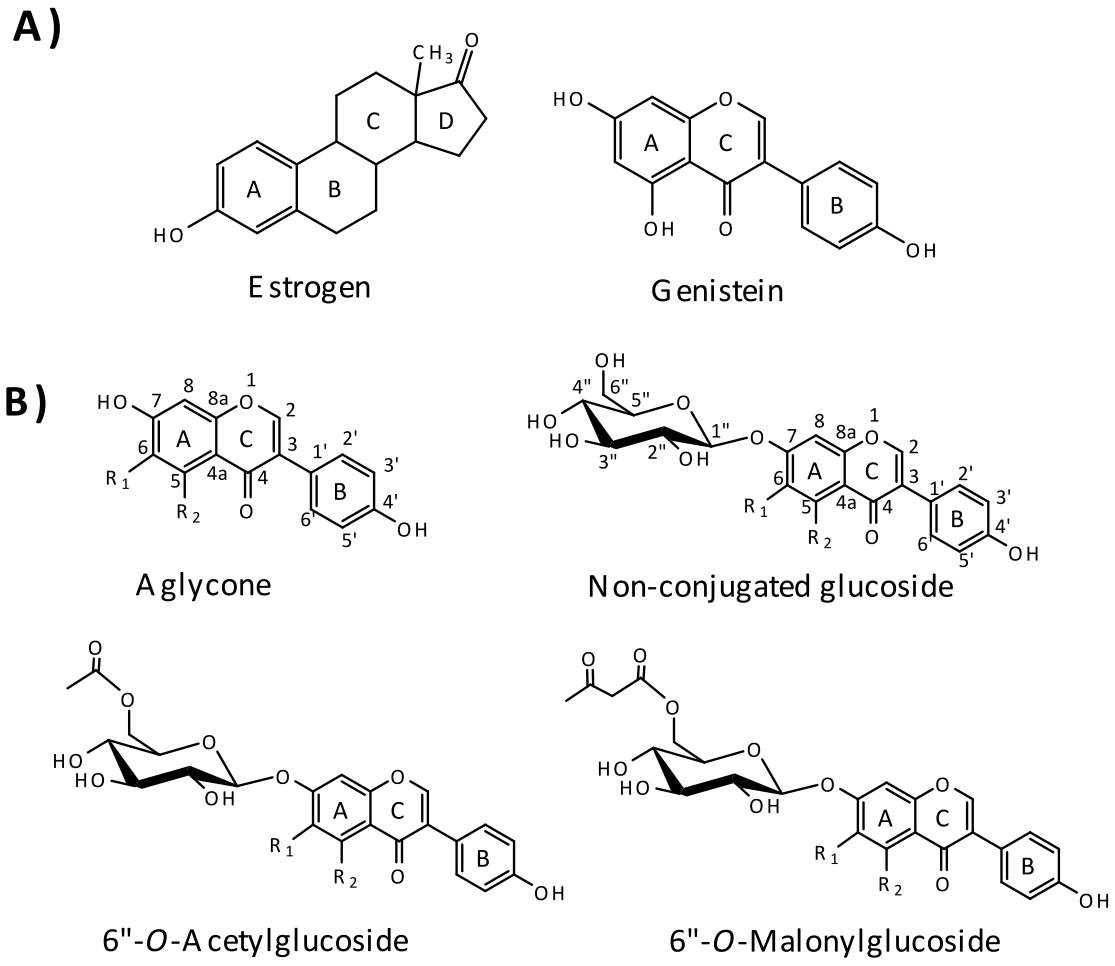

Figure 1. (A) Structures of human estrogen and isoflavone genistein showcasing their close structural resemblance. (B) Structures of the 12 known isoflavones categorized as aglycone, glucoside, acetylglucoside, and malonylglucoside. R1 can be -H in the case of daidzein and genistein or -OCH3 in the case of glycitein, while R2 can be -H in the case of daidzein and glycitein or -OH in the case of genistein.

The most abundant isoflavones in raw soybeans are the malonylglucosides, namely malonylgenistin and malonyldaidzin, followed by their respective non-conjugated glucosides. All of the four glycitein derivatives, acetylglucosides and aglycones are found in minute quantities (Wang and Murphy, 1996) (Figure 2). Based on the processing conditions employed to prepare soy products, the malonylglucoside content will vary. For example, malonylglucosides constitute about 52% of total isoflavone in soy protein isolate, 64% in soy protein concentrate, 72% in texturized vegetable protein, 64% in kinako, 82% in edamame, 33% in miso, and 26% in soymilk. Due to their high abundance in raw soybeans and various soy products, the bioavailability of malonylglucosides is crucial in order to contribute to the physiological benefits associated with isoflavones. Since, chemical structure can influence metabolism, absorption rate, bioavailability and subsequent bioactivity, consumption of different soy foods containing different isoflavone profile will not lead to the same physiological effect.

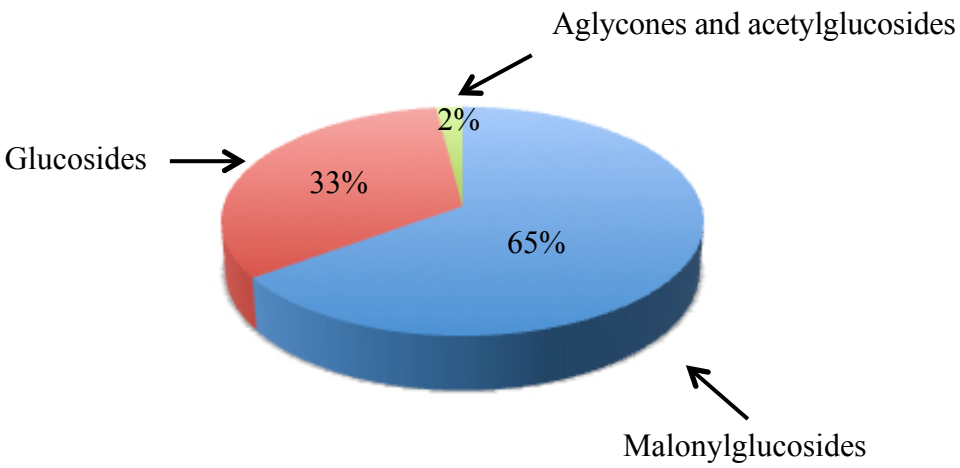

Figure 2. Distribution of isoflavones in raw soybean

1.3.3. Physiological properties of isoflavones

Owing to their structural similarity with human estrogen (Figure 1B), isoflavones are associated with numerous health benefits including alleviation of postmenopausal

symptoms (Shimizu et al., 2001); improved cardiovascular health (Kurzer et al., 2001; Kurzer et al., 2000; Burke et al., 1999); prevention of breast cancer (Lee et al., 2003; Severson et al., 1989), prevention of prostate cancer (Shu et al., 2001; Lee et al., 1991), prevention of colon cancer (Watanabe et al., 1993), prevention of osteoporosis (Takeshi et al. 2001; Kung et al., 2001; Leung et al., 2001), and anti-inflammatory activity (Ross, 1999). Following subsections provide examples of numerous studies that investigated isoflavone intake and its impact on health.

1.3.3.1. Postmenopausal symptoms

Estrogen replacement therapy (ERT) is a widely used technique for postmenopausal women to treat hot flushes and sweating. Owing to their structural similarity with human estrogen, soy isoflavones have been investigated as an alternative to the traditional ERT (Beck et al., 2005; Vincent and Fitzpatrick, 2000). For example, postmenopausal women that were placed on a soy-supplemented diet, containing aglycones (about 60 to 90 mg/day), showed a 40% decrease in the total number of hot flushes they experienced when they were on a soy-free diet (Murkies et al., 1995). However, modest reductions in the frequency and severity of hot flushes were also reported in a number of studies. For instance, a study reported no significant reduction in the frequency of hot flushes when test subjects were put on soy based diet (Lee et al., 2000).

1.3.3.2. Cardiovascular health

The important risk factors associated with cardiovascular health are high levels of low-density lipoprotein (LDL), high resistance of LDL to oxidation, low levels of high-density lipoprotein (HDL) in plasma, as well as high lipid peroxidation in tissues. These risk factors can potentially lead to heart attack or heart failure (Burke et al., 1999). Numerous clinical studies have investigated the relationship between soy intake and the reduction in the risk factors associated with cardiovascular diseases. Jenkins et al. (2000) reported a decrease in the concentration of circulating oxidized LDL in 31 hyperlipidemic

volunteers placed on soy-rich diet (86 mg isoflavones/day) over a period of 2 months. Teede et al. (2001) reported reduced systolic, diastolic, and mean blood pressure, and lowered triacylglycerol and LDL concentrations in men and postmenopausal women, after consumption of a beverage containing soy protein isolate (118 mg isoflavones/day) for a period of 3 months. However, studies also reported contradictory findings of isoflavones on cardiovascular risk factors. For example, Wiseman et al (2000) reported high levels of lipid peroxidation and a reduction in resistance of LDL to oxidation when a high phytoestrogen content diet (Containing 21.2 mg (84 μmol) daidzein and 34.8 mg (129 μmol) genistein) was administered. Thus, at present there is ambiguity in relation to the contribution of isoflavones to improvement in cardiovascular health.

1.3.3.3. Cancer

Cross-cultural studies reported a low occurrence of breast cancer among Japanese women as compared to their counterparts in the United States. This has been attributed to the fact that Japanese women consume more soy-based products (Lopez et al., 1997). Supporting this observation, Wu et al. (1996) found that the risk of breast cancer was higher for Asian Americans as compared to the native Asians that consume soy-rich diet.

After observing that isoflavones exert a beneficial effect against breast cancer, many studies were carried out to fully elucidate the mechanism involved. An *in vitro* study reported that genistein activated two detoxifications enzymes, quinone reductase and glutathione-S-transferase which are prominently responsible for controlling the development of breast cancer cell lines in women (Pahk and Delong, 1998). Furthermore, urinary isoflavone and equol concentrations were lower in women diagnosed with breast cancer as compared to well-matched control groups that were given a known amount of isoflavones (75 mg isoflavones/day) (Gorbach et al., 1995). Isoflavones were also reported to inhibit the development of prostate cancer cell lines. For example, genistein inhibited the growth of cultured prostate cell lines in an *in-vitro* study (Peterson and Barnes, 1993). The proposed mode of action was through the inhibition of focal adhesion kinases (Kyle et al., 1997). It was also postulated that the formation of new derivatives of

genistein by its interaction with halogenated or nitrated oxidants would also help in preventing prostate cancer (Kirk et al., 2001). In addition to the clinical studies, epidemiological studies also showed a direct relationship between soy isoflavone intake and reduction in prostate cancer risk. A significantly higher concentration of daidzein and equol in the prostatic fluid was observed in Asian men, coupled with a lower incidence of prostate cancer, as compared to European men (Morton et al., 1997).

In addition to the reported health benefits of isoflavones in preventing various forms of cancer, there is some data suggesting that isoflavones might not actually aid in the prevention of cancer. For example, breast cancer risk was not affected by phytoestrogen intake in a case-control study involving multi-ethnic American women (Horn-Ross et al., 2001). Thus, the results of the studies investigating the activity of isoflavones on various forms of cancer are not yet conclusive.

1.3.2.4. Osteoporosis

Osteoporosis is caused by reduced bone mineral density (BMD) and disrupted bone architecture, which might lead to an increased risk of bone fracture. These conditions are common in postmenopausal women due to an unbalanced estrogen level. Hence estrogen therapy is widely used by many postmenopausal women to treat osteoporosis (Christiansen et al., 1981). However, use of estrogen therapy might not always be useful as it might lead to an increased risk of breast cancer (Ronald et al., 2000). Isoflavones, which have both estrogen agonist/antagonist functions in the body, are being favored as a replacement for estrogen therapy. A large study conducted with around 24,000 postmenopausal Chinese women, reported an inverse relationship between soy isoflavone intake and risk of bone fracture (Zhang et al., 2005). Together with epidemiological studies, few clinical studies also showed association between soy intake and improvements in bone mineral density (BMD). Enhancemnent in BMD and reduction in spinal bone loss was observed in post-menopausal women that received a diet rich in isoflavone for 26 weeks (Potter et al., 1998).

There were also conflicting results reported for the prevention of osteoporosis by isoflavones. A study carried out in post-menopausal women did not confirm earlier conclusions that isoflavones improve BMD or have an affect on calcium metabolism (Duncan et al., 2003). Spence et al. (2005) reported that isoflavones had no effect on calcium absorption, bone turnover, and bone balance in post-menopausal women who consumed 40–50 g/day of soy protein containing isoflavones for 28 days.

1.3.2.5 Anti-inflammatory activity

Inflammation is generally considered as an early event in the pathogenesis of atherosclerosis (Ross, 1999; Libby, 2002), and can contribute to metabolic syndrome, type-II diabetes (Medjakovic et al., 2010) and cancer (Dijsselbloem et al., 2004). Endothelial cell adhesion molecules play an important role in the process of inflammation. These molecules are proteins that are located on the surface of endothelium and are involved in the binding of extracellular matrices, which is a process termed as cell adhesion. Expression of these endothelial cell adhesion molecules such as E- and P- selectins play an important role in the initiation of the inflammatory process (Dong et al., 2000; Ramos et al., 1999). Pro-inflammatory cytokines such as TNF-α and IL-1β have been reported in the up-regulation of the E- and P-selectins (Weber et al., 1995). Thus, inhibiting the cell adhesion molecules expression can result in controlling initial inflammatory response. Endothelial cells treated with isoflavone genistein (25-50 μM), inhibited TNF-α induced E- and P-selectins expression in human umbilical vein endothelial cells, highlighting the role of soy isoflavones in regulating inflammation at the initial stages (May et al., 1996).

The second step in the inflammatory process constitutes adhesion of inflammatory cells (a cell participating in the inflammatory response to a foreign substance) to the endothelium (Ross, 1999). Isoflavones, namely genistein, daidzein and equol have been reported to block the inflammatory process by inhibiting the adhesion of inflammatory cells to the endothelium (Nagarajan et al., 2006).

The third step in the inflammation process is transendothelial migration of the inflammatory cells (Ross, 1999). Transendothelial migration is often cited as a result of the presence of certain pro-inflammatory chemokines such as MIP1-α, MCP-1, RANTES and MIP1-β. Soy-based diets inhibited the expression of these chemokines, demonstrating that isoflavones have the ability to inhibit pro-inflammatory chemokines at the site of inflammation (Nagarajan et al., 2008).

Soy isoflavones also were shown to inhibit the final stages of inflammation processes by inhibiting foam cell formation (Kreiger, 1997). Foam cells are formed in our body by the scavenger receptor mediated uptake of oxLDL (oxidized LDL) by macrophages. Soy isoflavones inhibited oxLDL generation, thus prevented foam cell formation. Several *in vitro* studies have also reported that isoflavones might play a role in the inhibition LDL oxidation (Kerry and Abby, 1998).

On the other hand, few clinical studies have reported inefficacy of isoflavones in controlling inflammation at its various stages. For example, Beavers et al. (2010) reported that soymilk supplementation did not inhibit pro-inflammatory cytokines such as TNF-α. In another study, soy isoflavones did not show any effect on the inhibition of LDL oxidation (Vega-Lopez, 2005). Thus, there is no clear consensus regarding the plausible effects of isoflavones on inhibiting inflammation.

The mixed results that were obtained for the physiological effects of isoflavones could be attributed to many factors including but not limited to ethnic background, age, gender, gut microflora and source of isoflavones. Source of isoflavones can drastically affect the results, especially when different isoflavone forms are administered at different levels. Since different isoflavones may not all be bioavailable or biologically active (Setchell et al., 2001), it is important to identify the different chemical forms of isoflavones, determine the amounts in which they are consumed via different soy foods, and understand the effect of processing on these different forms. These topics will be dealt with in detail in the subsequent sections.

1.3.3. Isoflavone consumption

In western countries the sources of soy intake is generally in the form of soy products that are made from soy flour, soy grits, soy protein isolates or concentrates and textured soy proteins (Wang and Murphy, 1996). Consumption of these soy foods by western populations accounts to an average daily intake of 1 mg of isoflavones per capita (aglycone equivalents), which is far less than the daily intake of the Asian populations (Wei et al., 1995; Adlercreutz et al., 1991). In Asian countries, soy is consumed in traditional Asian diets in the form of soymilk, tofu, and as fermented soybean products such as miso, tempeh, soybean paste, natto and soy sauce (Wang and Murphy, 1996; Coward et al., 1993). The soy consumption by Asian populations on a daily basis is around 35 g per capita (Coward et al., 1993), which accounts for about 25-100 mg of isoflavones/day (aglycone equivalents) (Messina, 1999). Asian populations are exposed to soy very early in life and the consumption continues until later stages of life. Most of the clinical trials validating isoflavone health benefits have been conducted in Asian populations and it has been hypothesized that the exposure of Asians to isoflavones in early stages of life might be responsible for the health benefits occurring in the later stages of their life (Nagata et al., 2006). It has to be noted however, that the soy intake varies based on variables such as age, gender, ethnicity and socioeconomic status (Chun et al., 2009).

The types of soy foods consumed by Asians are often fermented, thus the main isoflavone forms ingested are aglycones, ranging between 10-30 mg/day (Messina et al., 2006). Western populations on the other hand consume other processed forms of soy that are not fermented. Examples include soymilk, and unfermented soy based products such as bakery goods and meat analogues formulated with either soy flour, textured vegetable protein, or soy protein isolate. These soy foods primarily constitute conjugated forms of isoflavones rather than aglycones. Hence, there is an apparent difference in the profile of isoflavones that are consumed by western and Asian populations (Wakai et al., 1999).

Difference in the isoflavone profile in various soyfoods is attributed to the different processing conditions that are employed. Thus, in order to determine the isoflavone profiles in various soy foods one has to understand the effect of processing on various isoflavone forms.

1.4. Effect of processing conditions on the profile and total content of isoflavones

There is a general consensus among researchers that isoflavones primarily undergo interconversions upon processing (Mathias et al., 2006). Of the twelve known isoflavone forms, malonylglucosides are the most thermally labile and contributes the most to the overall interconversions (Murphy et al., 2002). Generally, the extent of interconversions of the isoflavones is a factor of processing conditions employed. The three most important processing parameters that influence the change in isoflavone profile in various soy foods in comparison to raw soybeans are temperature, pH and time. These processing parameters have a substantial influence on the profile and content of isoflavones, mainly causing conversion of conjugates to their respective non-conjugates (Coward et al., 1998; Wang and Murphy, 1996). Some of the most common processing protocols employed to produce various kinds of soy products are discussed in the following sections.

1.4.1. Fermentation

The aglycone form is one of the major isoflavone forms found in fermented soybean products. During fermentation, the native glucosidase enzyme present in soybeans act on the non-conjugated glucosides, cleaving the glucose moieties, thus converting them to their respective aglycone forms (Murphy et al., 1999; Matsuura and Obata, 1993; Murakami et al., 1984). Examples of some of the fermented soy products are soy sauce, miso, and tempeh. It has to be noted, however, that conjugated isoflavones namely malonyl- and acetyl- glucosides are unaffected by the enzyme activity and their concentrations remain high in the end product (Wang and Murphy, 1994).

1.4.2. Low moisture processing

Processes such as toasting and extrusion can be categorized as low-moisture processing methods. Examples of soy products that undergo low-moisture processing are

toasted soy flour (Coward et al., 1998) and texturized soy protein isolates (Singletary et al., 2000). The main interconversions occurring upon low-moisture processing are the decarboxylation of malonylglucosides to form acetylglucosides (Figure 3). Toasting of soy flour at 150°C for 4 hours led to a substantial increase in acetylglucosides with a subsequent decrease in malonylglucosides (Murphy et al., 2002). There is minimum aglycone or non-conjugated glucoside formation under low moisture processing conditions (Murphy et al., 2002). Processing parameters can influence the rate of decarboxylation of malonylglucosides to acetylglucosides. For example, Mahungu et al. (1999) showed that acetylglucosides concentration significantly increased when temperature was raised from 110°C to 150°C.

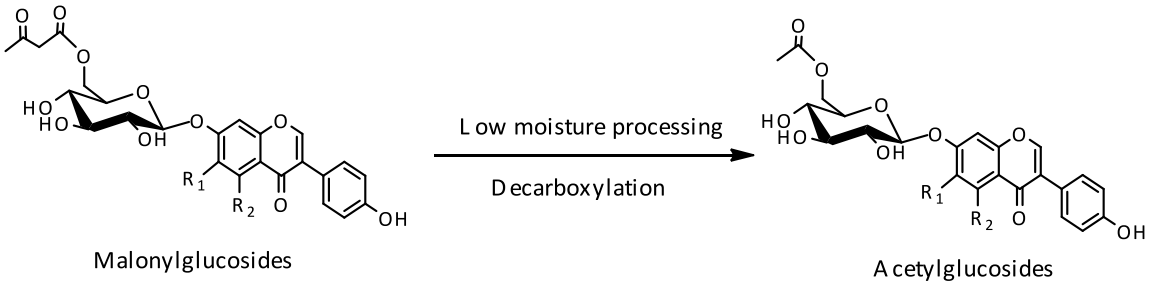

Figure 3: Interconversions of isoflavones subjected to low moisture processing

1.4.3. High moisture processing (aqueous processing)

An example of a soy product that is prepared by subjecting soybeans to aqueous processing is soymilk. The major interconversions observed during aqueous processing are the de-esterification of the abundant malonylglucosides to their respective heat stable non-conjugated glucosides (Kuduo et al., 1991) (Figure 4). Similar to low-moisture processing, the extent of interconversion depends largely on the processing parameters employed. A kinetic study showed that the de-esterification reaction rate of malonylglucosides increased with the increase in treatment temperature and time (Chien et al., 2002). Kinetic studies conducted by Vaidya et al. (2007) observed a similar effect, with the de-esterification reaction rate substantially increased as processing temperature was raised from 60°C to 100°C, and the pH increased from 8 to 10. Mathias et al. (2006)

showed similar results, where the rate of interconversion of malonylglucosides and acetylglucosides to non-conjugated glucosides increased substantially with the increase in temperature and pH. During aqueous processing, acetylglucoside formation was not favored. Similarly, aglycone formation was also not favored because of the thermal inactivation of the native glucosidase enzymes (Kuduo et al., 1991).

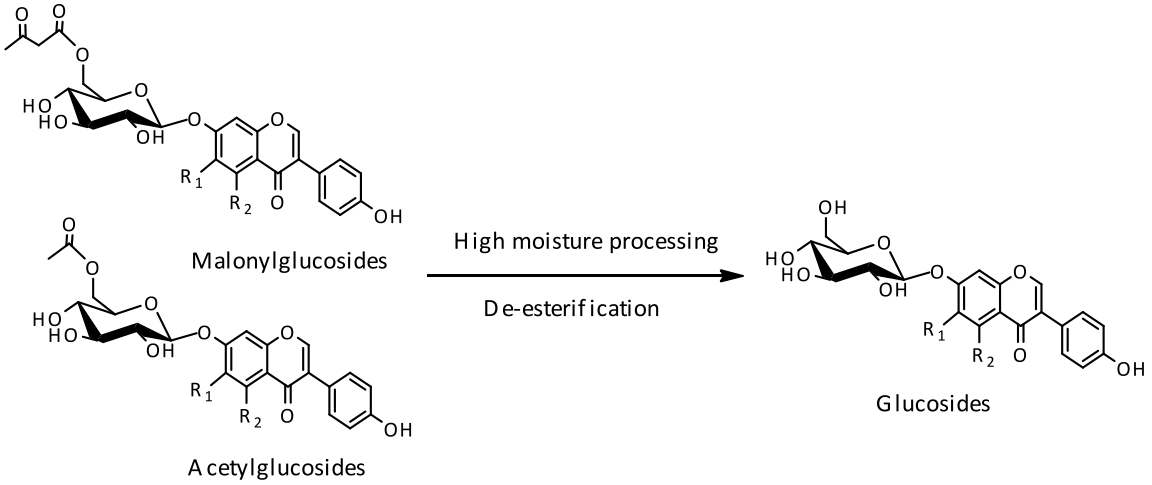

Figure 4: Interconversions of isoflavones subjected to high moisture processing

1.4.4. Loss in total isoflavone amount

Coupled with interconversions, significant amount of loss in total known isoflavone amount was also observed upon processing (Jackson et al., 2002). Since, the total isoflavone amount ingested is critical in inducing the desired health benefits, it is mandatory to determine the conditions that optimize isoflavone profile and minimize loss.

Initially, loss in isoflavones was assumed to be due to various processing steps such as soaking or leeching into waste stream (Hendrich and Murphy, 2001); dissolution of isoflavones in aqueous-alcohol solutions used in the production of certain soy products such as soy protein concentrates and isolates (Coward et al., 1993); or binding to the protein matrix (Murphy et al., 2002; Barnes et al., 1994). Jackson et al. (2002) observed 65% loss in the total isoflavone amount after processing of raw soybeans. Although, mass

balance studies accounted for a large part of the reported loss, about 20% remained unexplained.

Further research showed that loss in total isoflavones could also be attributed to complete degradation of isoflavones (Xu et al., 2002). Xu et al. (2002) employed a closed model system whereby the loss observed was not attributed to leaching or binding to proteins, instead was solely attributed to the complete degradation of isoflavones. They found a temperature dependent degradation of all the non-conjugated glucoside forms that were heated under dry conditions, as temperature was raised from 110°C to 135°C. Ungar et al. (2003) investigated the stability of genistein and daidzein at 120°C under alkaline (pH 9) and neutral (pH 7) conditions. At pH 7, degradation of daidzein was more than genistein and vice-versa at pH 9, indicating that pH along with temperature has a significant effect on degradation. Heating malonylglucosides in closed model systems, with temperature, time and pH as processing parameters, showed an increase in the de-esterification rate of malonylglucosides accompanied with up to 30% loss in the total isoflavone amount at elevated temperature and pH (Mathias et al., 2006). Loss in total isoflavones was also observed in complex soy food systems. Park et al. (2002) reported a 20% loss in total isoflavone amount after heating soy flour to a temperature of 121°C for 40 min. Mahungu et al. (1999) also observed significant losses due to degradation of malonylglucosides during extrusion of soy protein isolates and corn mixtures at 110°C, 130°C and 150°C.

The studies that have reported degradation of isoflavones made no attempt to characterize the degradation derivatives and hence labeled them as “loss”. A close look at chromatograms presented by researchers in their publications reveal the formation of unknown compounds that partially constitute the so-called “loss” (Figure 5 and 6). Chromatographic and spectral peaks corresponding to unknown compounds formed upon processing of isoflavones containing systems were not discussed.

It is still debatable whether interconversions affect bioavailability; however, since degradation products are labeled as “loss” it is thus assumed not to be bioavailable. Hence, if the loss is due to complete degradation, then it is important to investigate ways to limit it. However, if part of the calculated loss comprises a certain amount of

unidentified derivatives that might have biological relevance, then it would be necessary to identify these derivatives and investigate their physiological contribution. To date, there is no available data regarding isoflavone degradation derivatives. Many researchers investigating the processing effects on isoflavones often employ routine analytical approaches, which might mask the presence of the degradation derivatives. Hence, employing additional and more sophisticated analytical techniques may allow for the detection and identification of these derivatives.

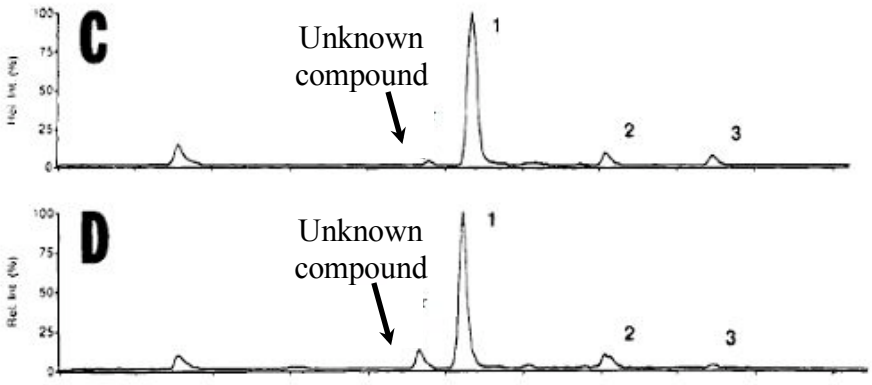

Figure 5: Selected positive ion chromatograms of genistein glucosidic conjugates in soybean hypocotyls (D) tofu following HPLC-APCI-HN-MS analysis. The reconstructed ion chromatograms were obtained from the sum of the m/z 519, 475 and 433 ions (Picture and text adopted from Barnes et al., 1994). The peaks eluting immediately before the peak labeled 1, correspond to an unknown compound that was not discussed by the authors.

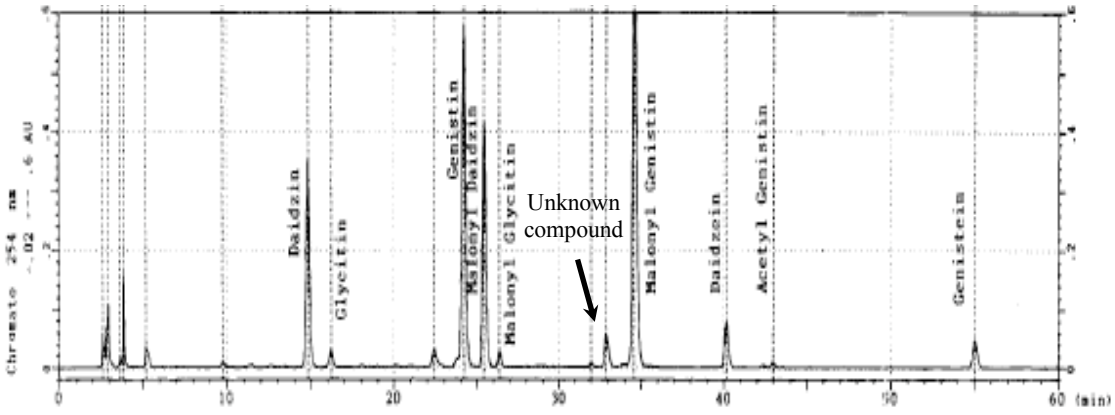

Figure 6: HPLC retention profiles and UV absorbance spectra of texturized vegetable protein (picture and text adopted from Wang and Murphy, 1994). It has to be noted that the peak labeled as isomer has the same absorbance spectra as malonylgenistin. The peak eluting immediately before the peak labeled malonylgenistin corresponds to an unknown compound that was not discussed by the authors.

1.5. Novel isomers of malonylglucosides

We have recently (Yerramsetty et al., 2011) detected derivatives of malonylglucosides formed upon heating at neutral and alkaline pH conditions (Figure 7). These derivatives constitute part of the calculated loss in total isoflavones reported previously (Mathias et al., 2006; Xu, et al., 2002; Nufer et al., 2009). The detected derivatives were deduced to be isomers of malonylglucosides based on liquid chromatography (LC) coupled with mass spectrometry (MS) analysis. The isomers had identical UV wavescan (Figure 8) and molecular mass (Figure 9), and had a slightly different fragmentation spectra (Figure 10) when compared with malonylglucosides. The fragmentation spectra for both isomer and malonylgenistin had m/z 271 as the base peak, representing the protonated form of the aglycone genistein. The formation of the aglycone peak after fragmentation at an optimum collision level is a unique identifier for non-conjugated as well as conjugated isoflavones (Rijke et al., 2004), thus confirming that both the isomer and malonylgenistin have genistein in their structure. An ion with m/z 433 (protonated form of genistin) was also present in the fragmentation spectrum of

malonylgenistin at low relative abundance, but was absent in that of the isomer. Similar observations were noted for malonyldaidzin and its isomer. These observations indicated that malonylglucosides and their isomers are either positional or stereoisomers. Since, chemical structure plays an important role in determining isoflavone bioavailability, complete structural elucidation of the isomers is necessary to determine their physiological relevance. Employing powerful analytical tools such as nuclear magnetic resonance (NMR) will provide structural characterization of the detected isomers.

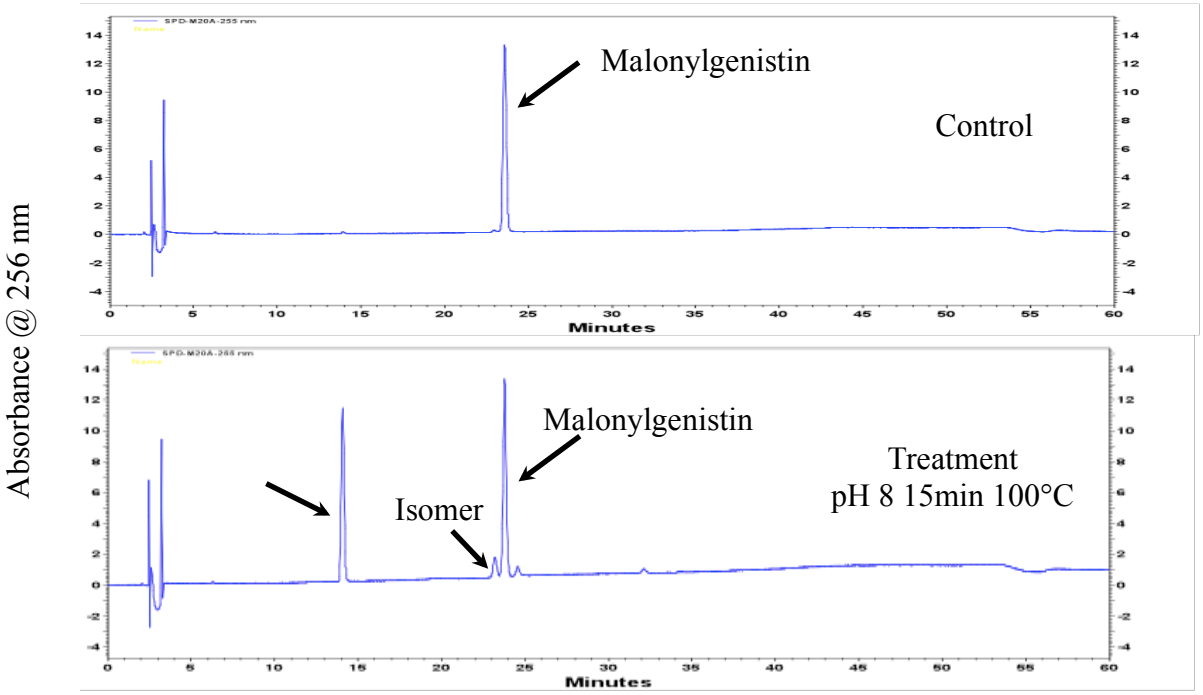

Figure 7: Formation of unknown compounds upon subjected to processing at various conditions

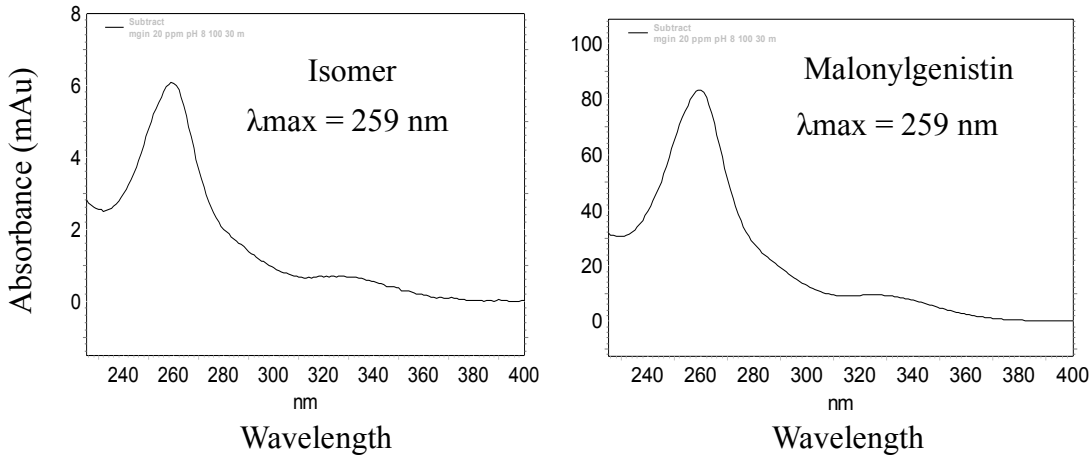

Figure 8: Wavescans of malonylgenistin and its isomer

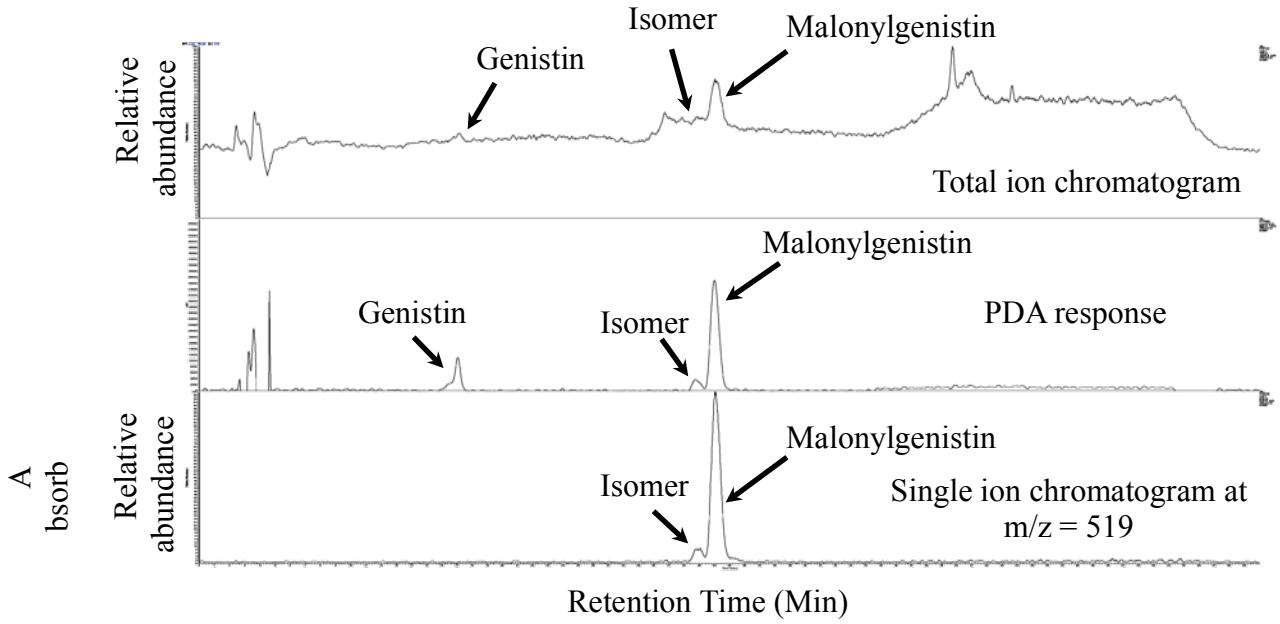

Figure 9: High performance liquid chromatography/mass spectrometry data showing that malonylgenistin and its isomer have the same mass (518 Da)

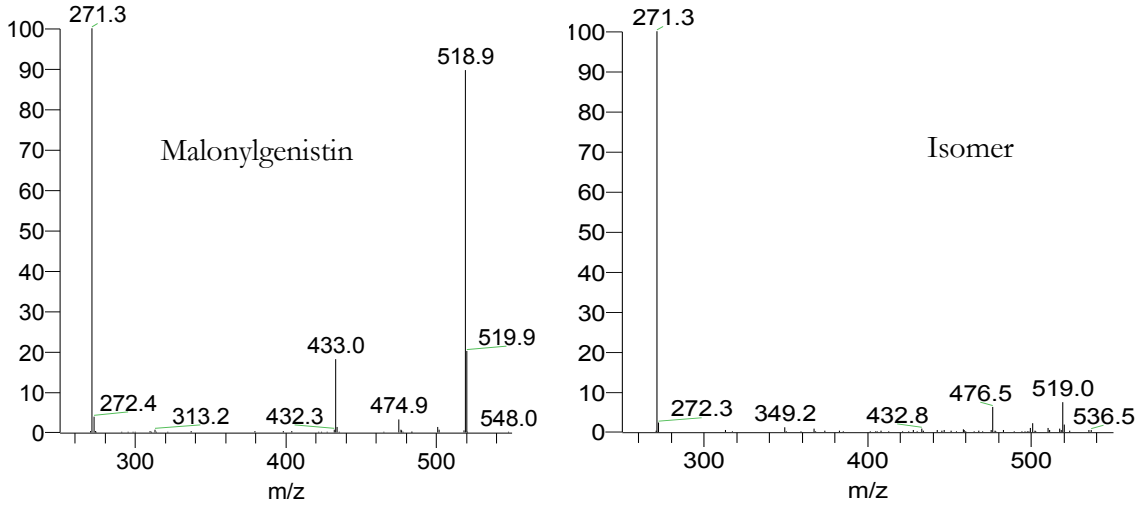

Figure 10: Fragmentation spectra (s) of malonylgenistin and its isomer. The parent ion of both malonylgenistin and its isomer (519 Da) fragmented into an ion with m/z = 271 for both compounds which corresponds to the aglycone, genistein. Data was collected at a collision level of 20%.

1.6. Analysis of isoflavones and structural characterization

1.6.1. High performance liquid chromatography/mass spectrometry (HPLC/MS)

Laboratories employ different analytical techniques for qualitative and quantitative analysis of isoflavones. The most widely used technique is HPLC. In addition to isoflavone separation, identification and quantification, HPLC can also be used on a preparative scale to purify and subsequently isolate isoflavones (Farmakalidis and Murphy, 1984). Different laboratories employ different HPLC methods to separate isoflavones. However, the common criteria for all the methods include the use of C18 columns and the optimization of resolution by changing solvent composition and temperature (Ismail and Hayes, 2005; Murphy et al., 2002). Commonly used detectors for isoflavone analysis are photodiode array (PDA) or ultraviolet (UV) detectors (Lijuan et al., 2007; Wilkinson et al., 2002). Compared to a standard UV detector, a PDA detector

allows more precise identification of isoflavones. Wavescans (190-370 nm) produced by a PDA detector allows for identification of isoflavones in the absence of authentic standards, and also for the structural characterization of unknown derivatives of isoflavones (Yerramsetty et al., 2011). However, structural characterization becomes rather challenging when the unknown derivatives share a similar structure with other known isoflavones, especially that of the UV absorbing phenolic moiety (Yerramsetty et al., 2011).

Other analytical techniques such as MS are also used in tandem with HPLC, primarily to perform qualitative and quantitative analysis of isoflavones (Griffith and Collision, 2001; Peterson et al., 1996). Among the various ionization techniques used during MS analysis, electrospray ionization has become prominent due to its ability to produce molecular ions (Wu et al., 2004; Prasain et al., 2003). With the knowledge of the m/z (mass to charge ratio) of molecular ions, mass determination of isoflavones becomes rather straightforward (Fenn et al., 1989). In order to obtain additional structural information of the compound of interest, tandem mass spectrometry is often employed to fragment the molecular ion and to produce daughter ions at various collision levels (Kang et al., 2007; Yerramsetty et al., 2011). Formation of molecular ions and fragmentation of ions aid in the mass determination and partial structural identification of unknown derivatives of isoflavones.

1.6.2. Nuclear magnetic resonance (NMR) analysis

Besides HPLC/MS, NMR analysis is also employed by various researchers for structural identification of isoflavones and derivatives in the absence of authentic standards (Yerramsetty et al., 2011; Chang et al., 1994; Coward et al., 1993). The most important information provided by NMR as compared to HPLC/MS is the molecule's skeletal connectivity. Although, HPLC/MS provides valuable structural information, often the skeletal connectivity information obtained from HPLC/MS is dubious. Hence, NMR is considered a more powerful analytical tool as compared to HPLC/MS.

The starting point for NMR analysis is the inspection of the proton (1H) spectrum. The proton spectrum is a 1-D (one dimensional) NMR technique with signal intensity as the Y- axis and chemical shift (in ppm) as the X-axis. Proton NMR spectra of most organic compounds are characterized by chemical shifts in the range +14 to -4 ppm. Often the position and number of chemical shifts are diagnostic of the structure of a molecule and gives information about the number of protons in the molecule. In some cases it might also be useful in predicting skeletal connectivity of few chemical bonds if not all. Further, based on the chemical shift of the peaks, one can deduce the hybridization or the functional group(s) present in the molecule. Coupling constant is another useful indicator to predict the type of chemical bond and in some instances their spatial orientations. For example, in the structure of glucose, coupling constant can be used as a useful indicator to differentiate between α and β anomers. The coupling constant of the anomeric proton (δH = 5.2) in α anomer is ~3.7 Hz whereas the coupling constant for the β-anomer is ~7.93 Hz. In case of α anomer, the coupling constant is low because of the smaller axial-equatorial dihedral angle at the H-C1-C2-H bond (Gurst, 1991).

Despite the wealth of information that can be obtained from the proton spectrum, sometimes, one can risk losing that information with the choice of the NMR solvent used, especially in the case of isoflavones that contain –OH groups. For example, some functional group information might be missing (such as in -OH or NH_3 groups) if a protic NMR solvent such as methanol (or) water is used. This is caused due to hydrogen/deuterium (H/D) exchange. To avoid this situation, researchers often employ aprotic solvents such as dimethyl sulphoxide (DMSO) or acetonitrile. However on the flipside, use of an aprotic solvent might result in poor solubility of isoflavones. Hence, in order to achieve complete solubility, the concentration of isoflavones in the aprotic solvent must be reduced. However, it has to be noted that low concentration warrants the use of a high strength NMR magnets ranging in the 700 to 950 MHz range.

In addition to problems caused by the choice of solvent, gathering skeletal connectivity information of complex molecules solely based on proton spectrum is very challenging. Often, many signals might overlap in the proton spectrum of complex

molecules which makes the interpretation tedious. Hence, additional NMR techniques have been developed that overcome these difficulties. A vast array of 2-D (two dimensional) techniques has been developed that provide different skeletal connectivity information depending upon the pulse sequence employed. Most common 2-D analysis techniques include correlation spectroscopy (COSY), heteronuclear single-quantum correlation spectroscopy (HSQC) and heteronuclear multiple-bond correlation spectroscopy (HMBC). While COSY is a homonuclear through-bond correlation technique that provides skeletal connectivity information of H-H linkages, HSQC and HMBC are heteronuclear through-bond correlation techniques that provide skeletal connectivity information about C-H linkages in a molecule. However, the difference between HSQC and HMBC techniques is that HSQC provides information about C-H linkages that are separated by only one bond, whereas HMBC can detect C-H linkages that are 2-3 bonds apart. Below is an example of the NMR analysis of isoflavone genistin as an illustration of the application of 1-D and 2-D techniques to completely elucidate isoflavone structure.

In the proton spectrum of genistin, there are two solvent peaks of DMSO-d_6, one is a multiplet at 2.50 ppm and the other is a singlet at 3.30 ppm. Excluding the solvent peaks, the proton spectrum of genistin can be divided into two distinct groups of signals that correspond to the aromatic and the glucose region of genistin (Figure 11). In the glucose region, there are 7 distinct peaks located between 5.08 ppm and 3.17 ppm. The doublet at 5.08 ppm is the most diagnostic component of the glucose region, as it represents the anomeric proton. It is typically found downfield relative to other ring protons due to the deshielding effect of the nearby ring oxygen atom. The coupling constant (7.7 Hz) is consistent with larger axial-axial coupling that is expected for the β-anomer, in which the H-C-C-H bond is approximately 180°. In addition to the anomeric proton, the doublet of doublet near 3.26 ppm is the proton attached to the C2 of the glucose. The H2 proton is coupled with two different protons (H1 and H3) with different coupling constants, and hence instead of a triplet, a doublet of doublet was observed for H2. A doublet of doublet was also observed at 3.71 ppm, and this signal belongs to one of the two H6 protons. Two protons are present at the C6 position and they experience preferential deshielding due to

the nearby oxygen atom that is part of the hydroxyl group at C4 position. As illustrated in Figure 12, one of the H6 protons will be spatially closer to the oxygen atom when compared to the other and hence results in preferential deshielding of the H6 protons resulting in the most deshielded proton to be relatively downfield as compared to the other. Assigning remaining glucose protons based on proton spectrum is difficult as there is significant overlapping of signals. For example, there was overlap between peaks with chemical shifts, 3.45 and 3.47 ppm. Hence, 2-D techniques will be of help in cases such as these.

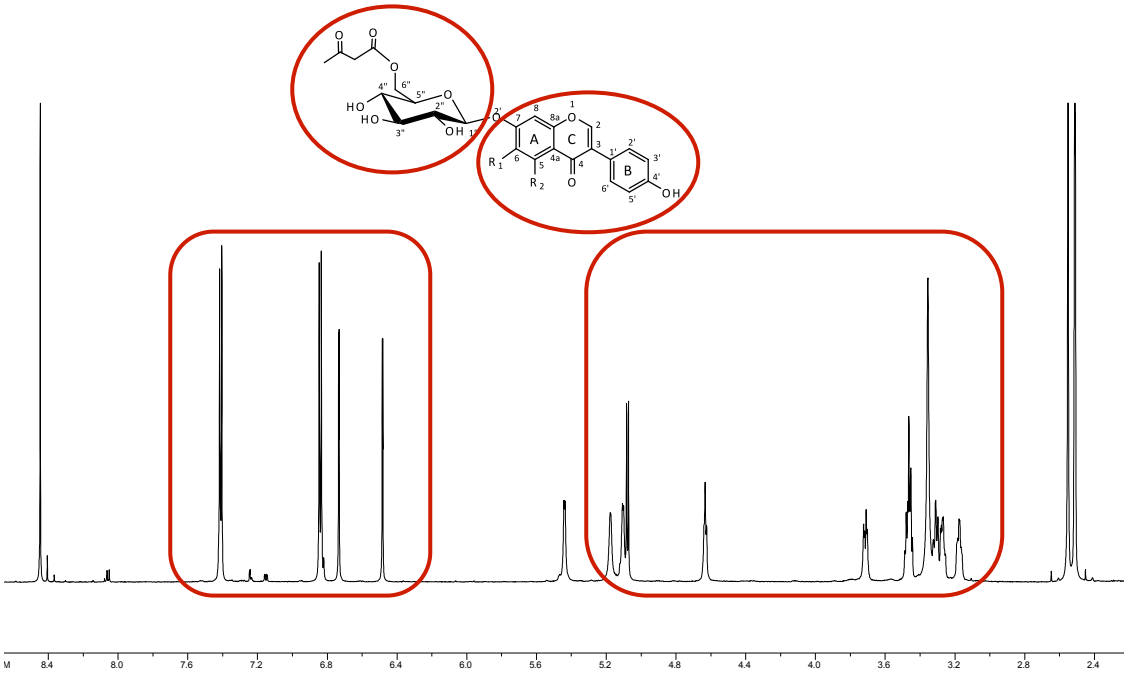

Figure 11: Proton NMR spectrum of genistin in DMSO-d_6. NMR experiments were carried out on a Bruker 700 MHz Avance spectrometer (Rheinstetten, Germany) equipped with a 1.7 mm TCI proton-enhanced cryoprobe.

Assigning chemical shifts to the aromatic protons is not complicated. A close look at the genistin structure reveals that in its proton spectrum there will be a singlet (H2) and four doublets (H6, H8, H2'/H6' and H3'/H5'). The singlet was observed at 8.44 ppm and it corresponds to the H2 proton. Due to the relatively high electron density of the

chromene system the H2'/H6' protons will experience higher deshielding effect than H3'/H5'. Thus, the peak at 7.41 ppm represents H2'/H6' and the peak at 6.83 ppm represents H3'/H5'. On the same grounds, the proton at 6.48 ppm represents H6 and the peak at 6.73 ppm represents H8. Another useful tool to differentiate the doublets is based on their coupling constants. The two doublets with a coupling constant of 2.20 Hz will be either H6 or H8 and the two doublets with 8.40 Hz belong to either H2'/H6' or H3'/H5'.

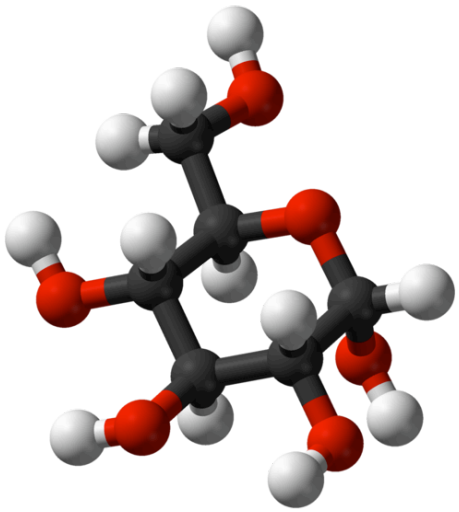

Figure 12: Three dimensional alignment of glucose (wikipedia.org/wiki/Glucose)

Two-dimensional NMR spectroscopy was employed to assign the undetermined peaks and to differentiate the overlapping peaks in the glucose region of the proton spectrum and also to confirm the proton assignments from the proton spectrum. Correlation spectroscopy was performed to establish the linkages between various protons (Figure 13). In the H,H-COSY spectrum of genistin we found correlation between the peaks at 3.71 ppm and 3.48 ppm indicating that these two peaks are coupled. Since the peak at 3.71 ppm is one of the H6 protons, the peak at 3.48 ppm can be deduced to be the second H6 proton. Similar correlations were established for all the unassigned protons and respective chemical shifts are 3.31 ppm (H3"), 3.17 ppm (H4") and 3.46 ppm (H5"). Additionally, HSQC was performed to validate all the information obtained from H,H-COSY and also to obtain carbon data. Structural information obtained from proton

and H,H-COSY was in excellent agreement with the structural information obtained from HSQC (Figure 14). The carbon data of genistin obtained from HSQC experiment is: Genistin (176 MHz, DMSO-d_6): β-D-glucose: C1'': 100.2, C2'': 74.1, C3'': 77.3, C4'': 69.9, C5'': 78, C6'': 61.4; aglycone: C2: 153.8, C3: 122.9, C4: 181.2, C4a: 106.5, C5: 162.4, C6: 99.7, C7: 163.4, C8: 94.8, C8a: 157.1, C1': 123.0, C2'/C6': 131.6, C3'/C5': 115.1, C4': 158.1.

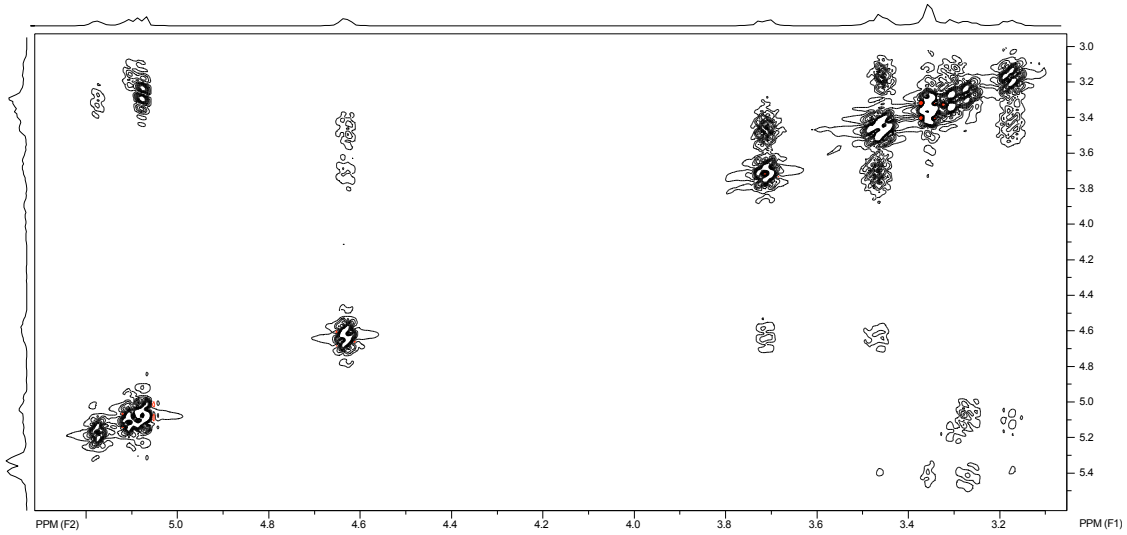

Figure 13: The COSY of the glucose region of genistin. The projection on the horizontal axis (F2) or on the vertical axis (F1) is the proton spectrum of the sample.

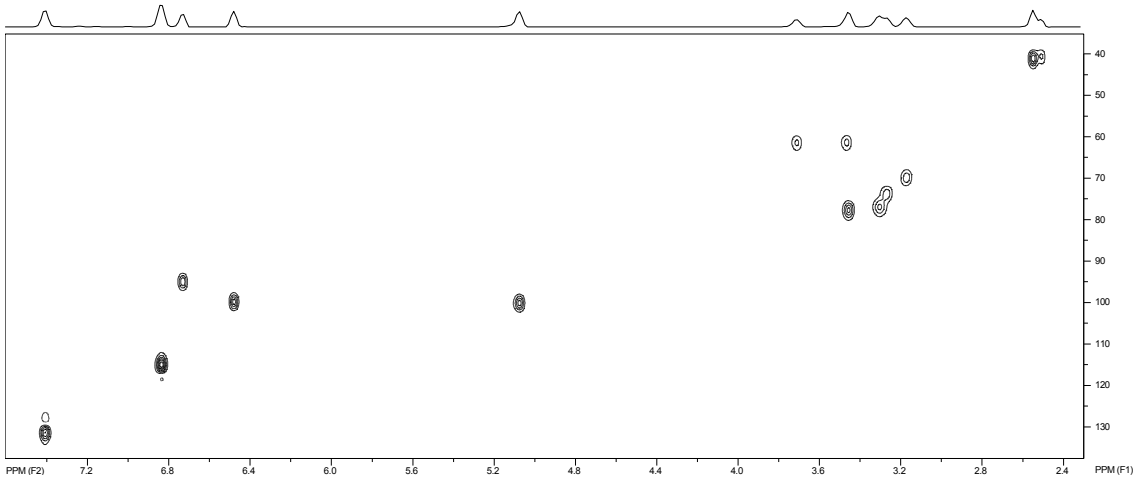

Figure 14: The HSQC of genistin. The projection on the horizontal axis (F2) is the proton spectrum and on the vertical axis (F1) is the carbon data.

The illustration above demonstrates that NMR has a unique advantage over HPLC/MS in obtaining complete structural information. Further, NMR can also be used as an analytical tool for the unambiguous verification of standards that are not available commercially and have to be either synthesized or separated using chromatographic techniques.

1.6.3. Isotope dilution mass spectrometry (IDMS) to determine plasma and urine isoflavone content

Obtaining accurate analytical results is the foremost requirement for any analytical method. With ever increasing need for trace analysis of analytes in various systems, a demand for a rugged and accurate analytical method has risen. Isotope dilution mass spectrometry (IDMS) is a method of proven accuracy and precision, with the sources of systematic errors well understood and controlled. In IDMS, an exact amount of an isotope is added to the analyte solution. By determining the isotope ratio of the spiked sample exact quantity of the analyte in the actual sample can be calculated, irrespective of the losses during sample preparation. This property is one of the principal advantages of IDMS over other contemporary analytical techniques, with the added advantage of surpassing their analytical accuracy. For this reason, IDMS has been widely employed in life sciences and to some extent in the analysis of isoflavones (Heinonen, et al., 2003; Twaddle, et al., 2002; Trdan, et al., 2011).

One of the main prerequisite in choosing isotopes is their stability during sample preparation and analysis. In case of instability, the calculated isotopic ratio would be altered and thus will result in inaccurate determination of the target analyte. Prominent isotopic standards for IDMS analysis of isoflavones are either carbon-13 or deuterium labeled. Many researchers preferred deuterated standards over carbon-13 standards, due to the ease with which one can synthesize deuterated standards (Cohen et al., 1986). For isoflavone analysis, researchers used either tri- or tetra- deuterated isoflavones as spike isotopes (Twaddle, et al., 2002; Trdan, et al., 2011). However, with increase in the number of deuteriums on the isoflavones structure, researchers observed that there was

significant separation between the deuterated isoflavone and its analyte. Researchers call this phenomena deuterium isotope effect, the extent of which is directly proportional to the number of deuteriums on the isoflavone structure, with significant chromatographic separation observed for isotopes that are 3-5 mass units more than the analyte (Lockley, 1989). Researchers saw a potential problem with the chromatographic separation caused by the deuterium isotope effect. Wang et al. (2007) reported that a chromatographic separation of 0.02 min between the analyte and its isotope that are five mass units apart can cause a 25% difference in their ion suppression(s), resulting in an inaccurate isotope ratio. This ion suppression can significantly impact the accuracy and precision of the IDMS method.

Despite the errors introduced by deuterium isotope effect investigators who used deutero labeled isotopes as internal standards in their experimental procedures have frequently used tri-deutero derivatives (Heinonen, et al., 2003) or tetra-deutero derivatives (Twaddle, et al., 2002). Researchers chose these isotopes to avoid isotopic overlap between the isotope and its analyte. Isotopic overlap is defined as the overlap between the isotopic envelopes of the isotope and its analyte, so that the analyte can be distinguished from the isotope when using mass spectrometry.

Although, IDMS is a proven method for high accuracy and precision and is often used to calibrate other analytical instruments, it is largely plagued by errors introduced by the choice of isotopes that are used as internal standards especially for isoflavone analysis. Thus, there is an immediate need to address the issue of deuterium isotope effect by choosing better isotopes, specifically with regard to isoflavone analysis without compromising the accuracy and precision. In order to synthesize the appropriate isotopes, the reactivity preferences of isoflavones needs to be understood to streamline the synthesis protocol. Computational chemistry is an excellent technique to determine various ground state characteristics of isoflavones that will give us a better understanding of their reactivity preferences.

1.6.4. Computational chemistry

Computational chemistry (or) theoretical chemistry is a field that is constantly evolving. Numerous quantum mechanical theories have been developed in the early part of the twentieth century. However, due to the complex mathematical nature of the theories, substantial data processing power was required to either validate the theories or use them to understand numerous quantum mechanical aspects of atoms or molecules. However, with the advent of the digital computer, computational chemistry has taken a major leap forward in terms of its application. The postulates and theorems of quantum mechanics can now be applied with much success to predict numerous physical or chemical properties of any atomic or molecular system.

Fundamental postulates of quantum mechanics state that the physical or chemical properties of any molecular system can be determined by predicting their "wave functions". In his seminal work in quantum mechanics, Heisenberg postulated that "it is impossible to predict with high accuracy and precision the position and momentum of a quantum particle simultaneously" (Ebbing and Gammon, 2007). In the backdrop of this quantum uncertainty, which later became known as "Heisenberg's uncertainty principle", the concept of electronic wave functions became prominent as postulated by Erwin Schrodinger (Ebbing and Gammon, General Chemistry *in* Quantum Theory of Atom, 2007). Schrodinger in his "wave equation" provided a mathematical proof to predict the probability of finding any quantum particle at any given point in time. By solving the "wave equation" and thereby by predicting the wave functions of a particular molecular system, numerous physical and chemical attributes can be predicted such as structure, potential energy surface, electron density, electrostatic potential and partial atomic charges.

In order to determine any attribute of a molecule using computational chemistry, one has to determine the molecule's lowest energy conformation, a conformation in which the spatial positions of all atoms in the molecule will amount to the lowest possible potential energy. Potential energy of a molecule is defined as the energy required to separate it into its constituent nuclei and electrons, all infinitely separated from one another and at rest. This is accomplished by constructing a potential energy surface (PES) by taking into account all the possible conformations of a given structure. Thus, PES is the potential

energy of the surface approximation of a collection of atoms over all possible atomic arrangements or spatial conformations. The PES is constructed by solving Schrodinger's wave equation, however, since, Schrodinger's wave equation by nature is very complex to solve (especially for large molecules), Born-Oppenheimer approximation has to be invoked to make the calculations relatively simplistic without compromising heavily on accuracy. In Born-Opperheimer approximation, energy and wavefunction of a molecule is calculated in two steps; in the first step the electronic Schrodinger equation is solved, yielding a wavefunction that is dependent on electrons only. During this calculation the nuclei are fixed in the equilibrium configuration. In the second step, the electronic wavefuntions calculated in the first step are used as a potential in a Schrodinger equation containing only the nuclei.

Despite the efficacy of Born-Opperheimer approximation in simplifying calculations when using Schrodinger wave equation, the accuracy of the approximation might not be satisfactory for many-body systems (like many electron systems). In cases such as these, density functional theory (DFT) has garnered wide spread use and acclaim over the past 20 years for its accurate quantum mechanical simulations of many body systems. Density functional theory simply provides an alternate approximate solution to the Schrodinger wave equation of a many-body system. According to DFT the electron density of a molecule (expressed as a functional of space and time) can be useful in predicting all its ground state properties (Hohenberg and Kohn, 1964). Some of the ground state parameters that are important for the current research are electron density, partial atomic charges (mulliken charges) and electrostatic potentials (ESP) (Figure 15). Electrostatic potential maps, also known as electrostatic potential energy maps, illustrate the charge distributions of molecules three dimensionally. Thus from an ESP map we not only can infer charge distribution but can also infer size and shape of any given molecule. By employing DFT to calculate various ground state characteristics, we hypothesize that we can better understand the electronic properties of isoflavones, which is important in understanding their reactivity preferences, which will be helpful in determining the conditions for the synthesis of appropriate deuterated standards. These standards will

potentially improve the accuracy of the currently employed IDMS method for isoflavone analysis.

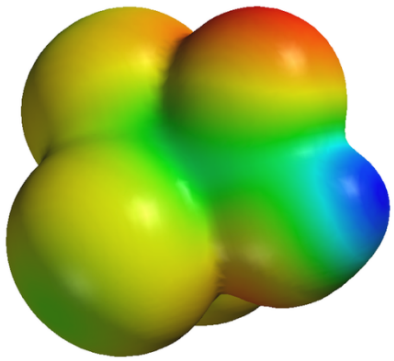

Figure 15: Electrostatic potential map of trichloro acetic acid (chemwiki.usdavis.edu)

1.7. Bioavailability of isoflavones

Bioavailability is defined as the "rate and extent at which the active ingredient or active moiety is absorbed from a drug product and becomes available at the site of action" (21CFR 320.1[a]). Thus, understanding the bioavailability of isoflavones is critical in predicting their potential physiological effects. *In-vivo* metabolism of isoflavones is depicted in Figure 16. Glucosides (both non-conjugated and conjugated forms) are poorly absorbed in the small intestine, due to their high molecular weight and hydrophilic nature (Liu and Hu, 2002). However, aglycones are easily absorbed through passive diffusion across the intestinal brush border, due to their hydrophobic nature and low molecular weight (Xu et al., 1995). Hence, hydrolysis of glucosides (both non-conjugated and conjugated forms) to aglycones is a prerequisite for efficient absorption of isoflavones through the small intestine (Scalbert and Williamson, 2000). Based on these findings, efforts have been made to produce aglycone-enriched soy products through enzymatic fermentation. However, enhancement in the aglycone concentration lead to a negative impact on the sensory attributes of the soy-derived products, primarily inducing off-flavors and bitter taste (Matsuura and Obata, 1993). Further research confirmed that glucosides can be hydrolyzed into aglycones in the small intestine by the action of glucosidase enzyme secreted by the intestinal microflora (Scalbert and

Williamson, 2000), and subsequently get absorbed. More studies were done to compare the bioavailability of isoflavones when ingested directly as aglycones or in the form of glucosides. Setchell et al. (2001) confirmed that the bioavailability of isoflavones was greater when ingested as glucosides contradicting the results of Izumi et al. (2000). On the other hand, Zubik and Meydani (2003) reported that the bioavailability of genistein and daidzein were not different when ingested either in the form of glucoside or aglycone. A logical explanation to the contradictory results could be the use of different sources of isoflavones. Setchell et al. (2001) compared the bioavailability of pure non-conjugated glucosides to pure aglycones. On the other hand, Izumi et al. (2000) and Zubik and Meydani (2003) compared the bioavailability of a mixture of both conjugated as well as non-conjugated glucosides with pure aglycones. Hence, the profile of the glucoside group that was compared to the aglycone group was different in each case, which most likely affected the results.

An *in vitro* study showed that the glucosidase enzyme is not effective in cleaving the glucose moiety of the conjugated glucosides (Ismail and Hayes, 2005). The glucosidase enzyme did not recognize the site of action or was hindered from cleaving the glucose, due to the bulky acetyl or malonyl group conjugated at the 6" carbon of the glucose moiety. This observation is of particular significance in soy foods that contain a high percentage (up to 63%) of conjugated isoflavones. Apart from this *in vitro* study, there has been no confirmatory *in vivo* work done to compare the bioavailability of non-conjugated vs. conjugated glucosides.

The obscurity in predicting the effect of chemical structure on isoflavone bioavailability can be largely attributed to variations in food matrix, inter-individual metabolism, gut microflora, and diet (Turner et al., 2003). However, lack of accurate profiling of the ingested isoflavone forms is often behind inconsistent conclusions. Investigators who had performed isoflavone bioavailability experiments often did not discuss their dietary compositions (Rufer et al., 2008; Faughan et al., 2004; Sepehr et al., 2009) and thus did not specify whether the β-glucosidic forms were conjugated and/or non-conjugated β-glucosides (Izumi et al., 2000; Faughan et al., 2004; Sepehr et al., 2009; Richelle, et al., 2002). Further, the comparison between β- glucosidic forms and

aglycones was not always done on an equimolar basis. Therefore, it is imperative to differentiate the bioavailability of conjugated glucosides, namely malonylglucosides from that of their non-conjugated counterparts. Although, malonylglucosides are abundant in many popular soy products (upto 80%), no attempt was made to determine their in-vivo bioavailability, and hence there is an urgent need to determine the in-vivo bioavailability of malonylglucosides in order to better understand the overall isoflavone bioavailability.

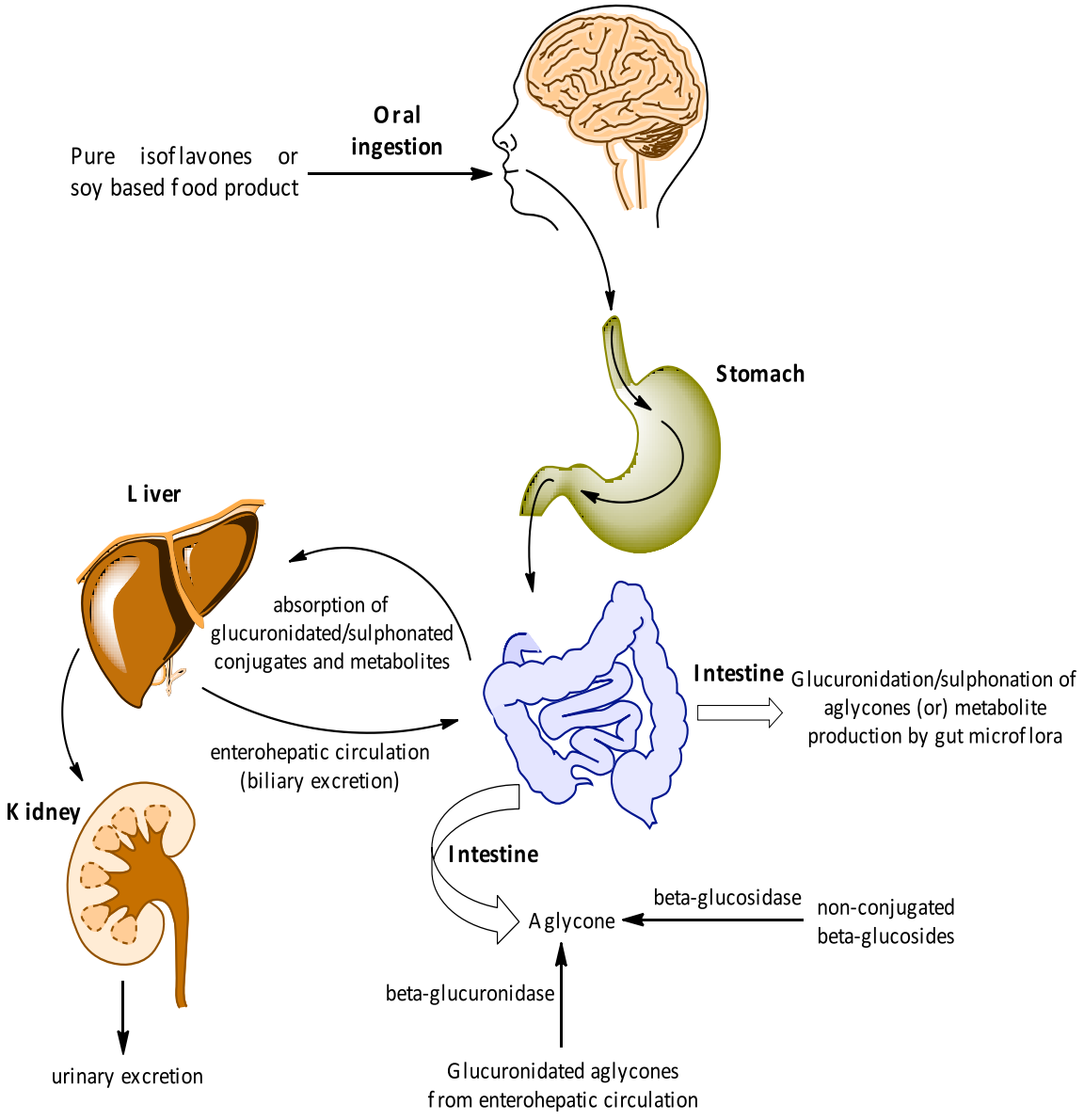

Figure 16: Metabolism of isoflavones.

1.8. Limitations of current isoflavone research

Despite the controversy in clinical research related to isoflavones, the evidence of their physiological benefits remains overwhelming. Also, although there has been some research indicating some adverse health effects of isoflavones, there is almost no credible evidence to suggest that traditional soy foods exert clinically relevant adverse effects in healthy individuals when consumed in amounts consistent with Asian intake (Messina, 2010). However, the extent of controversy posed great concerns, which a number of recent review articles have addressed (Patisaul et al., 2010; Mortensen et al., 2009). The reviews provided a wide range of reasons and limitations in clinical and animal studies that could have caused mixed and often conflicting results. These include many factors such as variations in ethnic background, age, gender, gut microflora and source of isoflavones. Source of isoflavones can drastically affect the results, especially when different isoflavone forms are administered at different levels.

The NIH sponsored a scientific workshop in July 2009 with an aim to provide guidance for the next generation of soy isoflavone research. Summarized recommendations from this workshop were published recently in the Journal of Nutrition (Klein, et al., 2010). The authors stated that "If clinical studies are to be pursued, then study sponsors, investigators, reviewers, and journal editors need to ensure that the experimental designs are optimal and the studies properly executed."

The inadequate profiling of isoflavones, lack of standardization of the source of isoflavones (different soy matrices and supplements), and lack of standard analytical methods for profiling and quantifying isoflavones present in different soy matrices, were among the main highlighted limitation in isoflavone research. Linking assessment of the bioavailability, including rate of absorption, of the administered isoflavones to their anticipated bioactivity was recommended for accurate conclusions. The choice of dosage administered in animal studies has to be relevant to human consumption. Use of an isotopically labeled internal standard was called upon for better method accuracy and traceability.

Our project was designed to investigate the bioavailability of the most abundant isoflavone forms taking into account the highlighted recommendations pertaining to accurate isoflavone profiling, bioavailability, reliable analytical techniques and relevant dosage.

2. DETECTION AND STRCUTURAL CHARACTERZIATION OF THERMALLY GENERATED MALONYLGLUCOSIDE DERIVATIVES IN BUFFER AND SOYMILK SYSTMES

* Contents of this chapter are published in Journal of Agricultural and Food Chemistry

Vamsidhar, Y.; Mathias, K.; Bunzel, M.; Ismail, B. 2011, *J. Agric. Food Chem.,* 59, 174-183.

2.1. Overview

Malonylglucoside isomers were identified by high performance liquid chromatography with mass spectrometric/ultraviolet detection and NMR. Two positional or stereoisomers of malonylgenistin and malonyldaidzin, showing similar UV-spectra and molecular weights yet different fragmentation patterns, were detected. In the proton spectra of malonylglucosides and their isomers, minor differences were observed in the glucose region. Heteronuclear multiple-bond correlation spectroscopy experiments showed a downfield shift of the H-4" proton of glucose in the isomer spectra, whereas, a downfield shift of H-6" proton was noted in the malonylglucoside spectra. Thus, NMR characterization of the malonylglucoside isomers revealed its structure to be 4"-*O*-malonylglucosides, suggesting a malonyl migration from the glucose-6-position to the glucose-4-position. The malonylgenistin isomer formation and interconversions were monitored in a soymilk system subjected to various heat treatments. The malonylgenistin isomer represented 6-9 % of the total calculated genistein content in soymilk heated at 100°C for various periods of time. Disregarding the content of malonylglucoside isomers in processed soy matrices can lead to erroneous results and misinterpretation of their biological contributions.

2.2. Introduction

Each of the genistein, daidzein, and glycitein isoflavones exist in up to four different forms, namely the aglycone, the non-conjugated glucoside, the acetylglucoside, and the malonylglucoside (Figure 17A). The effect of their chemical structures on bioavailability and physiological contributions is not fully understood yet. However, it is well agreed upon that the total amount of the biologically relevant isoflavones is one of the main determinants of the physiological benefits of soy products. Therefore, identifying the fate of isoflavones upon processing is essential for the accurate determination of their total content in the final product.

Processing conditions, namely pH, temperature, and time, have a substantial influence on the profile of isoflavones (Kudou et al., 1991), mainly converting the malonylglucosides to their more heat-stable non-conjugated β-glucosides (Barnes, et al., 1994; Wang et al., 1996; Coward et al., 1998). Malonylglucosides are the most abundant and the most thermally labile isoflavone forms (Wang, et al., 1996; Murphy, et al., 2002). In addition to interconversions between isoflavone forms, processing can also result in "loss" in the total amount of isoflavones. Measured losses of isoflavones were usually assumed to be a result of leaching into waste stream (Setchell, K. D. R., 1998; Henderich and Murphy, 2001; Jackson, et al., 2002), dissolving in aqueous alcohol solutions used in the production of certain soy products like soy protein concentrates and isolates (Coward, et al., 1993), or binding to the protein matrix (Barnes, et al., 1994; Murphy, et al., 2002). Jackson et al. (2002) observed a 65% loss in the total amount of isoflavones after processing raw soybeans. Although mass balance studies explained some of the loss, about 20% loss remained unexplained (Jackson et al., 2002). Further studies showed that isoflavone losses upon processing are potentially attributed to complete degradation (Xu et al., 2002; Park et al., 2002; Chein et al., 2005), and/or derivatization of isoflavones in a way that cannot be detected following standard analytical approaches. Thermal processing at elevated pH caused up to 30% and 15% loss in the form of undetectable degradation products in closed buffered (Mathias, et al., 2006) and soy systems (Nufer et al., 2009) systems, respectively.

While it is still debatable whether or not interconversions between known isoflavone forms affect bioavailability, undetected derivatives are labeled as "loss" and are thus assumed to have no biological relevance. We have recently detected derivatives of malonylglucosides formed upon heating at neutral and alkaline pH conditions (Yerramsetty Vamsidhar, MS thesis; Yerramsetty et al., 2011). These derivatives constitute part of the calculated loss in total isoflavones reported previously (Xu et al., 2002; Mathias et al., 2006; Nufer et al., 2009). The detected derivatives were deduced to be isomers of malonylglucosides based on liquid chromatography (LC) coupled with mass spectrometry (MS) analysis. The isomers had identical UV wavescan and molecular mass, and had similar fragmentation spectra when compared with malonylglucosides. Careful examination of the chromatograms presented by various researchers, investigating the isoflavone content in soybeans and various soy products, revealed the presence of these malonylglucoside isomers, however they were not discussed (Figure 5 and 6) (Barnes, et al., 1994; Wang and Murphy, 1994; Song, et al., 1998). Since, chemical structure plays an important role in determining isoflavone bioavailability, complete structural elucidation of the isomers is necessary to determine their physiological relevance.

Reported MS analysis of isoflavones indicated the presence of malonylglucoside isomers in soybeans and various soy based foods (Edwards et al., 1997; Griffith et al., 2001; Gu and Gu, 2001). Griffith and Collision (2001) also observed the formation of the isomers in standard solutions of malonylglucosides left at room temperature for several hours. Our recent work demonstrated that malonylglucosides convert to their isomeric forms when subjected to various processing conditions in model buffer systems (Yerramsetty et al., 2011). The extent of conversion was a function of the processing parameters employed. We also demonstrated that the isomers are thermally unstable and rapidly convert back to known isoflavone forms, namely malonylglucosides and their non-conjugated β-glucosides. The isomer conversion mechanism can be affected by the presence of soy protein in complex systems (Malapally and Ismail, 2010). There is no work done to characterize the formation and degradation of these isomers upon processing of soy based products. Disregarding the isomer's content can lead to erroneous results when calculating % loss in total isoflavones upon processing of soy products.

Therefore, the objective of this work is twofold: 1) Detect, identify and fully elucidate the structures of malonylglucoside isomers using an array of 1D and 2D NMR techniques; 2) Monitor the formation and conversion of malonylgenistin isomer during thermal processing in a soymilk system.

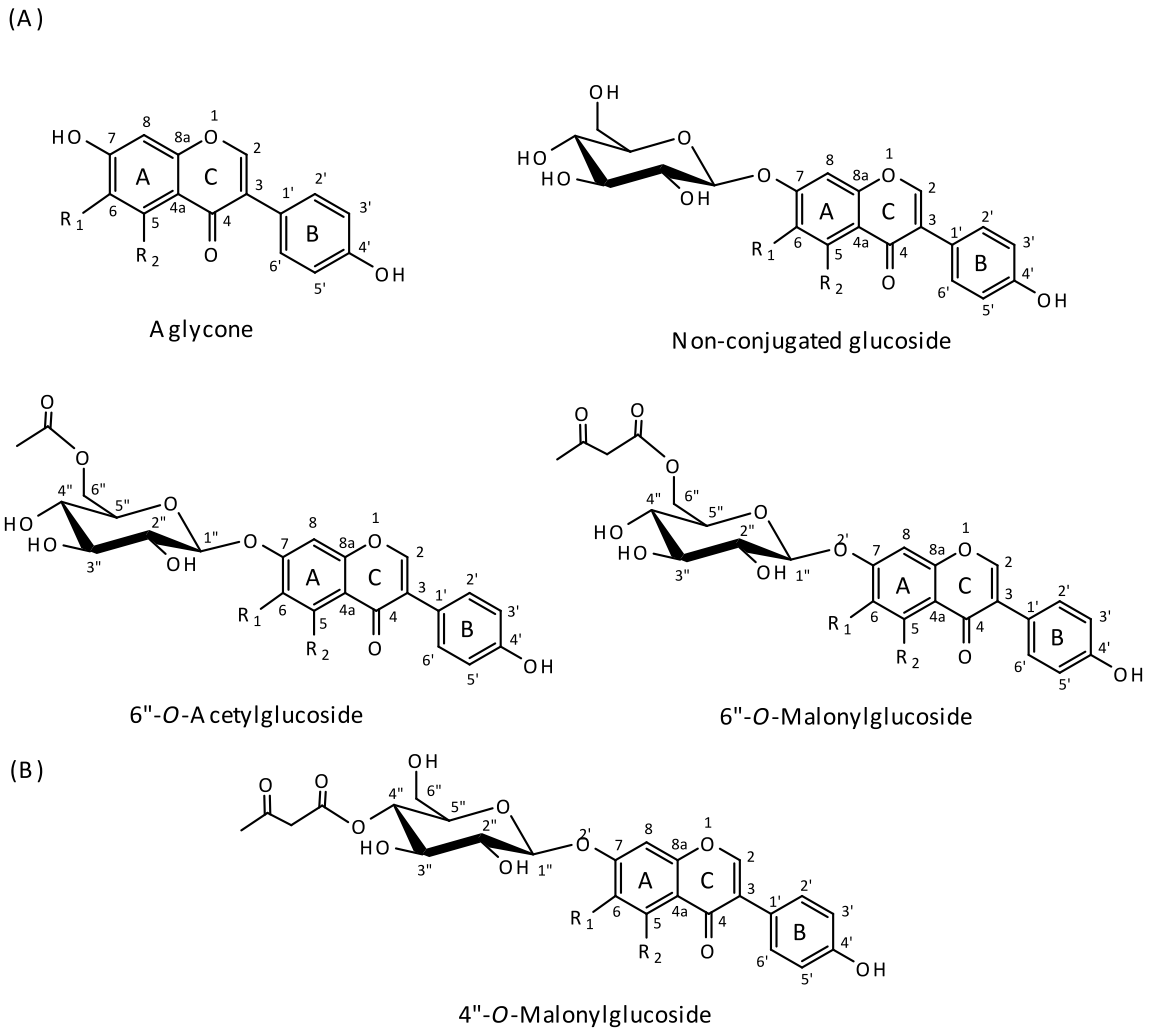

Figure 17: (A) Structures and numbering of the 12 known isoflavones categorized as aglycone, non-conjugated glucoside, acetylglucoside, and malonylglucoside. R1 can be -H in the case of daidzin and genistin or -OCH_3 in the case of glycitin, while R2 can be -H in the case of daidzin and glycitin or -OH in the case of genistin. (B) Structures and numbering system of 4''-*O*-malonylglucosides (malonylglucoside isomers)

2.3. Material and methods

2.3.1 Materials

High performance liquid chromatography (HPLC) grade acetonitrile and methanol (MeOH) were purchased from Fisher Scientific (Hanover Park, IL). Isoflavone standards malonyldaidzin, acetyldaidzin, acetylgenistin, malonylglycitin, and acetylglycitin were purchased from Wako Chemicals (Richmond, VA); genistein, genistin, malonylgenistin, daidzein, and daidzin were purchased from LC Laboratories (Woburn, MA); and glycitin and glycitein were purchased from Indofine Chemical Company (Hillsborough, NJ) (Table 1). Standard solutions (500 mg/L) were prepared using 80% (v/v) aqueous MeOH. Soy grits were kindly provided by Soylink (Product number: 27707-006, Oskaloosa IA).

Table 1. Purchased isoflavone standards

Isoflavone	Catalogue number	Company
Malonyldaidzin (>90%)	132-13821	Wako Chemicals
Acetyldaidzin (>90%)	013-1880	Wako Chemicals
Daidzin (>99%)	D-7878	LC labs
Daidzein (>99%)	D-2946	LC labs
Malonylgenistin (>98%)	M-8090	LC labs
Acetylgenistin (>90%)	010-18811	Wako Chemicals
Genistin (>99%)	G-5200	LC labs
Genistein (>99%)	G-6055	LC labs
Malonylglycitin (>90%)	139-13831	Wako chemicals
Acetylglycitin (>90%)	010-18791	Wako chemicals
Glycitin (>99%)	GL-002N	Indofine chemical company
Glycitein (>99%)	GL-001N	Indofine chemical company

2.3.2. Extraction of isoflavones from soy grits

Ground soy grits, containing the isomers of interest, were used to extract isoflavones using 53% (v/v) aqueous acetonitrile solution, as outlined by Murphy et al. (2002) and Malapally and Ismail (2010), with some modifications. Briefly, 0.05 gm of sample was weighed and mixed with 9 mL of deionized distilled water (DDW), followed by the addition of 10 mL acetonitrile. The samples then were stirred (400 rpm) at room temperature (23°C) for 2 h. After 2 hours of thorough mixing, extracts were centrifuged at 13,750 x g for 10 min at 15°C, and the supernatant was filtered through Whatman no. 42 filter paper. Acetonitrile was evaporated using a rotary evaporator at 37°C for 15 min. Subsequently, solid phase extraction (SPE) was used to extract isoflavones from the aqueous concentrated extract. Isoflavones were extracted using a Waters 500 mg Sep-Pak®Cl8 cartridge system (Waters Associates, Milford, MA) following a retention-cleanup-elution strategy. Briefly, Sep-Pak®Cl8 cartridges were preconditioned with 3 mL of 80% aqueous methanol (MeOH), followed by 3 mL of DDW. An aliquot (2 mL) of the sample was then passed through the cartridges at a flow rate of 5 mL/min, followed by rinsing with 3 mL DDW. Finally, isoflavones were recovered by passing 2 mL of 80% aqueous MeOH. The concentrated extracts were stored at -20°C in amber glass bottles until further analysis.

2.3.3. Semi-preparative isolation of the malonylglucosides and their isomers

To isolate the isomers of interest on a semi-preparative scale, a Shimadzu HPLC system equipped with SIL-10AF auto injector, two LC-20AT high pressure pumps, SPD-M20A photo diode array detector (PDA) and a CTO-20A column oven was used. The column used was a 250 mm x 10 mm i.d., 5 µm, YMC pack ODS AM-12S RP-18 column, with a 10 mm x 10 mm guard column of the same material (YMC pack ODS AM). The separation method outlined by Ismail and Hayes (2005) was modified by calculating a scale-up factor to ensure the same linear velocity of the mobile phases as used in the analytical run. The calculated flow rate after scale-up was 3.5 mL/min. An aliquot (300 µL) of the isoflavone extract was filtered through a 0.45 µm syringe filter and injected onto the column. A linear HPLC gradient was used: Solvent A was HPLC grade water, and solvent

B was acetonitrile, both containing 0.1% (v/v) glacial acetic acid. The initial gradient concentration was 15% solvent B, which was linearly increased to 18% in 25 min, kept constant for 5 min, linearly increased to 30% in 10 min, kept constant for 3 min, linearly increased to 90% in 2 min, and kept constant for 8 min, followed by column equilibration steps. The temperature was maintained at 45°C. Absorbance spectra were monitored over a UV wavelength range of 190-370 nm. Isoflavones and isomers were efficiently separated (Figure 18). The fractions containing malonylgenistin isomer and that containing malonyldaidzin isomer were collected and lyophilized. Several runs were performed and the obtained fractions of each isomer of interest were pooled. A portion of the lyophilized fraction was diluted with 80% (v/v) aqueous MeOH to prepare a standard solution of each isomer (~120 mg/L) and its identity was confirmed using HPLC/tandem mass spectrometry as described below. The remaining fractions were stored at -80ºC for further analysis using NMR analysis. The same separation procedure was employed to isolate malonylgenistin and malonyldaidzin for NMR analysis.

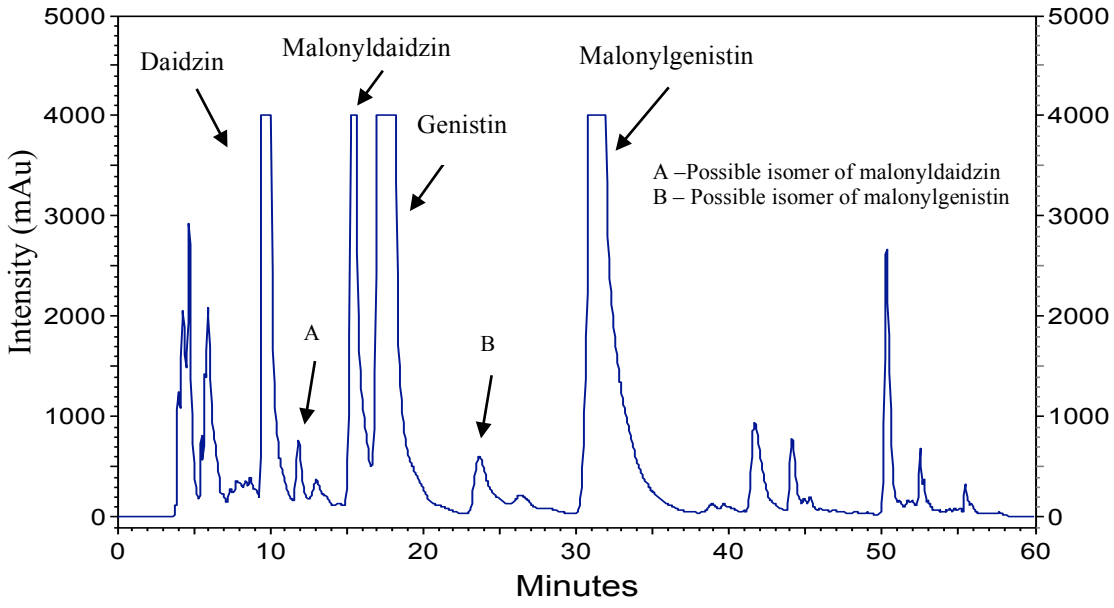

Figure 18. Chromatogram showing separation of malonylglucosides and their respective isomers.

2.3.4. HPLC/Tandem mass spectrometry (MS/MS) confirmation analysis of the isolated isomers

Identity and purity of the isomers were confirmed using liquid chromatography-tandem mass spectrometry (LC/MS/MS) analysis. Solutions (20 mg/L) of malonylglucosides and their respective isomers were analyzed by HPLC/MS/MS. A Spectra system P4000 HPLC system consisting of a SN 4000 model quaternary pump and a UV 600LP type photo diode array detector was used to analyze the isoflavones. The column used was a 250 mm x 4.6 mm i.d., 5 μm, YMC pack ODS AM-303 RP-18 column, with a 20 mm x 4 mm guard column of the same material (YMC pack ODS AM). Two linear HPLC gradients were used, one for the analysis of malonylgenistin isomer and the other for the analysis of malonyldaidzin isomer. Solvent A was HPLC grade water, and solvent B was acetonitrile, both containing 0.1% (v/v) glacial acetic acid. For separation of malonylgenistin and its isomer, the initial gradient concentration was 18% solvent B, which was kept constant at 18% for 40 min, linearly increased to 30% in 5 min, kept constant for 10 min, followed by column equilibration steps. For separation of malonyldaidzin and its isomer, the initial gradient concentration was 11% solvent B, which was linearly increased to 14% in 30 min, kept constant for 5 min, linearly increased to 30% in 10 min, kept constant for 10 min, followed by column equilibration steps. The flow rate was set at 0.8 mL/min and temperature was maintained at 45°C for both separation methods. Absorbance spectra were monitored over a UV wavelength range of 190-370 nm. The eluate from the HPLC column was split and 10% of the flow was passed into electrospray ionization (ESI) interface of a LCQ classic mass spectrometer (ion trap analyzer, ThermoElectron, CA, USA). The ionization conditions were as follows: heated capillary temperature 225°C; sheath gas (N_2, 99.99%, flow rate = 7.25 l/h); nebulizing pressure = 73.5 psi; spray voltage 4 kV; capillary voltage 16.7 V; positive ion spectra were recorded over an m/z range of 150-1000. Tandem mass spectrometry was employed to study the fragmentation pathway of the new derivatives as well as the known isoflavone forms. The precursor ions ($[M+H]^+$) were isolated and analyzed by collision-induced dissociation with 100% helium as the collision gas, and the daughter ion spectra were recorded. The relative collision energies were set to a value at

which ions of interest were produced in measurable abundance (varying from 9 to 31% in increments of 2).

2.3.5. NMR analysis of the malonylglucosides and their isomers

NMR experiments were carried out on a Bruker 700 MHz Avance spectrometer (Rheinstetten, Germany) equipped with a 5 mm TXI proton-enhanced cryoprobe. Structure identification was performed by using the usual array of one- and two-dimensional NMR experiments (1H, H,H-COSY, HSQC, HMBC). Carbon data were taken from the less time-consuming 2D experiments HSQC and HMBC instead of performing 1D 13C experiments. 6”-*O*-malonylgenistin (Figure 1A) was measured in MeOH-d_4 and dimethylsulfoxide (DMSO)-d_6; the malonylgenistin isomer (4”-*O*-malonylgenistin, Figure 1B) was measured in MeOH-d_4 only; 6”-*O*-malonyldaidzin (Figure 1A) and the malonyldaidzin isomer, (4”-*O*-malonyldaidzin, Figure 1B) were measured in (DMSO)-d_6. Chemical shifts (δ) were referenced to the central solvent signals (MeOH-d_4: δH 3.31 ppm, δC 49.0 ppm; DMSO-d_6: δH 2.50 ppm, δC 39.5 ppm (Gottlieb, et al., 1997)). J-values are given in Hz. NMR assignments follow the numbering shown in Figure 1.

6’’-*O*-malonylgenistin (700 MHz, DMSO-d_6): malonylated β-D-glucose: H1’’: 5.12 (d, J = 7.7 Hz); H2’’: 3.28, H3’’: 3.33; H4’’: 3.19 H5’’: 3.75, H6’’: 4.35, 4.12, malonyl-CH_2: 3.37; aglycone: H1: 8.40 (s), H6: 6.46 (s), H8: 6.71 (s), H2’/H6’: 7.39 (d, J = 8.1 Hz), H3’/H5’: 6.83 (d, J = 8.1 Hz). (176 MHz, DMSO-d6): malonylated β-D-glucose: C1’’: 99.3, C2’’: 72.7, C3’’: 76.1, C4’’: 69.4, C5’’: 73.6, C6’’: 63.9, malonyl-COOR: 167.0, malonyl-CH_2: 41.6, malonyl-COOH: 167.5; aglycone: C2: 154.6, C3: 122.5, C4: 180.5, C4a: 106.0, C5: 162.2, C6: 99.4, C7: 162.6, C8: 94.3, C8a: 157.1, C1’: 120.9, C2’/C6’: 130.2, C3’/C5’: 115.0, C4’: 157.4.

6’’-*O*-Malonylgenistin (700 MHz, MeOH-d_4) (n.d. – not determined): malonylated β-D-glucose: H1’’: 5.03 (d, J = 7.4 Hz); H2’’: 3.50, H3’’: 3.50, H4’’: 3.30, H5’’: 3.77, H6’’: 4.55, 4.27, malonyl-CH_2: n.d.; aglycone: H2: 8.15 (s), H6: 6.51 (s), H8: 6.71 (s), H2’/H6’: 7.40 (d, J = 8.2 Hz), H3’/H5’: 6.85 (d, J = 8.2 Hz). (176 MHz, MeOH-d4): malonylated β-D-glucose: C1’’: 101.0, C2’’: 74.2, C3’’: 77.1, C4’’: 70.9, C5’’: 75.1,

C6’’: 64.8, malonyl-COOR: 168.7, malonyl-CH_2: n.d, malonyl-COOH: n.d.; aglycone: C2: 155.0, C3: 124.1, C4: 182.1, C4a: 107.9, C5: 163.6, C6: 100.7, C7: 164.1, C8: 95.5, C8a: 159.0, C1’: 122.4, C2’/C6’: 130.8, C3’/C5’: 115.7, C4’: 158.5.

4’’-*O*-Malonylgenistin (700 MHz, MeOH-d_4): malonylated β-D-glucose: H1’’: 5.13 (d, J = 7.7 Hz); H2’’: 3.58, H3’’: 3.75, H4’’: 4.90, H5’’: 3.75, H6’’: 3.78, 3.62, malonyl-CH_2: n.d.; aglycone: H2: 8.16 (s), H6: 6.54 (s), H8: 6.73 (s), H2’/H6’: 7.40 (d, J = 8.2 Hz), H3’/H5’: 6.85 (d, J = 8.2 Hz). (176 MHz, MeOH-d4): malonylated β-D-glucose: C1’’: 100.9, C2’’: 74.2, C3’’: 75.5, C4’’: 72.3, C5’’: 75.5, C6’’: 61.5, malonyl-COOR: 169.0, malonyl-CH_2: n.d, malonyl-COOH: n.d.; aglycone: C2: n.d., C3: 125.0, C4: n.d., C4a: 108.0, C5: 164.0, C6: 100.7, C7: 164.6, C8: 95.4, C8a: 159.1, C1’: 122.9, C2’/C6’: 131.0, C3’/C5’: 115.9, C4’: 158.8.

6’’-*O*-Malonyldaidzin (700 MHz, DMSO-d_6): malonylated β-D-glucose: H1’’: 5.14 (d, J = 7.1 Hz); H2’’: 3.33, H3’’: 3.29, H4’’: 3.22, H5’’: 3.75, H6’’: 4.37, 4.10, malonyl-CH_2: 3.35; aglycone: H2: 8.36 (s), H5: 8.06 (d, J = 8.9 Hz), H6: 7.14 (d, J = 9.0 Hz), H8: 7.23 (s), H2’/H6’: 7.40 (d, J = 8.4 Hz), H3’/H5’: 6.82 (d, J = 8.4 Hz). (176 MHz, DMSO-d_6): malonylated β-D-glucose: C1’’: 100.2, C2’’: 72.7, C3’’: 76.9, C4’’: 70.2, C5’’: 74.5, C6’’: 64.5, malonyl-COOR: 167.0, malonyl-CH2: 42.7, malonyl-COOH: 169.6; aglycone: C2: 154.5, C3: 124.2, C4: 175.5, C4a: 118.9, C5: 128.1, C6: 115.5, C7: 161.8, C8: 104.2, C8a: 157.8, C1’: 122.7, C2’/C6’: 131.2, C3’/C5’: 115.2, C4’: 157.8

4’’-*O*-Malonyldaidzin (700 MHz, DMSO-d_6): malonylated β-D-glucose: H1’’: 5.24 (d, J = 7.2 Hz); H2’’: 3.41, H3’’: 3.12, H4’’: 4.62, H5’’: 3.38, H6’’: 3.77, 3.58, malonyl-CH_2: 3.88; aglycone: H2: 8.40 (s), H5: 8.06 (d, J = 8.8 Hz), H6: 7.11 (d, J = 8.6 Hz), H8: 7.27 (s), H2’/H6’: 7.41 (d, J = 7.9 Hz), H3’/H5’: 6.82 (d, J = 8.0 Hz). (176 MHz, DMSO-d_6): malonylated β-D-glucose: C1’’: 100.0, C2’’: 73.3, C3’’: 46.1, C4’’: 71.8, C5’’: 61.8, C6’’: 74.9, malonyl-COOR: 170.1, malonyl-CH2: 56.5, malonyl-COOH: n.d.; aglycone: C2: 153.9, C3: 124.1, C4: 175.2, C4a: 118.5, C5: 127.9, C6: 116.0, C7: 162.1, C8: 104.0, C8a: 158.1, C1’: 123.9, C2’/C6’: 130.7, C3’/C5’: 115.2, C4’: 157.7

2.3.6. Preparation of soymilk

Soymilk was prepared from soy grits. Soy grits (13 lb) were ground in a grinder (MZM/VK7, Fryma, Switzerland) after addition of 7 parts of water (60°C). The insoluble portion (okara) was then removed using a desludger unit (9749, Westfalia Clarifier, Centrico Inc., New Jersey). The total solids content was adjusted to 7% by the addition of water. The pH of the soymilk was close to neutral.

2.3.7. Thermal treatment of soymilk

The heat treatment of soymilk was carried out in triplicate with time (5 levels) as the independent factor while the temperature was held constant at 100°C. Aliquots (2 mL) of soymilk were dispensed into 2 mL-glass ampoules that were sealed and placed in a water bath at 100°C (± 1°C) for 2, 5, 10, 30, or 60 min. The contents of the ampoules of each treatment were pooled, frozen at -20°C and lyophilized. A non-heated control sample was treated accordingly. The lyophilized samples and control were stored at -80°C until further analysis.

2.3.8. Extraction of isoflavones from soymilk

Isoflavones were extracted from lyophilized samples following the method outlined by Murphy et al. (2002), however, using 0.05 gm sample instead of 2 gm (Malapally and Ismail, 2010), and without acidification. Briefly, 0.05 gm of sample was weighed and mixed with 9 mL of deionized distilled water (DDW), followed by the addition of 10 mL acetonitrile. The samples then were stirred (400 rpm) at room temperature (23°C) for 2 h. The extract was subjected to centrifugation at a speed of 13,750 × g for about 10 min at 15°C and supernatant was filtered through Whatman no. 42 filter paper. Acetonitrile from filtrate was evaporated under vacuum using a rotary evaporator at 37°C for 15 min. The condensed extracts were re-dissolved in 80% methanol, placed in amber glass bottles and stored at -20°C until analyzed by HPLC.

2.3.9. HPLC/Ultra violet (UV) analysis

The Shimadzu HPLC system described in section 2.3.3 was used. The column used was a 250 mm x 4.6 mm i.d., 5 µm, YMC pack ODS AM-303 RP-18 column, with a 20 mm x 4 mm guard column of the same material (YMC pack ODS AM). Isoflavone analysis was achieved as outlined by Ismail and Hayes (2005) with minor modifications. A linear HPLC gradient at a flow rate of 1.2 mL/min was used: Solvent A was HPLC grade water, and solvent B was acetonitrile, both containing 0.1% (v/v) glacial acetic acid. The initial gradient concentration was 17% solvent B, which was linearly increased to 25% in 25 min, kept constant for 5 min, linearly increased to 30% in 10 min, kept constant for 10 min, followed by column equilibration steps. Column temperature maintained at 35°C and absorbance was monitored over a wavelength range of 190 - 370 nm. Integration for quantitation purposes was performed at 256 nm. A seven-point external calibration with standard solutions (0.1, 0.5, 1.0, 2.0, 4.0, 8.0, 10.0 mg/L) containing all 12 forms of isoflavones genistein, daidzein and glycitein was performed. Calibration curves are presented in Appendix A.

2.3.10. Statistical analysis

Analysis of variance (ANOVA) was carried out utilizing SPSS 15 for Windows (Vaidya, et al., 2010). When a factor effect or an interaction was found significant, indicated by a significant F test ($P \leq 0.05$), differences between the respective means (if more than 2 means) were determined using Tukey-Kramer multiple means comparison test.

2.4. Results and discussion

2.4.1. Identification and purity confirmation of malonylglucosides and their respective isomers using LC/MS/MS

Initial structural identification and verification of the purified malonylglucosides and their respective isomers was confirmed using LC/MS/MS. As reported earlier (Yerramsetty et al., 2011), the UV spectrum of the isomers was similar to that of their respective malonylglucosides with λ_{max} for malonyldaidzin and its isomer at 249 nm and for that of malonylgenistin and its isomer at 259 nm (Figure 19). Similar wavescan and λ_{max} confirmed that each malonylglucoside and its isomer share the same aromatic moiety, which is the aglycone. Liquid chromatography/MS data confirmed that the isomers had the same mass (502 for malonyldaidzin isomer and 518 for malonylgenistin isomer) as the quasi molecular ion of their respective malonylglucosides (Figure 20 and 21).

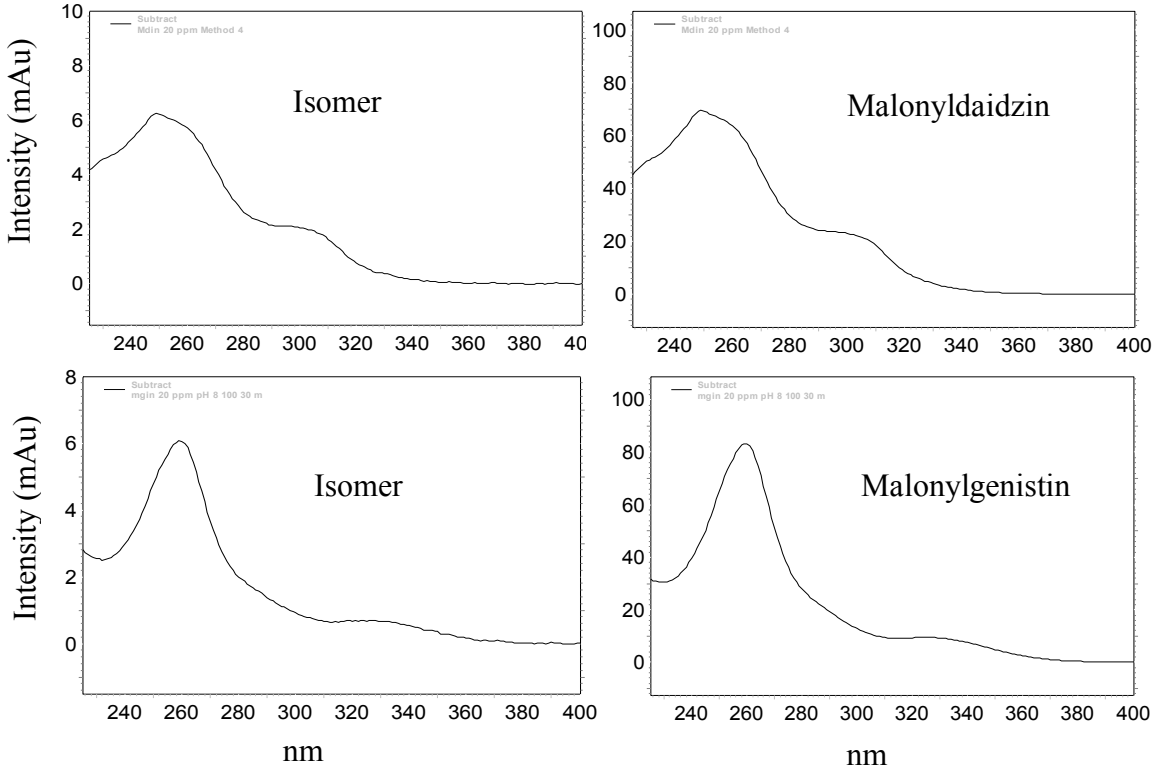

Figure 19: Wavescans of malonylglucosides and their respective isomers

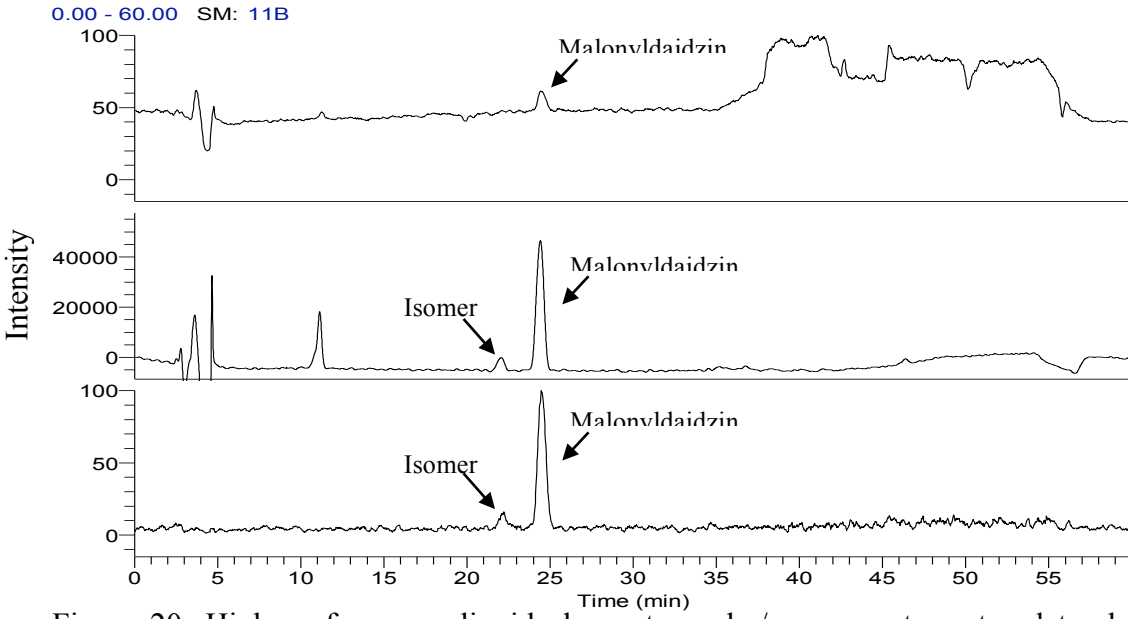

Figure 20: High performance liquid chromatography/mass spectrometry data showing that malonyldaidzin and its isomer have the same mass (502 Da). A) A) Total ion chromatogram (m/z range = 150 – 1000) B) UV/Vis spectrum (data collected at 256 nm) C) Extracted single ion spectrum with m/z = 503 Da

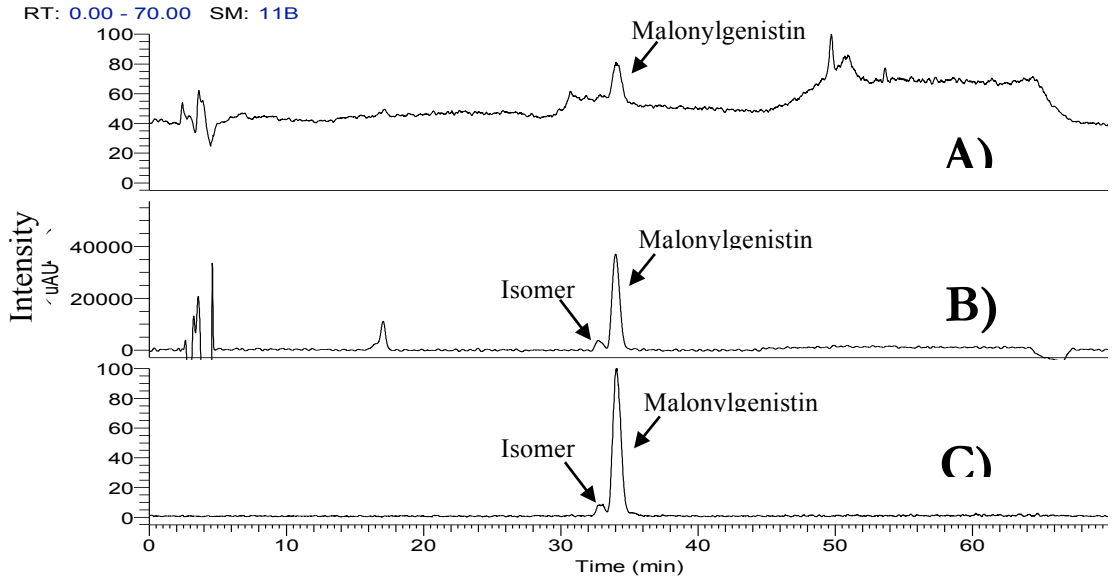

Figure 21: High performance liquid chromatography/mass spectrometry data showing that malonylgenistin and its isomer have the same mass (518 Da). A) Total ion chromatogram (m/z range = 150 – 1000) B) UV/Vis spectrum (data collected at 256 nm) C) Extracted single ion spectrum with m/z = 518 Da

Fragmentation patterns obtained after ESI-MS/MS analysis of the quasi molecular ions of the isomers and their respective malonylglucosides at various collision levels (17% and 20%) revealed the same differences (Figure 22 and 23) we have observed previously (Yerramsetty et al., 2011). The fragmentation spectra for both the isomer and malonylgenistin obtained at a collision level of 20% had a base peak of m/z = 271, corresponding to the protonated form of the aglycone genistein. However, the fragmentation spectrum of malonylgenistin had an ion with m/z = 433 (protonated form of genistin), which was absent in the fragmentation spectra of the isomer (Figure 22 A, B). Additionally, at a collision level of 17%, it was noted that the ion with m/z=271 was formed more readily from the precursor ion of the isomer as compared to that of malonylgenistin (Figure 22 C, D). The relative abundance of the 519 and 271 ions were 100 and 30, and 35 and 100, for the isomer and malonylgenistin, respectively. Similarly, the fragmentation spectra of both malonyldaidzin and its isomer obtained at a collision level of 20% had a base peak of m/z = 255 which corresponds to the aglycone daidzein. However, fragmentation spectrum of malonyldaidzin had two ions with m/z = 417 (protonated form of daidzin) and m/z = 459 (protonated form of acetyldaidzin) that were absent in the isomer fragmentation spectra obtained at the same collision level (Figure 23 A, B). Differences were also observed in the fragmentation spectra of malonyldaidzin and its isomer obtained at a lower collision level of 17%. The ion with m/z=271 was formed more readily from the precursor ion of the isomer as compared to that of malonyldaidzin (Figure 23 C, D). Thus, based on UV and LC/MS/MS analysis we were successfully able to confirm the identity of the purified isomers and their respective malonylglucosides.

Based on the LC/MS/MS data obtained, the isomers were thought to be either positional or stereoisomers of their respective malonylglucosides (Yerramsetty et al., 2011). It is hypothesized that isomerization is due to migration of the malonyl group from the *O*-6-glucose position to the *O*-4-glucose position. A similar isomerization was demonstrated for formononetin glucoside malonate (Rijke et al., 2004). The authors reported an isomer of 7-*O*-β-D-glucoside 6”-*O*-malonate in *Trifolium pretense* leaves and identified it as 7-*O*-β-D-glucoside 4”-*O*-malonate; i.e. they only differed in the substitution position of the malonate group on the glucoside ring. To validate our hypothesis NMR analysis was pursued for

complete structural elucidation of the isomers and determination of the type of isomerism they exhibited.

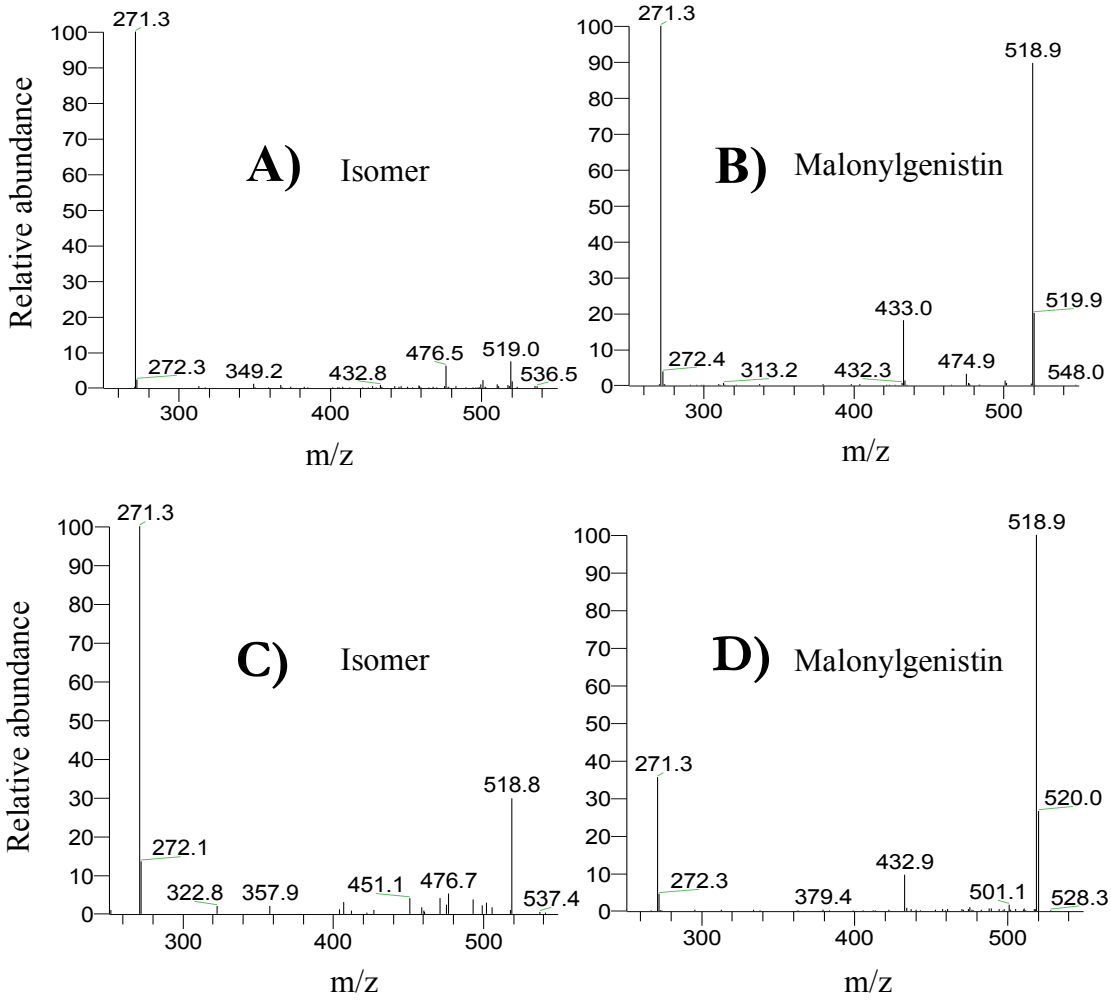

Figure 22: ESI-MS/MS analysis of the protonated forms of malonylgenistin and its isomer at various collision levels: (A) Isomer at 20%, (B) malonylgenistin at 20%, (C) isomer at 17%, and (D) malonylgenistin at 17%.

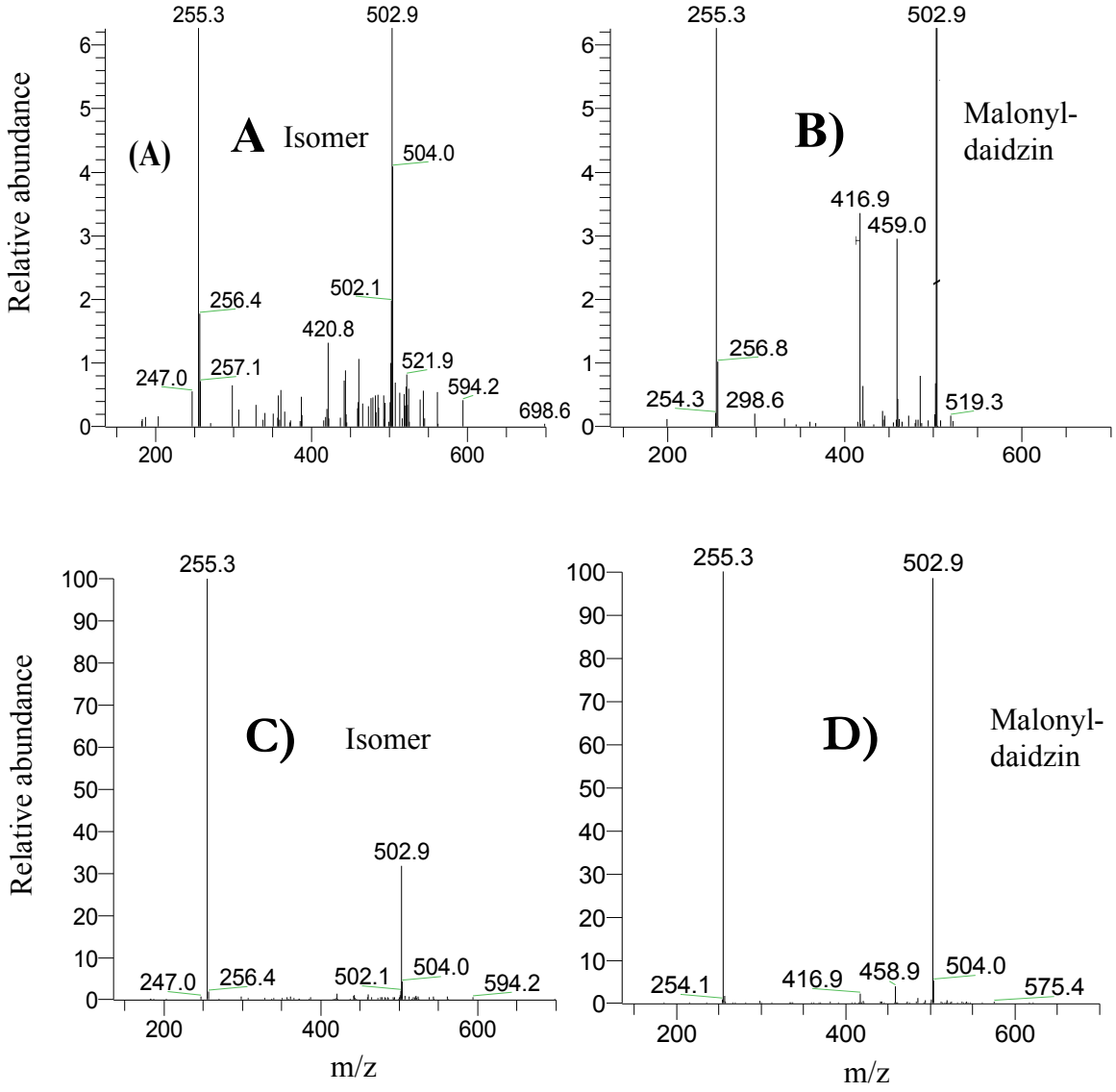

Figure 23: ESI-MS/MS analysis of the protonated forms of malonyldaidzin and its isomer at various collision levels: (A) Isomer at 20%, (B) malonyldaidzin at 20%, (C) isomer at 17%, and (D) malonyldaidzin at 17%

2.4.2. Structural elucidation of the malonylglucosides isomers by NMR

NMR data for malonylglucosides and their respective isomers were recorded in MeOH-d_4 and DMSO-d_6. The enhanced acidity of α-protons in β-dicarbonyls (keto-enol-tautomerization) leads to a proton-deuterium exchange in MeOH-d_4. As a result, the malonyl-CH_2 group was not detected using MeOH-d_4 as a solvent. However, using DMSO-d_6, which minimizes proton exchange, a whole NMR data set for malonylglucosides and their isomers was obtained.

In the proton spectra of both the isomer and malonylglucosides, the signals between 3.2 - 5.1 ppm originate from the glucose moiety and the signals between 6.5 - 8.2 ppm represent the aromatic protons. The coupling constant of the anomeric carbon (H1", δ = 5.03 ppm in MeOH-d_4) in all structures was ~7.93 Hz, which is expected from the β-anomer due to large axial-equatorial dihedral angle at the H-C1-C2-H bond. There were no differences between the proton signals in the aromatic range of malonylglucosides and their respective isomers (Figure 24). However, differences were noticeable in the glucose region implying that the structural change between the malonylglucoside and their isomers is confined to the glucose moiety thus complementing LC/MS/MS data.

Glucose proton signals were assigned using the H,H-COSY experiment. The linkage of the malonyl-group to the glucose 6-position in malonylgenistin was demonstrated by cross-peaks at 4.55 ppm/168.7 ppm and 4.27 ppm/168.7 ppm in the HMBC spectrum. Formation of an ester linkage at the glucose 6-position shifts the signals of the glucose 6-protons (4.55 and 4.27 ppm, Figure 25) and, although less dramatic, the 6-carbon (64.8 ppm) downfield, as also shown for 6"-*O*-acetylgenistin (Steuertz et al., 2006). The NMR spectra of the malonylgenistin isomer revealed its structure to be 4"-*O*-malonylgenistin (Figure 1B). The signal for the glucose 4-proton shifted downfield as did the glucose carbon-4 signal (Figure 25), indicating that the malonyl group is linked in this position. HMBC spectrum shows a weak cross peak at 4.90 and 169.0 ppm that, however, needs careful interpretation. Because the signal for the 4-glucose proton shifted extensively downfield (as also demonstrated in Rijke et al., 2004), it is located underneath the water signal, making this region rather prone to fragments in the HMBC spectrum. The removal of the malonyl group from glucose position 6 is well demonstrated by the upfield shift of the glucose-6 proton signals (Figure 25).

The NMR spectra of the malonyldaidzin isomer also revealed its structure to be 4”-*O*-malonyldaidzin (Figure 50, Appendix B). Heteronuclear multiple-bond correlation spectroscopy experiments indicated a downfield shift of the H-4” proton of glucose (δH-4” = 4.62) in the isomer spectra, whereas, a similar effect was observed for H-6” protons in malonyldaidzin (δH-6” = 4.37; 4.11). This indicated that the malonate group is present on the 4th carbon of the glucose moiety of the isomers as compared to 6th carbon of that of the malonyldaidzin (6”-*O*-malonyldaidzin).

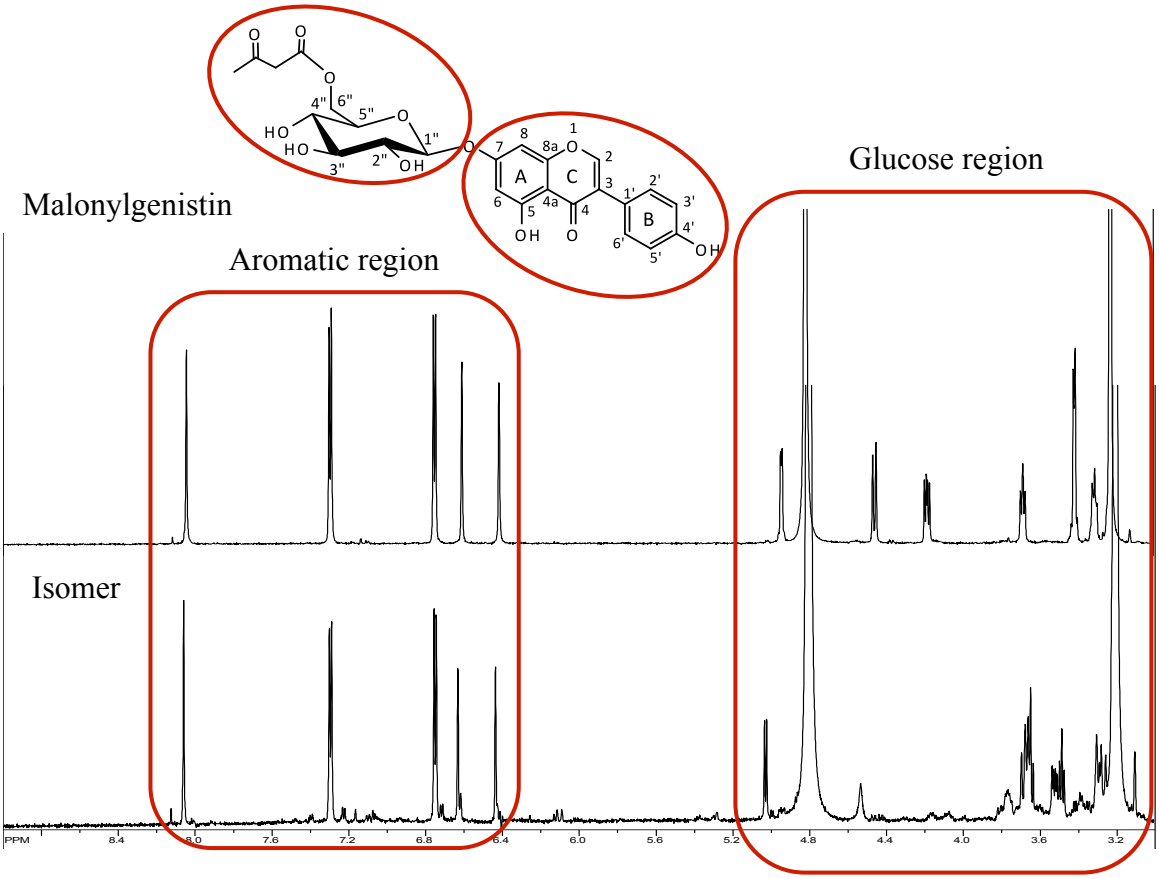

Figure 24: Proton NMR spectrum of malonylgenistin in MeOH-d_4. NMR experiments were carried out on a Bruker 700 MHz Avance spectrometer (Rheinstetten, Germany) equipped with a 1.7 mm TCI proton-enhanced cryoprobe

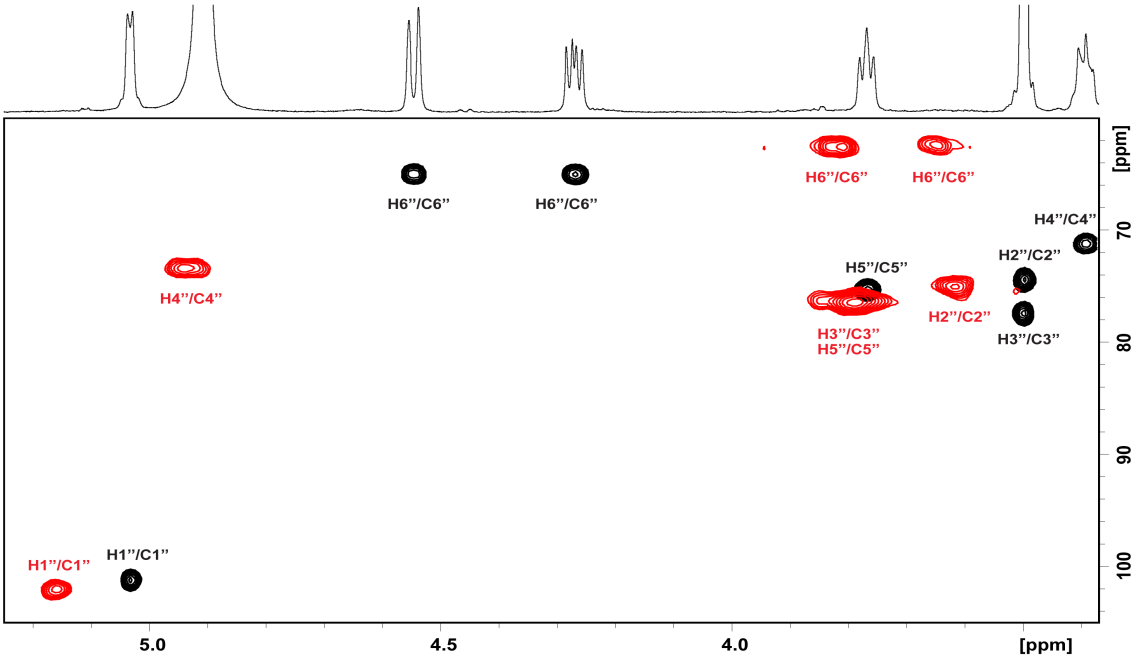

Figure 25: Overlay of the HSQC spectra (carbohydrate region) of malonylgenistin (6''-*O*-malonyl-genistin) (black cross peaks) and the malonylgenistin isomer (4''-*O*-malonyl-gensitin) (red cross peaks). The 1D proton spectrum represents 6''-*O*-malonyl-genistin

Considering all NMR experiments, the data demonstrated the malonyl group migration between position 6 and 4 of the glucose moiety. After the first whole set of NMR experiments was performed, we recorded two more proton and HMBC spectra over the following 20 hours for malonylgenistin and its isomer. Especially in the proton spectra a small but appreciable conversion from the 4''-*O*-malonylgenistin back to the 6''-*O*-malonylgenistin was noted.

Acyl migration was first noted in organic synthesis and frequently described for acetates in early and recent literature (Doerschuk, 1952; Bonner, 1959; Tsuda and Yoshimoto, 1981; Hsiao et al., 1994). As a general trend, migrations following the direction glucose 1-position to glucose 6-position are more favoured, with the 4→6 migration being frequently described (Tsuda and Yoshimoto, 1981). Intramolecular acyl migration is based on the formation of ortho-acid ester intermediates (Bonner, 1959), which are 5 or 6-membered ring systems requiring proper spatial relationships. Malonyl migration was less frequently described than acetyl migration (Rijke, et al., 2004).

Wybraniec (2008) described 4→6 and 6→4 malonyl migrations on malonyl-betanins (malonyl group ester-linked to a β-glucose unit) depending on the pH conditions. In general, migrations were faster under alkaline conditions, e.g. 4→6 migration occurred almost instantly at pH 10.5 and 20˚C (Wybraniec, 2008). As a result of these studies the glucose 6-position was described as the most favoured one for malonylation. A 4→6 migration was also observed for the conjugated isoflavone formononetin glucoside malonate (Rijke, et al., 2004). A migration of the malonyl group to the glucose 6-position was noticed over the course of several hours in an acidic aqueous/MeOH medium while gathering NMR data for the isolated 4”-*O*-malonate isomer.

2.4.3. Interconversions between malonylgenistin and its isomer (4”-*O*-malonylgenistin) in thermally treated soymilk

Since similar structural information was obtained for malonyldaidzin and malonylgenistin, further interconversion work was focused only on the malonylgenistin isomer. The formation and interconversion of the malonylgenistin isomer was monitored in thermally treated soymilk. Formation of the malonylgenistin isomer and its interconversions in complex systems, such as soymilk, are potentially different from the reactions in model systems as interconversions can be influenced by various soy components, specifically soy proteins (Malapally and Ismail, 2010).

Genistin formation started to occur after 10 min of thermal treatment of soymilk, and increased gradually thereafter. There was no decarboxylation of malonylgenistin to acetylgenistin. The formation of genistein (the aglycone form) was also not favored as the concentration remained constant for all the treatment times (Table 2). Thus, the changes in the isoflavone profile were driven by the malonylglucosides as was observed in studies done by Mathias et al. (2006) and Vaidya et al. (2007).

Malonylgenistin isomer was detected in the control and all thermally treated samples. A representative chromatogram of isoflavones extracted from a soymilk sample subjected to thermal treatment at 100°C for 60 min is shown in Figure 26. Identity of 4”-*O*-malonylgenistin isomer in the soymilk samples was confirmed by LC/MS/MS analysis.

On a molar basis, an increase in malonylgenistin isomer was observed upon heating soymilk at 100ºC for 2 min, followed by a gradual decrease after 10 min of thermal treatment (Table 2, see Appendix C for ANOVA Table 11). The observed rate of interconversions between malonylgenistin and its isomer is noticeably different from that observed in buffered systems. The isomer concentration in buffered systems peaked after 10 min (Yerramsetty et al., 2011), while that in soymilk system peaked after 2 min.

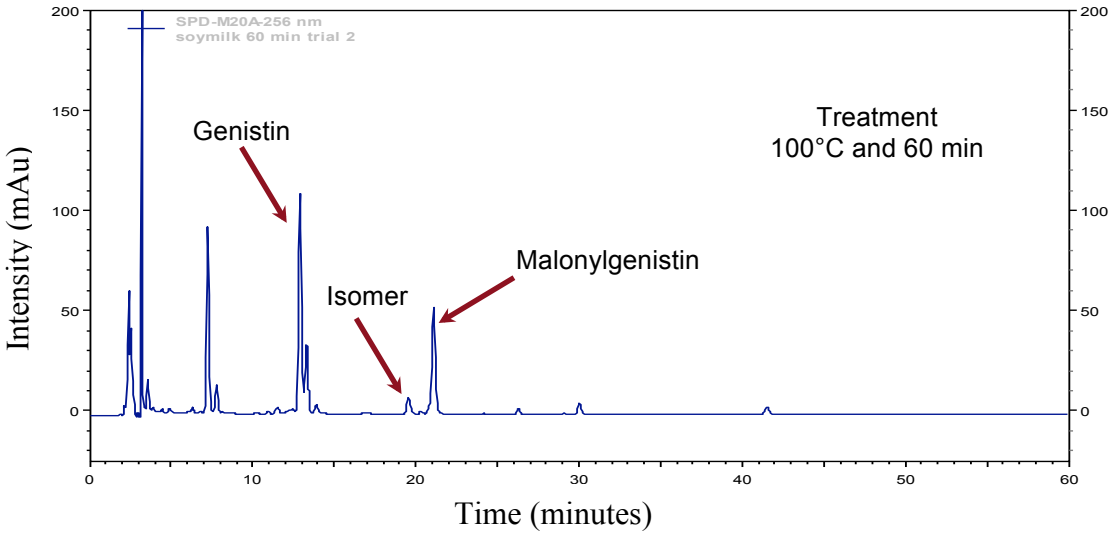

Figure 26: HPLC chromatograms at 256 nm showing a malonylgenistin isomer, which was present after heating a soymilk sample at 100°C for 60 min.

Researchers observed significant differences in the amount of observed loss and extent of interconversions of isoflavones between buffer and complex systems (Mathias et al., 2006; Nufer et al., 2009). The noted differences in the isoflavone profile in buffer and complex systems are mostly attributed to protein-isoflavone interactions.

Isoflavones are phenolic compounds and hence they tend to hide from the aqueous phase and instead interact with the hydrophobic interior of the globular soy proteins (Rawel et al., 2004). The interactions involved in the formation of protein-phenolic complex include hydrogen bonding, ionic and covalent binding, and mainly hydrophobic interactions. This protein-isoflavone association is believed to be a function of protein content as well as protein denaturation state, which in turn is dependent on processing

conditions such as pH, temperature and time (Malapally et al., 2010). In this study we saw a similar effect of protein on the conversion rate of malonylgenistin isomer in a complex soymilk system. The malonylgenistin isomer was present at all treatment times which is different from what was observed previously in buffered systems (Yerramsetty et al., 2011). The isomer was present even after 60 min of treatment time in the soymilk system whereas it disappeared under the same conditions in the buffered systems (Yerramsetty et al., 2011), thus showcasing the effect of protein on the stability of malonylgenistin isomer when subjected to processing. Overall, little is known about the effect of isoflavone-soy matrix interaction on isoflavone conversion and degradation under different temperature, time and pH conditions. Therefore, more research has to be done to investigate the individual association of isoflavones with the protein moiety under various processing conditions. Understanding the protective effect of the protein against isoflavone degradation and interconversion among various isoflavone forms, including isomers, will allow soy processors to tailor processing conditions based on the protein content and denaturation state, to minimize loss in isoflavones.

Table 2. Mean amounts (nmol/g dry weight) of MGin isomer, MGin, Gin, AGin, and total detected genistein derivatives in soymilk samples subjected to thermal treatment at 100°C for several intervals of time ranging from 0-60 min.

Time (min)	Isomer*	MGin*	Gin*	AGin*	Gein*	Total Gin^
0	677.8 c	6235 a	1049 d	151.1 cd	125.2 a	8239 a
2	785.9 a	6224 a	1117 d	147.8 d	124.2 a	8399 a
5	762.5 ab	5626 b	1238 d	158.3 cd	114.4 ab	7899 ab
10	719.1 bc	5285 c	1647 c	172.1 c	107.7 b	7932 ab
30	622.5 d	4082 d	2968 b	236.6 b	119.3 b	8029 a
60	462.9 e	2657 e	3845 a	276.0 a	116.1 bc	7357 b

*Isomer, malonylgenisting isomer; Gin, genistin; MGin, malonylgenistin; AGin, acetylgenistin; Gein, genistein. ^Total detected genistein derivatives (Isomer + Gin + Mgin + Agin + Gein). Means in each column with different small letters are significantly different across the treatment times according to Tukey-Kramer multiple means comparison test ($P \leq 0.05$); n=3.

Under all the heat treatment times employed, malonylgenistin isomer represented 6-9% of the total genistein derivatives. Disregarding the concentration of 4''-*O*-malonylgenistin thus leads to at least a 6% (up to ~ 15 %, considering malonyldaidzin isomer as well) underestimation of the isoflavone concentration of a given soy food. For accurate determination of total isoflavone content and any incurred loss in isoflavones due to processing, it is thus crucial to account for the present isomers. To better characterize the interconversions of the malonylglucosides and their isomers in complex systems further studies are required covering wider ranges of temperature, pH, and time.

2.5. Conclusions

While the existence of isomers in soy matrices was reported earlier, the present work provided further structural characterization with full elucidation of the malonylglucoside isomers. We demonstrated for the first time that the formation of the soy malonyl isomers is governed by thermal processing time in a soymilk system. Further, a clear distinction was observed between the rates of interconversions between malonylgenistin and its isomer when compared between buffered and soymilk systems. Results highlighted the role of isoflavone-protein interactions in the determination of isomer stability in complex systems that are subjected to processing. Since the identified isomers can convert to biologically relevant forms, it is crucial to include the isomers in the calculation of total isoflavone content, profile and loss. Disregarding the isomer formation upon heating can result in overestimation of loss in total isoflavone content and misinterpretation of the biological contributions.

3. DEVELOPMENT OF A SIMPLE, FAST AND ACCURATE METHOD FOR THE DIRECT QUANTITATION OF FEW ESTROGEN RECEPTOR MODULATORS IN RAT PLASMA USING STABLE ISOTOPE DILUTION MASS SPECTROMETRY*

*: Content of this chapter was submitted to Journal of Agricultural and Food Chemistry **Yerramsetty, V.,** Mikel, R., Hegeman, A., Cohen, J., and Ismail, B. *Journal of Agricultural and Food Chemistry.,* submitted, Dec 3rd of 2012.

3.1. Overview

A rapid analytical procedure was developed to quantify major selective estrogen receptor modulators (SERMs) simultaneously in biological fluids using stable isotope dilution mass spectrometry (SID-LCMS). Two novel isotopically labeled (SIL) analogues of natural SERMs, genistein and daidzein were synthesized using a H/D exchange reaction mechanism. Computational chemistry coupled with MS and NMR data confirmed the site and mechanism of deuteration. The SIL analogues, which were mono- and dideutero substituted at the ortho positions, exhibited minimal deuterium isotope effects, and were stable under the employed sample preparation protocol and MS analysis. An isotopic overlap correction was successfully employed to improve the accuracy and precision of the analytical method. The developed method, which was found to be sensitive, selective, precise and accurate, is a valuable tool for the research focused on determining the bioavailability of individual SERMs.

3.2. Introduction

Selective estrogen receptor modulators (SERMs) are non-hormonal compounds that can bind to estrogen receptors and selectively interact with specific coactivators and corepressors depending on the type of tissue. Tamoxifen and raloxifene (Figure 27) are two of the only three synthetic SERMs that are approved by the Food and Drug Administration (FDA) for human use. Naturally occurring isoflavones also exhibit SERM activity (Brezezinski et al., 1999; Arjmandi et al., 2002; Oseni et al., 288). Upon ingestion, the metabolic pathway of SERMs and their ensuing bioactivity is dictated by their chemical structure. For instance, equol, which is a metabolite of daidzein, is more estrogenic than daidzein, while the genistein metabolite *p*-ethyl phenol (Figure 27) is not estrogenic (Turner et al., 2003).

Liquid chromatographic (LC) techniques coupled with mass spectrometry (MS) are the preferred analytical methods for isoflavone analysis in biological fluids (Wu et al., 2004; Heinonen et al., 2003; Twaddle et al., 2002; Trdan et al., 2011). To account for losses during sample preparation, researchers have utilized a variety of internal standards including structural analogues such as apigenin (Barnes et al., 1999), biochanin A (Barnes et al., 1998), fluorescein (Coward et al., 1998), and dihydroxyflavone (Setchell et al., 1997). Researchers also used stable isotopically labeled (SIL) analogues, either deuterium (^{2}H) or carbon-13 (^{13}C) labeled, coupled with stable isotope dilution LCMS (SID-LCMS) analysis (Adlercreutz et al., 1995; Clarke et al., 2002). Stable isotopically labeled analogues, which are chemically identical to their respective analytes, have a great advantage over structural analogues because they experience similar chemical stresses during sample preparation and analysis (chromatography and ionization). One of the major deliverables of an NIH sponsored scientific workshop on soy isoflavone research (Klein et al., 2010) was the importance of using appropriate SIL analogues to guarantee better quantitation accuracy and traceability.

Due to their high stability, ^{13}C labeled analogues are preferred over ^{2}H labeled analogues. Nevertheless, ^{2}H labeled analogues are gaining popularity due to their simple synthesis approach (hydrogen/deuterium (H/D) exchange) compared to that of ^{13}C

labeled analogues. Investigators who had used ^{2}H labeled SIL analogues in their experimental procedures have used trideutero derivatives (Antignac et al., 2009), tetradeutero derivatives (Ferrer et al., 2009), pentadeutero derivatives (Teunissen et al., 2009) or hexadeutero derivatives of SERMs (Teunissen et al., 2009). However, deuterium isotopic effect, which is a chromatographic separation between the analytes and the deuterated analogues, has been reported (Lockley, 1989). Wang et al. (2007) reported that a chromatographic separation between the analyte and its deuterated analogue can cause up to 25% difference in their ion suppression(s), resulting in an inaccurate analyte-to-internal standard peak ratio.

In addition to the current predicament in the choice of internal standards, literature lacks an accurate method that can simultaneously quantify all major SERMs. Isoflavones can interact with certain cytochrome class enzymes that take part in the metabolism of tamoxifen, thus altering its physiological activity (Shin et al., 2006; Chen et al., 2004). Although, there is no information on raloxifene-isoflavone interaction on the raloxifene metabolic pathway, a report recommended the use of phytochemicals in tandem with raloxifene to improve its bioavailability (Panay, 2004). Thus, there is a growing interest to test synthetic SERMs concomitantly with natural isoflavones in an effort to effectively treat various health issues. Therefore, the overall objective of this study is to develop and validate an accurate and rapid analytical procedure to quantify tamoxifen, raloxifene, genistein, daidzein, and equol simultaneously in biological fluids using SID-LCMS.

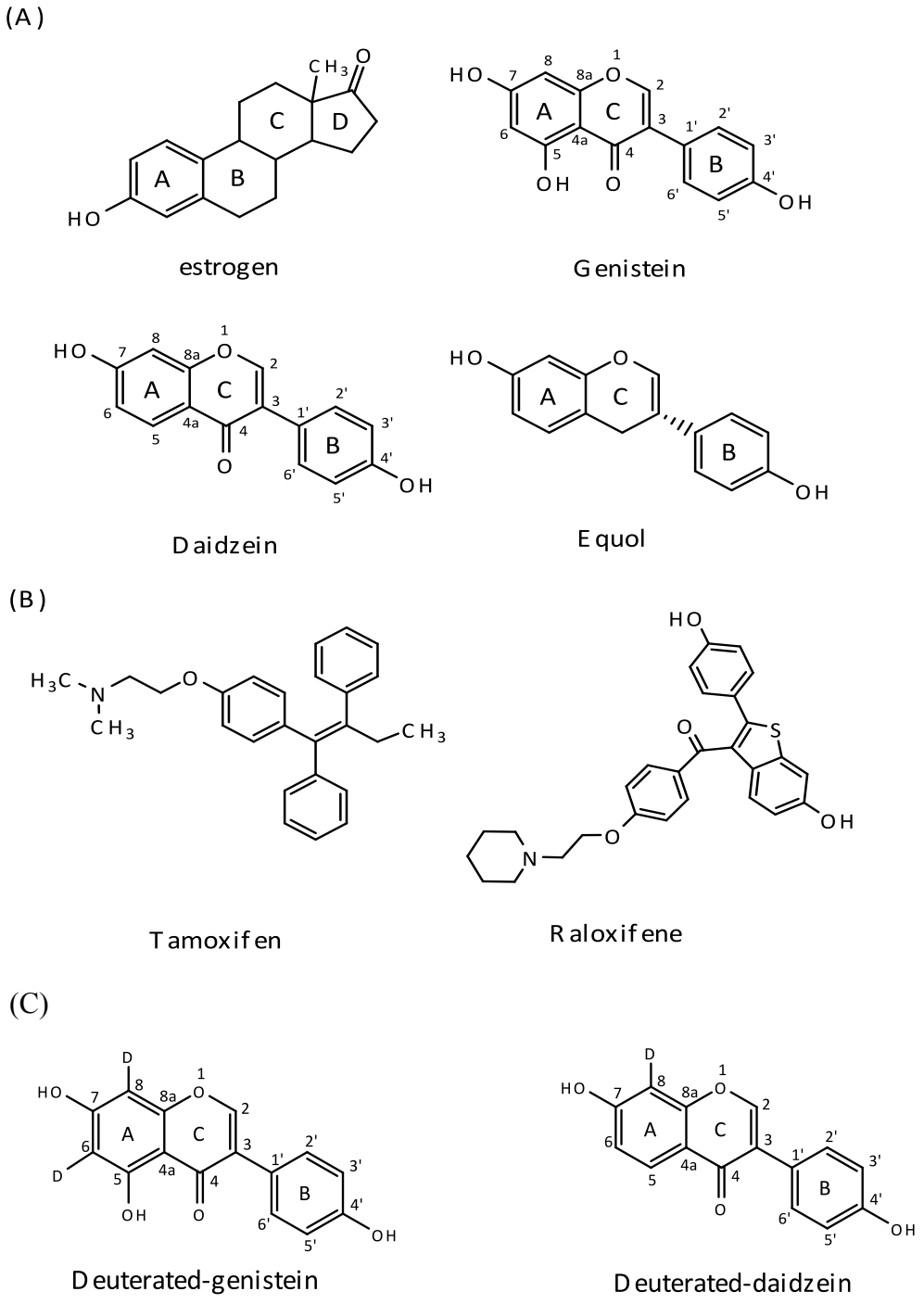

Figure 27. (A) Structures of human estrogen, genistein, daidzein, and equol. (B) Structures, tamoxifen and raloxifene. (C) Structures of deuterated genistein, 6,8-dideutero-5,7-dihydroxy-3-(4-hydroxyphenyl) chromen-4-one, and deuterated daidzein, 8-monodeutero-7-hydroxy-3-(4-hydroxyphenyl) chromen-4-one.

3.3. Materials and methods

3.3.1 Materials

High performance liquid chromatography (HPLC) grade acetonitrile and methanol were purchased from Fisher Scientific (Hanover Park, IL, USA). Isoflavones genistein and daidzein were purchased from LC Laboratories (Woburn, MA, USA). Tamoxifen was purchased from MP Biomedicals (Santa Ana, CA, USA). Sulphatase/glucuronidase enzyme (S9626), deuterated methanol (CD_3OD), deuterated water (D_2O), raloxifene, phenolphthalein-β-D glucuronide, *p*-nitrocatechol sulfate, phenolphthalein, and *p*-nitrocatechol were purchased from Sigma Aldrich (St. Louis, MO, USA). Deuterated standards tamoxifen-d_5, raloxifene-d_4 and equol-d_4 were purchased from Toronto research chemicals (North York, Ontario, Canada). Rat plasma was generously donated by Professor Daniel Gallaher (University of Minnesota, St. Paul, US).

3.3.2. Reagents

3.3.2.1. Preparation of sodium citrate buffer (0.01M, pH 5.0)

Equal volumes of sodium citrate (0.05 M) and citric acid (0.05 M) solutions were mixed and diluted to a final concentration of 0.01M. The pH was adjusted to 5.0 using HCl (0.05 M).

3.3.2.2. Preparation of sulphatase/glucuronidase enzyme

The enzyme solution was prepared in sodium citrate buffer (0.01 M, pH 5.0) to a final enzyme activity of 500 U/mL of sulphatase and ~15,000 U/mL of glucuronidase.

3.3.3. Reference standards

Reference standards of phenolphthalein-β-D glucuronide, *p*-nitrocatechol sulfate and *p*-nitrocatechol were prepared in double distilled water (DDW) (500 mg/L). Reference standards of phenolphthalein, genistein, daidzein, raloxifene, tamoxifen, equol, deuterated standards of daidzein and genistein, tamoxifen-d_5, raloxifene-d_4 and equol-d_4 were prepared in 80% aqueous methanol solution (500 mg/L). Reference standards of genistein and daidzein (500 mg/L) were also prepared in deuterated methanol (CD_3OD) for use in the preparation of their respective deuterated standards.

3.3.4. Working standards

Reference standards were diluted in either DDW or 80% aqueous methanol solution to obtain working standards. Working standards of individual compounds were diluted to 1 µg/L for MS analysis. Working standards for calibration were (1) a cocktail of the analytes (genistein, daidzein, equol, tamoxifen, raloxifene) at concentrations ranging from 20 µg/L - 18 mg/L, and (2) a cocktail of all the respective internal standards at a concentration of 6 mg/L prepared in 80% aqueous methanol solution. Working standards of a cocktail of phenolphthalein-β-D glucuronide, *p*-nitrocatechol sulfate, phenolphthalein, *p*-nitrocatechol (10 mg/L) were also prepared in DDW after appropriate dilutions using the reference standards. Validation standards were also prepared in 80% aqueous methanol solution at three different levels 200 µg/L, 2 mg/L and 15 mg/L.

3.3.5. Preparation of isoflavone deuterated standards

Genistein and daidzein were individually dissolved to a final concentration of 25 mg/L in 94.9:5:0.1 (v/v) D_2O, CD_3OD and deuterated formic acid, respectively. Deuteration solvent composition was optimized to obtain rapid and complete deuteration. Genistein solution was incubated for three days, while daidzein solution was incubated for five days in a heating block maintained at 90°C. After incubation, deuterated isoflavones were separated from the reaction volume using Sep-Pak^{TM} C_{18} reverse-phase cartridges (Water's Associates, Milford, MA, USA). Before sample loading, Sep-Pak^{TM}

C_{18} cartridges were primed with 2 mL of methanol, followed by conditioning with same volume of DDW. The sample was then loaded onto the cartridge and the deuterated formic acid was subsequently washed with 3 mL DDW. The deuterated isoflavones were recovered with 1.2 mL of methanol, which aids in reinstating the protic hydroxyl groups via H/D back exchange. Methanol was subsequently evaporated using a speed-vac (Savant, DNA110), and the residue was either re-dissolved in 5% (v/v) acetonitrile solution or dimethylsulfoxide (DMSO)-d_6 and immediately analyzed by MS and nuclear magnetic resonance (NMR) to determine the extent of deuteration.

3.3.6. Determination of deuteration site

3.3.6.1. MS analysis

Individual solutions (1.0 µg/L) of isoflavones and deuterated isoflavones were directly infused into the heated electrospray ionization (HESI) interface of a triple stage quadrupole mass spectrometer (5500 QTRAP, AB Sciex, Washington, D.C., USA) operating in the positive ion mode. The Q1 and Q3 mass resolutions were set at 0.4 Dalton (Da) full width at half maximum (FWHM). Fifteen spectra were collected with a scan time of one second. Instrument parameters, namely sheath gas flow (N2, 99.99%, flow rate = 5-20 units), vaporization temperature 150°C, collision cell exit potential (10-17 V), spray voltage (4.0-4.5 kV), entrance potential (5-18 V), declustering potential (38-55 V), and collision energy (15-35 units), were optimized for each isoflavone such that ions of interest were produced in measurable abundance. Tandem MS/MS was employed to determine the fragmentation pathway of the isoflavones and deuterated isoflavones. The precursor ions ($[M+H]^+$) were isolated and analyzed by collision induced dissociation (CID) and daughter ion spectra were recorded. The collision energy was set to a value (30 units) at which ions of interest were produced in measurable abundance. Spectra were collected in triplicate.

3.3.6.2. Proton NMR experiments

NMR experiments were carried out on a Varian 500 MHz Inova spectrometer equipped with a 5 mm triple resonance probe. Proton spectra for isoflavones and deuterated isoflavones were measured in (DMSO)-d_6 at ambient temperature. As a non-protic solvent, (DMSO)-d_6 facilitates the detection of phenol hydroxyl proton resonances due to the absence of proton-deuterium (H/D) exchange, which is commonly observed when protic solvents such as deuterium oxide (D_2O) or CD_3OD are used. Chemical shifts (δ) were referenced to the central solvent signal of (DMSO)-d_6 (δH 2.50 ppm) (Gottlieb, et al., 1997). J values are given in hertz. NMR assignments follow the numbering shown in Figure 27.

Genistein (500 MHz, DMSO-d_6): H6, 6.21 (d, 2.4 Hz); H8, 6.37 (d, 2 Hz); H3' and H5', 6.81 (d, 8.4 Hz); H2' and H6', 7.36 (d, 8.4 Hz); H2, 8.31 (s); C4'-OH, 9.57 (s); C7-OH, 10.86 (s); C5-OH, 12.94 (s).

Deuterated genistein: H3' and H5', 6.81 (d, 8.4 Hz); H2' and H6', 7.36 (d, 8.4 Hz); H2, 8.31 (s); C4'-OH, 9.56 (s); C7-OH, 10.85 (s); C5-OH, 12.93 (s).

Daidzein: H3' and H5', 6.81 (d, 8.4 Hz); H8, 6.85 (s); H6, 6.93 (d, 8.9 Hz); H2' and H6', 7.38 (d, 8.4 Hz); H5, 7.96 (d, 8.7 Hz); H2, 8.28 (s); C4'-OH, 9.53 (s); C7-OH, 10.78 (s).

Deuterated daidzein: H3' and H5', 6.80 (d, 8.4 Hz); H6, 6.93 (d, 8.9 Hz); H2' and H6', 7.38 (d, 8.4 Hz); H5, 7.96 (d, 8.7 Hz); H2, 8.28 (s); C4'-OH, 9.53 (s); C7-OH, 10.78 (s).

3.3.6.3. Quantum mechanical modeling of genistein and daidzein

Density functional theory (DFT) was employed to perform quantum mechanical modeling of genistein and daidzein. Structures of both genistein and daidzein were optimized to the lowest energy conformations using DFT calculations at the B3LYP level and 6-31G(d,p) basis set using Gaussian 03 software (2003) (Gaussian, Inc. Wallingford, CT, USA). The chosen basis set and polarization functions yielded excellent results for structurally similar compounds (Krishnakumar et al., 2004). Single point energy calculations were performed on the lowest energy conformations of genistein and

daidzein at the same level and basis set to plot their electrostatic potential (ESP) maps. Mulliken charges were also determined, which serve as a good indicator for estimating partial atomic charges.

3.3.7. Optimization of the hydrolysis conditions of sulphonated and glucuronidated isoflavones

In triplicates, an aliquot (20 µL) of rat plasma was mixed with 10 µL of a solution containing both phenolphthalein-β-D glucuronide and *p*-nitrocatechol sulfate (10 mg/L), vortexed, and sonicated for 10 min. Sulphatase/glucuronidase enzyme (200 µL) was added and the samples were incubated at 37°C, pH 5 for 15, 30, 45, 60, or 360 min. After hydrolysis the synthetic substrates and products were extracted into ethyl ether (1 mL × 3), vortexed, and centrifuged at 5,000 x g for 10 min at 15°C. The supernatant was evaporated under a stream of nitrogen gas, and the residue was dissolved in 200 µL of 80% aqueous methanol. Samples were stored at -80°C or analyzed immediately by LC/MS. Time required for complete hydrolysis of the synthetic substrates was determined by monitoring their complete disappearance and appearance of their respective de-conjugated forms (phenolphthalein and *p*-nitrocatechol).

3.3.8. Stability of the synthesized deuterated standards

The stability of the synthesized SIL analogues was tested after subjecting them to the optimized enzymatic conditions by monitoring their isotopic profile before and after the enzymatic hydrolysis. An aliquot (10 µL) of SIL analogues of genistein or daidzein (200 µg/L) was added, in triplicates, to rat plasma (20 µL), which was then subjected to the optimized hydrolysis conditions followed by the extraction procedure described above. The final concentration of SIL analogues in the extract was 10 µg/L. Stability was also monitored during MS analysis by varying vaporization temperature from 100°C to 400°C, with a step size of 100°C during the SID-LC/MS analysis.

3.3.9. Calibration

An aliquot (10 µL) of each of six working standards containing all five SERMs (20 µg/L, 1 mg/L, 2mg/L, 6mg/L, 12mg/L and 18 mg/L) and an aliquot (10 µL) of the cocktail containing the respective SIL analogue of each SERM (6 mg/L) were added to 20 µL of plasma, which was then subjected to the optimized hydrolysis conditions followed by the extraction procedure described above. The final concentrations of the five SERMS in the standard extracts were 1, 50, 100, 300, 600, and 900 µg/L, and the final concentration of their respective SIL analogues in each standard extract was 300 µg/L. All standards were analyzed following the LC/MS method described below. Calibration curves were obtained by plotting the response ratio of the variable analyte to that of the constant internal standard against the analyte concentration. Analyte response was measured in the multiple reaction monitoring (MRM) mode. An additional step was included to correct for the isotopic overlap between genistein/daidzein and their respective SIL analogues. Daidzein and genistein were run separately in the absence of their respective SIL analogues, and the MRM transitions of their natural isotopic peaks, which can interfere with their respective SIL analogues, were monitored. Subsequently, the obtained responses were subtracted from that obtained from the calibration. All analyses were performed in triplicate.

3.3.10. LC/MS analysis

LC/MS analysis was conducted on an ultra-high pressure LC system (Shimadzu UFLC XR) online with a triple stage quadrupole mass spectrometer (5500 QTRAP, AB Sciex, Washington, D.C., USA) equipped with a 50 × 2.1 mm inner diameter, 5 µm, YMC C18 column. The column temperature was maintained at 25°C. An injection volume of 5 µL was chosen. A linear binary gradient at a flow rate of 0.4 mL/min with water and acetonitrile as solvents were used, both containing 0.1% (v/v) formic acid. The initial gradient concentration was 20% acetonitrile, which was kept constant for one min, linearly increased to 95% in 4.50 min, kept constant for one min, followed by column equilibration steps. The LC column eluate entered the electrospray ionization (ESI) interface of the mass

spectrometer operating in the positive ion mode. The MS parameters were: sheath gas (N_2 99.99%, flow rate = 20 units); vaporization temperature 150°C; collision cell exit potential 17 V; spray voltage 4.5 kV; entrance potential 10 V; declustering potential 55 V; collision energy 28 units. Acquisition was carried out in the MRM mode, so as to achieve maximal sensitivity and reliable quantitation over several orders of magnitude of compound abundance (Sawada et al., 2009; Bhat et al., 2011). The MRM transitions of the analytes of interest are summarized in Table 3. Concentrations of SERMSs were calculated based on peak areas integrated by MultiQuantTM (version 2.0.2).

Table 3. Multiple reaction monitoring (MRM) transitions of all the compounds used in the present study.

Analyte	**MRM transitions**	
	Q1* mass	**Q3^ mass**
Genistein	271	153
Deuterated genistein	273	155
Daidzein	255	199
Daidzein-d_1	256	200
Tamoxifen	372	72
Tamoxifen-d_5	377	72
Equol	243	105
Equol-d_4	247	108
Raloxifene	474	112
Raloxifene-d_4	478	116
Phenolpthalein	319	225
Phenolphthalein β-D-glucuronide	495	225
p-Nitrocatechol	156	123
p-Nitrocatechol sulfate dipotassium salt	234	154

* first quadrupole; ^ third quadrupole

3.3.11. Validation of the analytical procedure

3.3.11.1. Linearity

Calibration curves were constructed by performing least square linear regression using Microsoft Excel (2010), and correlation coefficients (R^2) were determined. A R^2 value greater than 0.99 was considered acceptable.

3.3.11.2. Accuracy and precison

Three validation standards of a low range (10 µg/L), middle range (200 µg/L), and an upper range (750 µg/L) of the calibration curve were prepared as follows. An aliquot (10 µL) of each of three working standards containing all five SERMs (200 µg/L, 4 mg/L and 15 mg/L) and an aliquot (10 µL) of the cocktail containing the respective SIL analogue of each SERM (6 mg/L) were added to 20 µL of plasma, which was then subjected to the optimized hydrolysis conditions followed by the extraction procedure described above. Extracts were analyzed following the LC/MS method described above. Accuracy was determined by comparing the measured concentration of the validation standards to the nominal concentration. Accuracy criterion for the measured concentration was set at nominal concentration ±7% (measured in terms of percentage relative error, % E_{rel}). Precision criteria were set at ≤7% (measured in terms of percent relative standard deviation, % RSD) for both intra-assay precision and instrument precision (re-injection repeatability).

3.3.11.3. Stability of working standards

Working standards of the analytes (5 µg/L for daidzein and10 µg/L for the rest of the analytes) were analyzed, in triplicate, immediately after preparation and after being held at room temperature (25°C) for 3 h. The stability of the SIL analogues was tested by monitoring their isotopic profiles before and after being held at 25°C for 3 h. Stability of the validation standards was also monitored after holding them in the auto sampler at 4°C for 12 h. The analysis time never exceeded 12 h. The same acceptance criterion stated for the determination of accuracy and precision was chosen.

3.3.11.4. Carry over

A blank plasma extract was analyzed, in triplicates, immediately after analyzing the standard with the highest concentration (900 µg/L). Concentration of the analytes should not be more than 5% of the lowest standard concentration (1 µg/L).

3.3.12. Method application in a model rat system

Two male Wistar rats (100 – 125 g) were housed and cared for in the Research Animal Resources (RAR) facility by trained personnel. The RAR animal facility is guided by the Reagents' policy, USDA Animal Welfare Act, NIH guide for the Care and Use of laboratory Animals, AAALAC and public health Service Policy. The rats were subjected to an adjustment period of 10 days, during which they were fed a casein-based diet following the formulation described by the American Institute of Nutrition (AIN – 93M). After the adjustment period each rat was gavaged with either genistin or daidzin at a concentration of 100 µmole/kg body weight. The dose is based on an average intake of ~10 mg/day of isoflavones by humans, which was converted to an equivalent amount based on an energy equivalent intake for rats compared to a human diet. Blood (125 µL) was collected from the saphenous vein of each rat at various time intervals including 0, 2, 4, 6, 8, 10, 12 and 24 h. The collected blood was centrifuged for 3 min at 4°C, 6000 × *g*, and plasma was collected and stored at -80°C until analysis. SIL analogues (300 µg/L) were added to the plasma samples on the day of analysis, and the plasma samples were subjected to the optimized hydrolysis and extraction condition as outlined above. Dilution of the extracts was experimentally determined to fit within the tested linear range. Isoflavones extracts were stored at -80°C for later analysis. Plasma concentrations of genistein, daidzein and its metabolite equol were monitored following the SID-LC/MS analysis method outlined above.

3.3.13. Statistical analysis

All statistical analysis including calculation of mean, standard deviation, coefficient of variation, percentage relative error and linear regression analyses were performed using Microsoft Excel (2010).

3.4. Results and discusion

3.4.1. Structural characterization of deuterated genistein and daidzein

3.4.1.1. Mass spectrometry analysis

The employed deuteration conditions produced deuterated isoflavones with high isotopic purity (>98%). The quasi-molecular ion of genistein in the positive ion mode was m/z 270.99 $[M+H]^+$ and that of deuterated genistein was 272.95 $[M+H]^+$, indicating an incorporation of two deuteriums on the genistein molecule (Figure 28 A, B). The main fragment ion of genistein was m/z 153 (Figure 28 A), which has the A ring intact and is formed from the parent compound by retro Diels-Alder fragmentation at the C ring (Figure 29). There was 2 mass units increase for this ion (m/z 155) in the deuterated genistein spectra (Figure 28, B). Therefore, the site of deuteration on the genistein molecule is most likely at the ortho positions of the A ring.

The quasi-molecular ion of daidzein in positive ion mode was m/z 255.07. Unlike what was observed in the case of genistein, we only observed an increase of 1 m/z for deuterated daidzein (m/z = 256.05), indicating an incorporation of 1 deuterium on its structure (Figure 28 C, D). The main fragment ion, observed in the fragmentation spectra of daidzein was m/z 199. This fragment ion which is composed of three fused benzene rings representing a phenanthrene framework, is formed by retro- Diels Alder fragmentation upon the loss of 2CO groups at ring C ($[M+H-2CO]^+$) and has both A and B rings intact. The ion with m/z 137 has it's A ring intact (Figure 29). There was 1 mass unit increase for this ion (m/z 138) in the deuterated daidzein fragmentation spectra (Figure 28, D), indicating that the site of deuteration on the daidzein molecule was on the A ring, probably at an ortho position to C7 similar to what was observed for genistein.

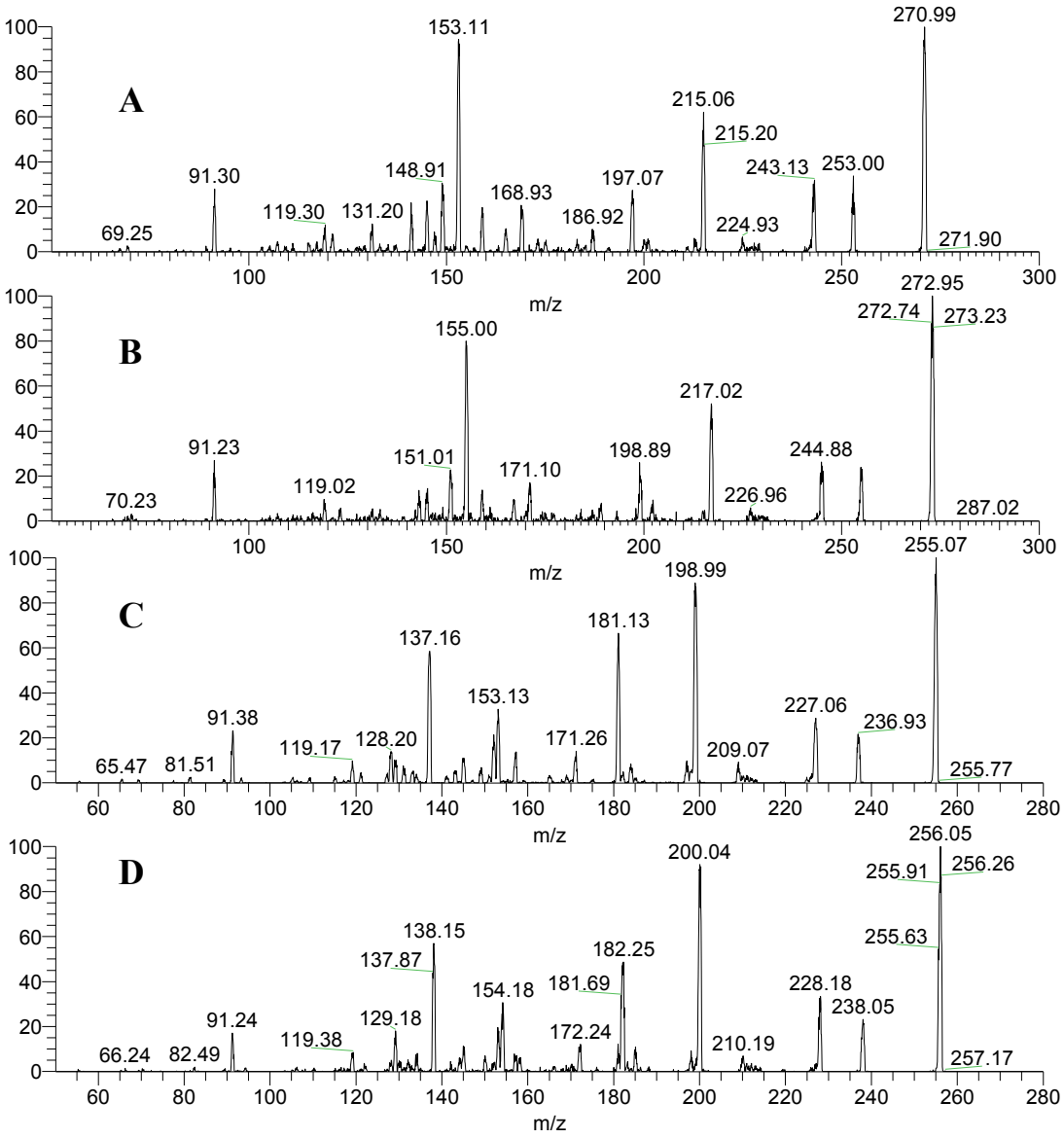

Figure 28. Tandem MS of (A) genistein and (B) deuterated genistein (C) daidzein (D) deuterated daidzein.

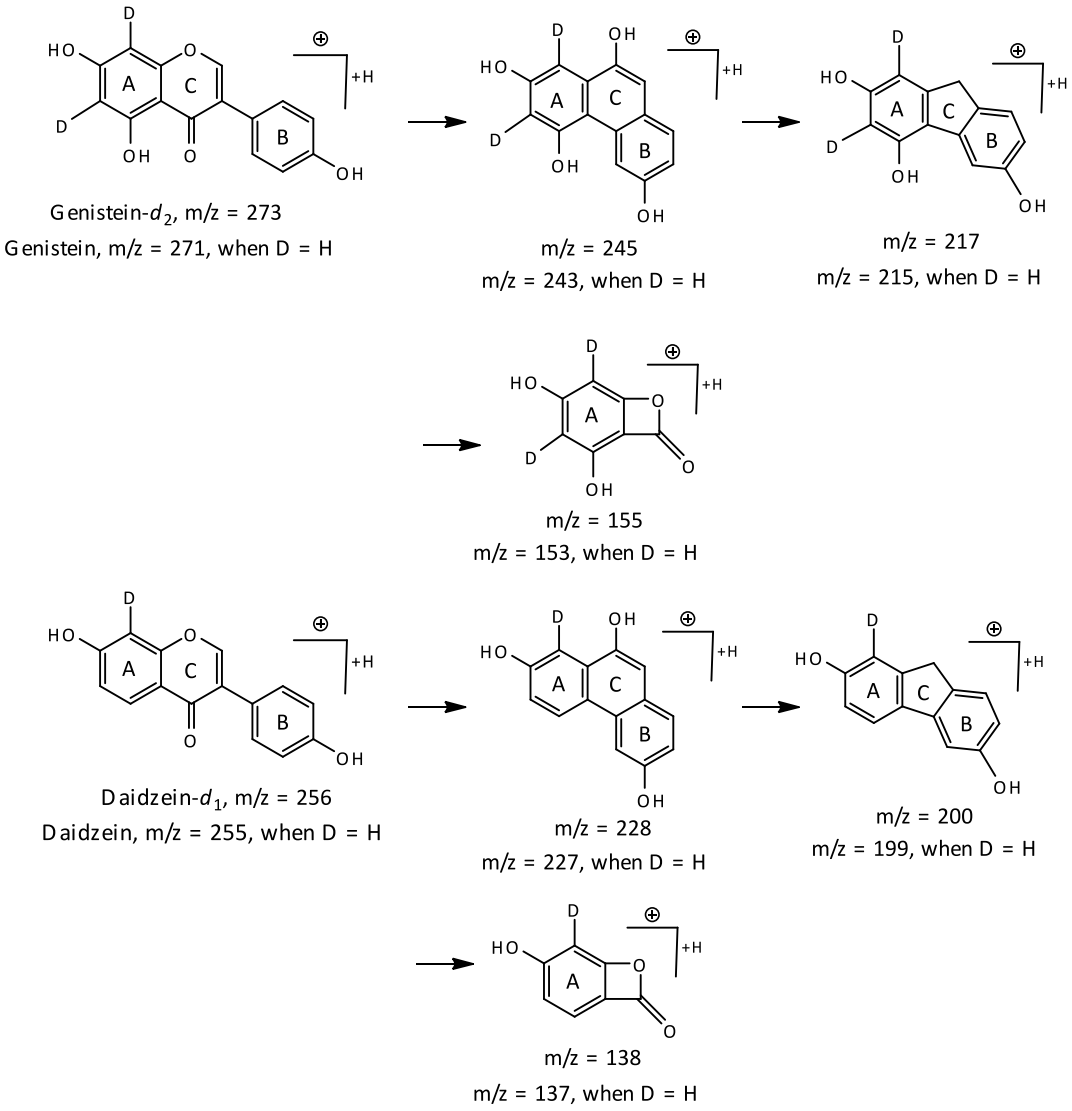

Figure 29. Fragmentation pathway of quasi-molecular ions of genistein, deuterated genistein and daidzein, deuterated daidzein

3.4.1.2. NMR analysis

NMR data obtained for genistein and daidzein were consistent with previously published data (Lori et al., 2011; Yu-Chen et al., 1994). The signals corresponding to the H6 and H8 protons (δH 6.21 and δH 6.37 ppm, respectively) in the genistein spectra were

absent in the deuterated genistein spectra. This indicates that the two protons present in the ortho positions to C7 in genistein took part in the H-D exchange, thus complementing the MS data. In the case of daidzein only the H8 proton (δH 6.85) was replaced with deuterium. Thus, the deuterated standards of genistein and daidzein are 6,8-dideutero-5,7-dihydroxy-3-(4-hydroxyphenyl) chromen-4-one and 8-monodeutero-7-hydroxy-3-(4-hydroxyphenyl) chromen-4-one, respectively (Figure 27 C).

3.4.1.3. Quantum mechanical modeling

In spite of using an extended basis set and polarization functions, no differences in electron densities at the sites of deuteration were detected based on ESP maps (Figure 30). To overcome this predicament, the Mulliken charges on each atom were determined. Mulliken charges represent partial atomic charges, making it possible to probe the electron population in a given region of the molecule (e.g. sites of deuteration). Partial atomic charges were used to predict the reactivity preference of the abundant deuterium ion (D^+) in the deuteration of isoflavones. Although partial atomic charges are not quantum mechanical observables, the charge scheme employed could represent all the properties that can be obtained from the quantum mechanical wave functions. Calculation of the Mulliken charges revealed that the C6 of the genistein molecule is more electron dense than C8. Thus, deuteration of genistein would be favored at C6 followed by C8. However, in the case of daidzein, C8 is more electron dense than C6. Thus, for daidzein, deuteration at C8 would be favored over C6. The difference in the preference of deuteration between genistein and daidzein is due to the presence of an additional hydroxyl group at C5 in genistein. Being an electron withdrawing group, the hydroxyl group reduces the electron density at the C5 position, which invokes a pronounced asymmetric distribution of electrons between C5 and C6, resulting in a higher electron density at C6. Further, a comparison of the overall partial atomic charges between genistein and daidzein at the deuteration sites reveals that the nucleophilic nature of genistein is greater than that of daidzein. This explained the necessity to incubate

daidzein for an extended period of time (5 days) as compared to genistein (3 days) to achieve deuteration.

A reaction in which the hydrogen attached to an aromatic system is replaced by an electrophile (D^+) is an example of the classical electrophilic aromatic substitution reaction (Wahala et al., 2002). The reaction is initiated with the addition of deuterium(s) to the π complex resulting in the formation of a resonance stabilized cyclohexadienyl cation intermediate (Figure 31). Presence of electronegative hydroxyl groups in the structures of isoflavones aids in the additional stabilization of the cyclohexadienyl cation intermediate. The hybrid resonance intermediate formed during electrophilic aromatic substitution reaction allows delocalization of the electrons over a greater volume of the isoflavone molecule (five resonance forms) resulting in its enhanced stability (Figure 31). The final deuterated compound is formed by restoration of the aromatic sextet upon the loss of the original hydrogen bound at the site of the electrophilic attack (Jones, 2005). Hydroxyl groups in the isoflavone structures also significantly affect the regioselectivity of deuterium substitution, predominantly favoring ortho or para substitution (Jones, 2005). This is in agreement with the experimental results where substitution for both genistein and daidzein occurred at positions ortho to C7-OH and to C5-OH in case of genistein.

It is reported that deuteration at the ortho positions has far less effect on isotopic fractionation when compared to meta or para positions (Lockly, 1989). Hence, we predict that the SIL analogues reported in this work will exhibit less deuterium isotopic effect as compared to the tetra/tri/hexa deuterated isotopes of isoflavones.

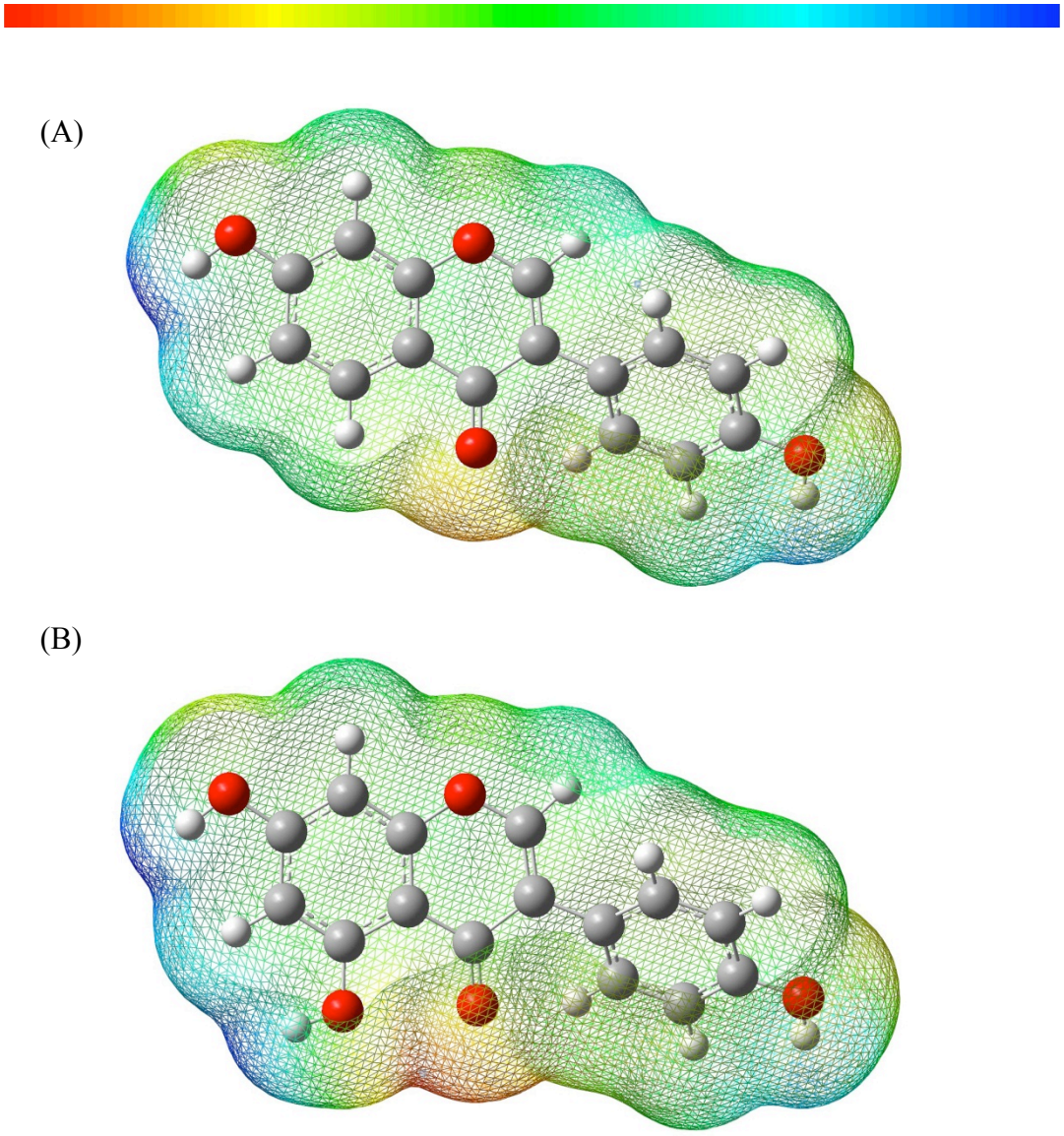

Figure 30. Electrostatic potential maps of (A) daidzein and (B) genistein. The most negative potential (high electron density) is clolored red while the most positive potential (low electron density) is colored blue.

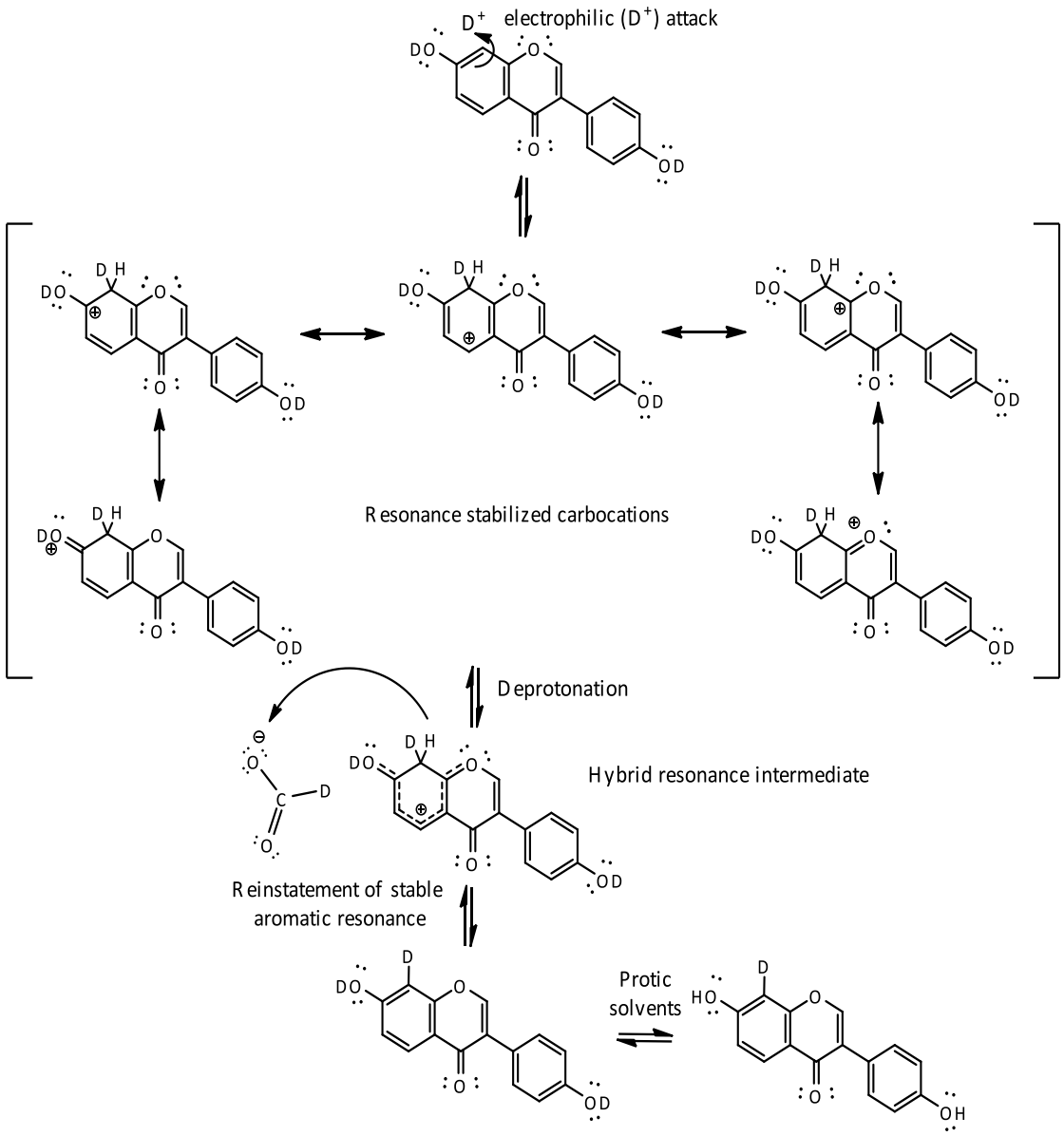

Figure 31. The five intermediate cyclohexadienyl cations involved in the electrophilic aromatic substitution of daidzein with the subsequent formation of stable deuterated daidzein.

3.4.2. Determination of optimum hydrolysis time

Complete hydrolysis of phenolphthalein-β-D glucuronide and *p*-nitrocatechol sulfate by sulphatase/glucuronidase was achieved after 60 min of incubation at 37°C, pH 5 (Figure

32). Using MRM transitions, completion of hydrolysis was determined by the disappearance of the conjugated forms of the standards (phenolphthalein-β-D glucuronide and *p*-nitrocatechol sulfate) and appearance of their respective deconjugated forms (phenolphthalein and *p*-nitrocatechol). After incubation for 60 min, as compared to the control, the presence of *p*-nitrocatechol sulfate (monitored by 234-154 MRM transition) was negligible (Figure 32). The disappearance of *p*-nitrocatechol sulfate was accompanied by the appearance of a new peak (156-123 MRM transition) corresponding to the MRM transition of *p*-nitrocatechol. The complete disappearance of phenolphthalein-β-D-glucuronide and the formation of its deconjugated form, phenolphthalein, was also accomplished after 60 min of incubation.

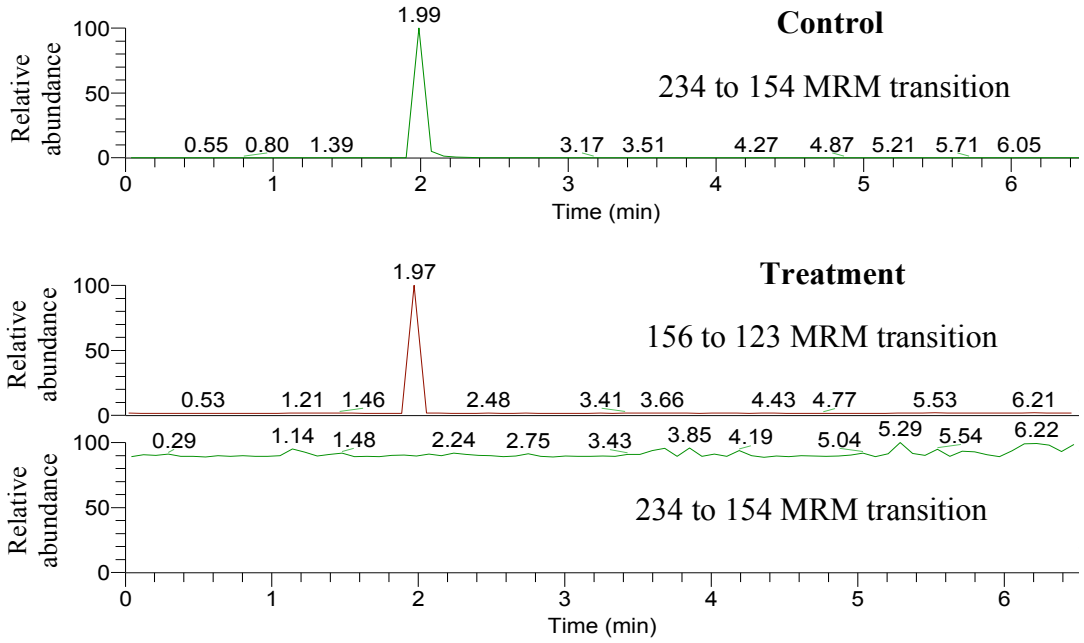

Figure 32. MRM of m/z = 234 to 154 transition for p-nitrocatechol sulphate and m/z = 156 to 123 transition for p-nitrocatechol, before and after incubation at 37°C, pH 5 for 60 min.

3.4.3. Stability of SIL analogues of genistein and daidzein

The optimized hydrolysis conditions (60 min at pH 5, 37°C) did not impact the stability of the SIL analogues of genistein and daidzein. Based on the relative abundances of the ions that constitute the isotopic profiles of the SIL analogues, we observed no significant change in their intensities before and after hydrolysis, indicating the absence of loss in deuteration from the structures of the SIL analogues of genistein and daidzein upon hydrolysis (Figure 33).

Operation in the heated electrospray ionization (HESI) mode subjects analytes and their SIL analogues to high temperatures. In HESI mode the auxiliary gas is heated to temperatures ranging between 50°C to 400°C to aid in solvent evaporation. These high temperatures can result in the loss of deuterium from the SIL analogues. Based on the relative abundances of the ions that constitute the isotopic profiles of the SIL analogues, we observed no significant changes in the intensities for temperatures up to 300°C. However, for temperatures greater than 300°C, a decrease in the intensities of the monoisotopic deuterated peaks for SIL analogues (m/z = 273 for deuterated genistein and m/z 256 for deuterated daidzein) in their isotopic profiles was observed. This was accompanied with a subsequent increase in the intensities of the monoisotopic peaks of genistein (m/z = 271) and daidzein (m/z 255) indicating a loss in deuteration. However, the vaporization temperature was maintained at 150°C during the duration of the SID-LC/MS analysis.

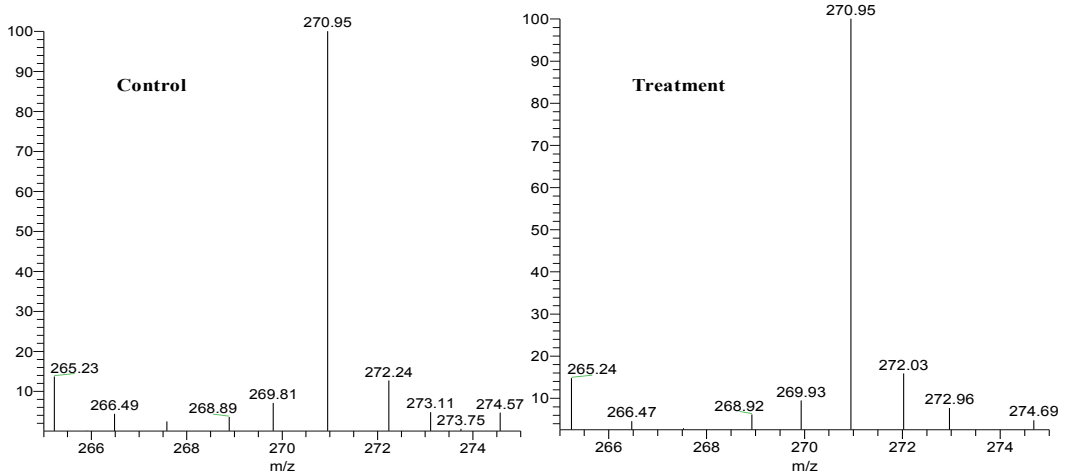

Figure 33. ESI-MS/MS analysis of the deuterated genistein in both control and treatment samples incubated at 37ºC for 60 min.

3.4.4. Proposed changes to SID-LC/MS methodology

One of the preemptive conditions for SID-LC/MS is the absence of mass overlap between the analyte of interest and its SIL analogue. However, due to the choice of the SIL analogues for genistein and daidzein in the present study there was an overlap between the naturally occurring isotopes of genistein/daidzein (M+1 or M+2 peaks) and their respective SIL analogues. For example, the base peak of the molecular ion of daidzein-d_1 (m/z = 256 in positive ion mode) has the same mass as the naturally occurring ^{13}C isotopic peak of daidzein (M+1 peak, m/z = 256, in positive ion mode). It is thus difficult to separate these two ions during SID-LC/MS analysis when operating the MS in either single ion monitoring (SIM) mode or MRM mode. This isotopic overlap will introduce an error during the calculation of the isotopic ratio and may lead to overestimation of the analytes of interest. The extent of the error, however, depends on the abundance of the naturally occurring isotopic peaks that contribute to an isotopic overlap. To correct for this error, the isotopic profiles of the individual compounds that undergo isotopic overlap during analysis must be determined. Based on theoretical calculations, using the MassLynx software (Micromass, Water's Associates, Milford, MA, USA), the isotopic overlap is 16% in the case of daidzein (M+1 peak) and 2.2% in the case of genistein (M+2 peak). Experimentally, the abundances of the naturally occurring isotopic peaks were calculated relative to the abundance of the monoisotopic peak. The theoretical and the experimental isotopic profiles were similar, with standard deviations less than <1% for the abundances of the monoisotopic as well as for the naturally occurring isotopic peaks.

Several strategies were proposed by various researchers to correct the isotopic overlap between compounds of interest during SID-LC/MS analysis (Liebish et al., 2004; Scherer et al., 2010; Haimi et al., 2009). Of these strategies, the subtraction method was chosen for the present study. In spite of being a straightforward approach in single ion monitoring mode, the subtraction method in the MRM mode is rather challenging (Ejsing et al., 2006). This is due to the fact that the distribution of the higher isotope in the [M+1] peak is random and hence the daughter ion formed upon fragmentation may or may not

contain the higher isotope in its structure (Figure 34). Depending upon the daughter ion chosen for the analyte (the choice of which varies among researchers) and its SIL analogue, the occurrence of the higher isotope in the daughter ion(s) follows a probabilistic behavior. Thus, in theory, the probability of the occurrence of the higher isotope in the daughter ion (13/15 as shown in Figure 34) has to be multiplied by the higher isotope peak abundance (16% in case of daidzein) in order to account for the isotopic overlap. Based on this theoretical approach, the daughter ion, especially for monodeutero SIL analogues can be chosen such that the error due to the isotopic overlap is at its minimum. While a theoretical understanding can be established we decided to experimentally eliminate the isotopic overlap.

Daidzein was analyzed separately using the same calibration protocol and the MRM transition of daidzein-d_1, which is equivalent to the M+1 peak of the naturally present ^{13}C isotope, was monitored. The area response obtained was subtracted from the corresponding area responses obtained from the calibration assay that included the SIL analogues. Following this approach the error caused by the isotopic overlap was successfully eliminated and the linearity of the standard curve for daidzein was improved from $R^2 = 0.95$ before compensating for isotopic overlap to a R^2 value > 0.99. A similar protocol was employed to compensate for the error caused due to the isotopic overlap between genistein and its SIL analogue, genistein-d_2. The obtained data strongly supported the viability of the isotopic correction strategy that was employed and subsequently provided a basis for the use of mono- or dideuterated internal standards for the quantification of isoflavones

3.4.5. Validation of the analytical assay

3.4.5.1. Linearity, accuracy and precision

All calibration curves were linear with R^2 values > 0.99 within the concentration range tested. Accuracy (in terms of % E_{rel}) for all the analytes of interest varied between -4.55% and 5.91% (Table 4). Intra-assay precision (in terms of % RSD) also varied between 0.95%

and 6.66% (Table 4). Instrument precision (re-injection repeatability) was also tested with % E_{rel} < 5% and % RSD < 8% (Table 5). Results indicated that the analytical method is both accurate and precise within the concentration range tested.

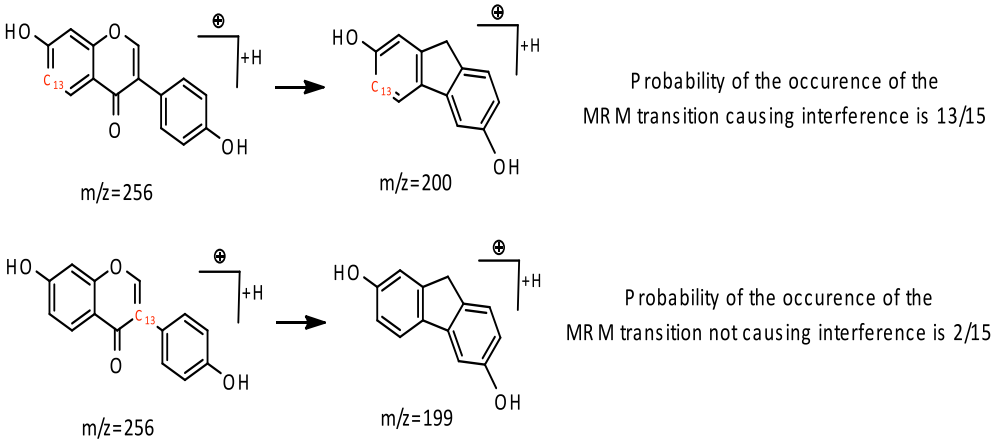

Figure 34. The probability of the occurrence of the higher isotope (13C) in the daughter ion (m/z = 200) of daidzein monitored in the MRM mode.

Table 4. Accuracy and precision of the developed analytical method determined upon analysis of three validation standards at 10, 200 and 750 µg/L.

	Nominal concentration (µg/L)	Calculated concentration (µg/L)	Accuracy (% E_{rel})	Precision (% RSD)
Genistein	10	9.63	-3.63	4.69
	200	193.29	-3.35	4.44
	750	787.99	5.03	3.66
Daidzein	10	10.33	3.37	0.95
	200	196.59	-1.71	1.98
	750	786.52	4.86	3.21
Equol	10	9.74	-2.56	2.88
	200	192.11	-3.94	5.43
	750	733.72	-2.17	5.42
Tamoxifen	10	10.56	5.67	1.43
	200	199.62	-0.186	6.66
	750	794.37	5.91	1.65
Raloxifene	10	10.47	4.77	1.56
	200	190.89	-4.55	3.58
	750	771.38	2.85	2.23

* % E_{rel} – Percent relative error; % RSD – Percent relative standard deviation

Table 5. Re-injection reproducibility data to determine instrument precision.

	First injection (µg/L)	Second injection (µg/L)	Accuracy (% E_{rel})	Precision (% RSD)
Genistein	9.95	9.92	-0.64	0.45
	190.95	190.21	-0.39	0.27
	780.33	798.3	2.23	1.56
Daidzein	10.26	9.67	-2.91	4.23
	193.38	195.99	0.67	0.94
	804.03	781.18	-1.42	2.03
Equol	9.54	10.63	5.71	7.63
	181.42	183.45	0.56	0.78
	727.24	691.39	-2.46	3.57
Tamoxifen	10.67	10.52	-1.41	2.03
	188.31	202.89	3.87	5.27
	808.35	770.29	-2.35	3.41
Raloxifene	10.59	10.51	4.77	1.56
	191.31	188.99	-0.61	0.86
	777.55	802.66	1.61	2.24

* % E_{rel} – Percent relative error; % RSD – Percent relative standard deviation

3.4.5.2. Stability

Working standards of the analytes were stable at room temperature (25°C) after 3 h with % E_{rel} < 5% and % RSD < 5% (Table 6). Working standards of the SIL analogues were also stable, as there was no significant change in their isotopic profiles before and after holding them at room temperature for 3 h. All validation standards were stable in the auto sampler after 12 h at 4°C, with % E_{rel} < 5.5% and % RSD <5% (Table 7).

3.4.5.3. Carry over

No carry over was observed. The concentration of the analytes observed after running a blank plasma extract was < 5% of that of the standard with the lowest concentration (1 µg/L).

Table 6. Stability of working standards of analytes (10 µg/L) held at room temperature (25°C) for 3 h.

	Concentration at 0 h (µg/L)	Concentration after 3 h (µg/L)	Accuracy (% E_{rel})	Precision (% RSD)
Genistein	10.11	9.89	-2.22	1.56
Daidzein	5.04	4.86	-3.70	2.57
Equol	10.15	10.03	-1.20	0.84
Tamoxifen	10.23	10.11	-1.19	0.83
Raloxifene	9.96	9.84	-1.22	0.86

* % E_{rel} – Percent relative error; % RSD – Percent relative standard deviation

Table 7. Stability the validation standards held in the auto sampler at 4°C for 12 h.

	Concentration at 0 h (µg/L)	Concentration after 12 h (µg/L)	Accuracy (% E_{rel})	Precision (% RSD)
	9.63	9.47	-1.63	1.16
Genistein	193.29	187.44	-3.02	2.17
	787.74	756.41	-3.97	2.87
	10.33	10.41	0.75	0.52
Daidzein	196.59	200.03	1.75	1.22
	786.52	819.22	4.15	2.88
	9.74	10.01	2.73	1.96
Equol	193.11	195.39	1.71	1.19
	733.72	732.98	-0.11	0.07
	10.56	10.96	3.81	2.63
Tamoxifen	199.62	189.56	-5.04	3.65
	794.37	785.53	-1.12	0.79
	10.47	10.53	0.51	0.36
Raloxifene	190.89	187.14	-1.96	1.41
	771.38	729.58	-5.41	3.93

* % E_{rel} – Percent relative error; % RSD – Percent relative standard deviation

3.4.6. Method application

The proposed analytical method was successfully applied in a rat system to quantitate the analytes of interest at concentrations within the linear range tested. Peak plasma concentration of daidzein (2.61 nmole/L) and genistein (9.11 nmole/L) was reached 4 h post ingestion of daidzin and genisten, respectively (Figure 35). Plasma concentration of equol continued to increase over time. The rate of disappearance of daidzein in the plasma was slower than that of genistein.

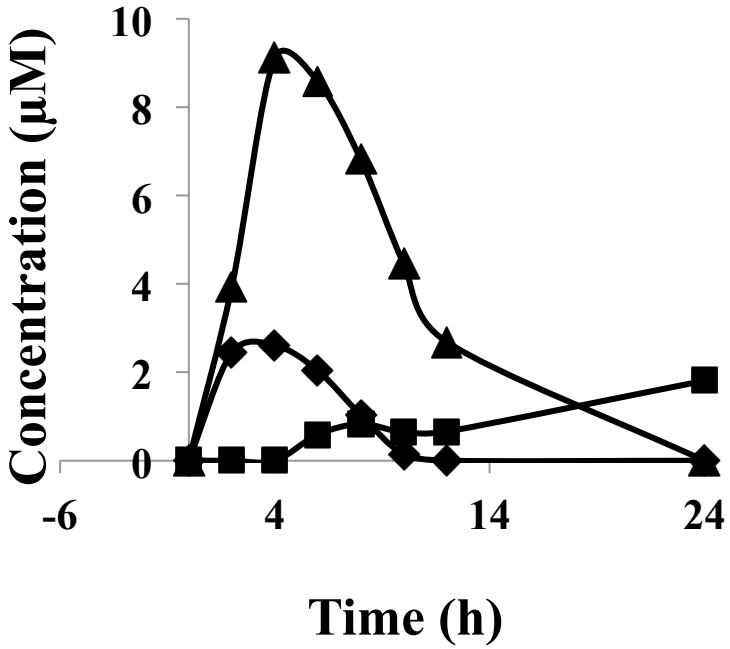

Figure 35. Plasma concentrations of daidzein (▲), genistein (■) and equol (♦) obtained from two male Wistar rats at 0, 2, 4, 6, 8, 10, 12 and 24 h after being gavaged with a single dose of either genistein or daidzein at a concentration of 100 µmole/kg body weight.

3.5 Conclusions

Two deuterated SIL analogues of daidzein and genistein were successfully produced using a novel and simple approach. The deuteration approach followed in this study

greatly reduced the efforts and costs associated with the preparation of SIL analogues following a syntheses-based approach using predeuterated starting materials. Results based on computational chemistry coupled with MS and NMR data confirmed the site and mechanism of deuteration. The produced SIL analogues, mono- and dideutero substituted at the ortho positions exhibited minimal deuterium isotopic effect, and were stable under the employed sample preparation protocol and MS analysis. Differential matrix effects due to the slight differences in retention times between SIL analogues and their respective analytes were minimal. A strategy to eliminate errors due to the isotopic overlap between the synthesized SIL analogues of isoflavones and their respective analytes of interest was developed in the MRM mode, thereby improving the accuracy of the proposed analytical method. Applying this unique isotopic overlap correction strategy will allow for the expanded use of similar SIL analogues in SID-LCMS analysis. This work provided, for the first time, a validated analytical SID-LC/MS method to detect natural and known synthetic SERMs in a single analytical assay. The method proved to be sensitive, selective, rapid and accurate. Such analytical method would be valuable for the research focused on determining the bioavailability of individual SERMs and the effect of isoflavones on tamoxifen/raloxifene metabolic pathways and vice-versa.

4. EFFECT OF MALONYL- CONJUGATION ON THE BIOAVAILABILITY OF ISOFLAVONES

4.1. Overview

Bioavailability of the malonylglucoside form of isoflavones and their respective non-conjugated glucosides was determined in rats. Rats were gavaged with an assigned isoflavone form on an equi-molar basis. Blood and urine samples were collected at different time intervals. Isoflavone metabolites in plasma were determined using SID-LCMS analysis. Bioavailability was determined by calculating pharmokinetic parameters such as $C_{max\ and}$ AUC, assuming first order disposition kinetics. The pharmokinetic parameters obtained for malonylglucoside forms differed significantly from their respective non-conjugated β-glucosides. The AUC values of the respective aglycones and equol in the plasma and urine obtained after the administration of non-conjugated β-glucosides were 2-6 times greater than those of their respective malonylglucosides, indicating that non-conjugated β-glucosides are relatively more bioavailable than their respective malonylglucosides. The lower initial absorption rates of malonylglucosides, when compared to non-conjugated glucosides, confirmed that the malonyl group hinders the extent and rate of malonylglucoside hydrolysis by β-glucosidases to their respective aglycones, and consequently limits their absorption. Thus, structural differences among isoflavone glucosides in evaluating their bioavailability. Obtaining bioavailability data for all major isoflavone forms and determining the differences in their bioavailability will help understand discrepancy in the reported isoflavone clinical research.

4.2. Introduction

Isoflavones have gained considerable attention over the past 20 years due to their association with prevention of cancer, cardiovascular diseases, osteoporosis, postmenopausal symptoms, and their putative anti-inflammatory activity (Cohen et al., 2000; Kwon et al., 1998; Lamartiniere et al., 1995; Song et al., 1999; Setchell et al., 1998; Messina, 1999). However, the demonstration of these physiological effects by isoflavones is highly inconsistent. Several studies have reported negative or marginal effects of isoflavones on the aforementioned conditions and diseases (Alekel et al., 2010; Weaver et al., 2009; Lethaby et al., 2007; Jacobs et al., 2009; Campagnoli et al., 2005; Khaodhiar et al., 2008; Upmalis et al., 2000; Burke et al., 2000). These inconsistent results could be attributed to many factors including but not limited to ethnic background, age, gender, gut microflora and source of isoflavones. The source of isoflavones can drastically affect the results, especially when different isoflavone forms are administered at different levels without accounting for differences in their relative bioavailability.

For isoflavones to be bioavailable, they must undergo hydrolysis to their respective aglycones by gut and microbial enzymes, mainly β-glucosidases (Xu et al., 1994; King and Bursill, 1998, Setchell et al., 2001; Walle et al., 2005). Upon hydrolysis, the aglycones pass through the intestinal epithelium and undergo conjugation, mainly sulfonation or glucuronidation (Liu et al., 2002). Intestinal microflora also produces metabolites, such as equol and p-ethyl phenol, that are predominantly used as bio-markers to predict isoflavone bioavailability (Turner et al., 2003).

Based on pharmokinetic data, Zhang et al. (1999) showed that genistein is more bioavailable than diadzein. Xu et al. (2000), on the other hand, found the opposite (King, 1999). Due to these and other contradictory results, there is no consensus among researchers as to which form of isoflavone is more bioavailable. The inconclusiveness about the effect of isoflavone chemical structure on bioavailability escalated when some researchers reported that isoflavones are more bioavailable when ingested in β-glucosidic forms as compared to the aglycone forms (Setchell et al., 2001; Rufer et al., 2008), while some reported the opposite (Izumi et al., 2002) and others found no significant difference

(Zubik and Meydani, 2003). These inconsistencies in predicting the effect of chemical structure on isoflavone bioavailability can be largely attributed to lack of accurate profiling of the ingested isoflavone forms and the use of different sources.

Investigators who had performed isoflavone bioavailability experiments often did not discuss the composition of the diet (King and Bursill, 1998; Rufer et al., 2008; Sepehr et al., 2009). When comparing the bioavailability of β-glucosides to that of aglycones, it was not clear whether the administered β-glucosids mainly conjugated (namely malonylglucosides) and/or non-conjugated β-glucosides (Zubik and Meydani, 2003). Our in vitro studies confirmed that bacterial β-glycosidase can hydrolyze completely the non-conjugated glucosides into aglycones, however, it is not effective in hydrolyzing the malonyl- and acetyl- glucosides, even with prolonged incubation and increased levels of the enzyme (Ismail and Hayes, 2005). Because enzyme activity is structure specific, conjugation on the sixth carbon of the glucose moiety might give rise to steric hindrance, which reduces drastically the rate at which β-glucosidases can hydrolyze conjugated β-glucosides (Ismail and Hayes, 2005). Therefore, ingesting a mixture of conjugated and non-conjugated glucosides (Izumi et al., 2002; Zubik and Meydani, 2003) vs. only non-conjugated glucosides (Setchell et al., 2001) will obviously lead to the noted discrepancies in the bioavailability reports. Despite their abundant nature (> 50% of total isoflavones in some soy products), no attempt was made to determine the in-vivo bioavailability of malonylglucosides compared to their non-conjugated counterparts.

The National Institute of Health (NIH) conducted a scientific workshop to address the conflicting results in the current isoflavone research ((Klein et al., 2010). The inadequate profiling of isoflavones and the lack of standardization of the source of isoflavones (different soy matrices and supplements) were among the main highlighted limitations in the current isoflavone research (Klein et al., 2010). Therefore, to address these limitations, the objective of this study was to determine the effect of malonyl conjugation on isoflavone bioavailability by comparing the pharmokinetic parameters of malonyldaidzin and malonylgenistin to that of their non-conjugated counterparts in a model rat system.

4.3. Materials and methods

4.3.1 Materials

High performance liquid chromatography (HPLC) grade acetonitrile and methanol were purchased from Fisher Scientific (Hanover Park, IL, USA). The isoflavones genistein, equol and daidzein were purchased from LC Laboratories (Woburn, MA, USA). Sulphatase/glucuronidase enzyme (S9626), deuterated methanol (CD_3OD), and deuterium oxide (D_2O) were purchased from Sigma Aldrich (St. Louis, MO, USA). Sulphatase/glucuronidase enzyme solution was prepared in sodium citrate buffer (0.01 M, pH 5.0) to a final enzyme activity of 500 U/mL of sulphatase and ~15,000 U/mL of glucuronidase. Equol-d_4 was purchased from Toronto research chemicals (North York, Ontario, Canada). Control rat plasma was generously donated by Professor Daniel Gallaher (University of Minnesota, St. Paul, US).

4.3.2. Reference standards

Reference standards of genistein, daidzein, equol, deuterated standards of daidzein and genistein, equol-d_4 were prepared in 80% aqueous methanol solution (500 mg/L). Reference standards of genistein and daidzein (500 mg/L) were also prepared in deuterated methanol (CD_3OD) for the production of their respective deuterated standards.

4.3.3. Working standards

Reference standards were diluted in 80% aqueous methanol solution to obtain working standards. Working standards for calibration were (1) a cocktail of the analytes (genistein, daidzein, equol) at concentrations ranging from 20 µg/L - 18 mg/L, and (2) a cocktail of all the respective internal standards at a concentration of 6 mg/L.

4.3.4. Extraction of malonylglucosides and their respective non-conjugated β-glucosides from soy grits

Isoflavones were extracted from ground soy grits using 53% (v/v) aqueous acetonitrile solution following the method outlined by Yerramsetty et al. (2011) and Malapally and Ismail (2010), with some modifications. A sample (0.05 g) was mixed with 9 mL of deionized distilled water (DDW), followed by the addition of 10 mL acetonitrile. The samples then were stirred (400 rpm) at room temperature (23°C) for 2 h. Extracts were centrifuged at 13,750 x g for 10 min at 15°C, and the supernatant was filtered through Whatman no. 42 filter paper. Acetonitrile from the filtrates was evaporated using a rotary evaporator at 37°C for 15 min. Subsequently, solid phase extraction (SPE) was used to extract isoflavones from the aqueous concentrated extract. Isoflavones were extracted using a Waters 500 mg Sep-Pak®C_{18} cartridge system (Waters Associates, Milford, MA) following a retention-cleanup-elution strategy. Briefly, Sep-Pak®Cl8 cartridges were preconditioned with 3 mL of 80% aqueous methanol (MeOH), followed by 3 mL of DDW. An aliquot (2 mL) of the sample was then passed through the cartridges at a flow rate of 5 mL/min, followed by rinsing with 3 mL DDW. Finally, isoflavones were recovered by passing 2 mL of 80% aqueous MeOH. The concentrated extracts were stored at -20°C in amber glass bottles until further analysis.

4.3.5. Semi-preparative isolation of malonylglucosides and their respective non-conjugated glucosides

Isoflavones of interest were separated on a semi-preparative scale following the method outlined by Yerramsetty et al. (2011). A Shimadzu HPLC system was used equipped with SIL-10AF auto injector, two LC-20AT high pressure pumps, SPD-M20A photo diode array detector (PDA) and a CTO-20A column oven. The column used was a 250 mm x 10 mm i.d., 5 µm, YMC pack ODS AM-12S RP-18 column, with a 10 mm x 10 mm guard column of the same material (YMC pack ODS AM). An aliquot (500 µL) of the isoflavone extract was filtered through a 0.45 µm syringe filter and injected onto the column. A linear HPLC gradient at a flow rate of 3.5 mL/min was used: Solvent A was HPLC grade water, and solvent B was acetonitrile, both containing 0.1% (v/v)

glacial acetic acid. The initial gradient concentration was 15% solvent B, which was linearly increased to 18% in 25 min, kept constant for 5 min, linearly increased to 30% in 10 min, kept constant for 3 min, linearly increased to 90% in 2 min, and kept constant for 8 min, followed by column equilibration steps. The temperature was maintained at 45°C. Absorbance spectra were monitored over a UV wavelength range of 190-370 nm. The fractions containing malonylgenistin, malonyldaidzin, genistin and daidzin were collected individually and lyophilized. Several runs were performed and the collected fractions of each isoflavone were pooled. Solutions (~500 mg/L) each of the lyophilized isoflavone fraction were prepared in 100% (DMSO)-d_6 for nuclear magnetic resonance (NMR) analysis to confirm their identity and purity. The remaining isoflavone fractions were stored at -80 ºC until their use for the oral administration in rats.

4.3.6. Nuclear Magnetic Resonance (NMR) analysis of isoflavones

NMR experiments were carried out on a Bruker 700 MHz Avance spectrometer (Rheinstetten, Germany) equipped with a 5 mm TXI proton-enhanced cryoprobe. Structure identification was performed by using the usual array of one- and two-dimensional NMR experiments (1H, H,H-COSY, HSQC, HMBC). Carbon data were taken from the less time-consuming 2D experiments HSQC and HMBC instead of performing 1D 13C experiments. All the data was acquired in (DMSO)-d_6. Chemical shifts (δ) were referenced to the central solvent signal of (DMSO)-d6 (δH 2.50 ppm) (Gottlieb, et al., 1997). J values are given in hertz. NMR assignments follow the numbering shown in Figure 27.

6’’-O-Malonylgenistin (700 MHz, DMSO-d_6): malonylated β-D-glucose: H1’’: 5.12 (d, J = 7.5 Hz); H2’’: 3.30, H3’’: 3.34; H4’’: 3.20 H5’’: 3.76, H6’’: 4.36, 4.13, malonyl-CH2: 3.38; aglycone: H2: 8.40 (s), H6: 6.48 (s), H8: 6.71 (s), H2’/H6’: 7.40 (d, J = 8.4 Hz), H3’/H5’: 6.83 (d, J = 8.4 Hz). (176 MHz, DMSO-d6): malonylated β-D-glucose: C1’’: 99.9, C2’’: 72.7, C3’’: 76.2, C4’’: 69.9, C5’’: 74.3, C6’’: 64.3, malonyl-COOR: 167.0, malonyl-CH2: 42.3, malonyl-COOH: 168; aglycone: C2: 157.5, C3: 123.0, C4: 181.2, C4a: 106.6, C5: 162.5, C6: 99.8, C7: 163.4, C8: 94.3, C8a: 157.1, C1’: 123.0, C2’/C6’: 130.7, C3’/C5’: 115.5, C4’: 158.2

6’’-O-Malonyldaidzin (700 MHz, DMSO-d_6): malonylated β-D-glucose: H1’’: 5.14 (d, J = 7.1 Hz); H2’’: 3.29, H3’’: 3.33; H4’’: 3.22 H5’’: 3.75, H6’’: 4.37, 4.10, malonyl-CH2: 3.35; aglycone: H2: 8.36 (s), H5: 8.06 (s), H6: 7.14 (s), H8: 7.23 (s), H2’/H6’: 7.40 (d, J = 8.3 Hz), H3’/H5’: 6.82 (d, J = 8.3 Hz). (176 MHz, DMSO-d6): malonylated β-D-glucose: C1’’: 100.2, C2’’: 72.7, C3’’: 76.9, C4’’: 70.2, C5’’: 74.5, C6’’: 64.5, malonyl-COOR: 167.0, malonyl-CH2: 42.7, malonyl-COOH: 169.6; aglycone: C2: 154.5, C3: 124.2, C4: 175.5, C4a: 118.9, C5: 128.1, C6: 115.5, C7: 161.8, C8: 104.2, C8a: 157.8, C1’: 122.7, C2’/C6’: 131.2, C3’/C5’: 115.2, C4’: 157.8

Genistin (700 MHz, DMSO- d_6): β-D-glucose: H1’’: 5.08 (d, J = 7.5 Hz); H2’’: 3.26, H3’’: 3.31; H4’’: 3.17 H5’’: 3.46, H6’’: 3.71, 3.48; aglycone: H2: 8.44 (s), H6: 6.48 (d, J = 2.2 Hz), H8: 6.73 (d, J = 2.2 Hz), H2’/H6’: 7.41 (d, J = 8.4 Hz), H3’/H5’: 6.83 (d, J = 8.4 Hz). (176 MHz, DMSO-d6): β-D-glucose: C1’’: 100.2, C2’’: 74.1, C3’’: 77.3, C4’’: 69.9, C5’’: 78, C6’’: 61.4; aglycone: C2: 153.8, C3: 122.9, C4: 181.2, C4a: 106.5, C5: 162.4, C6: 99.7, C7: 163.4, C8: 94.8, C8a: 157.1, C1’: 123.0, C2’/C6’: 131.6, C3’/C5’: 115.1, C4’: 158.1

Daidzin (700 MHz, DMSO- d_6): β-D-glucose: H1’’: 5.11 (d, J = 7.2 Hz); H2’’: 3.31, H3’’: 3.32; H4’’: 3.19 H5’’: 3.48, H6’’: 3.72, 3.47; aglycone: H2: 8.40 (s), H5: 8.05 (s), H6: 7.15 (s), H8: 7.24 (s), H2’/H6’: 7.41 (d, J = 8.4 Hz), H3’/H5’: 6.83 (d, J = 8.4 Hz). (176 MHz, DMSO-d6): β-D-glucose: C1’’: 100.6, C2’’: 74.1, C3’’: 77.4, C4’’: 70.0, C5’’: 78.1, C6’’: 61.6; aglycone: C2: 155.3, C3: 124.0, C4: 175.5, C4a: 118.6, C5: 128.2, C6: 115.5, C7: 161.9, C8: 104.0, C8a: 157.8, C1’: 122.9, C2’/C6’: 131.6, C3’/C5’: 114.7, C4’: 157.8

Genistein (700 MHz, DMSO- d_6): H6, 6.21 (d, 2.4 Hz); H8, 6.37 (d, 2 Hz); H3’ and H5’, 6.81 (d, 8.4 Hz); H2’ and H6’, 7.36 (d, 8.4 Hz); H2, 8.31 (s); C4’-OH, 9.57 (s); C7-OH, 10.86 (s); C5-OH, 12.94 (s).

Deuterated genistein (700 MHz, DMSO- d_6): H3’ and H5’, 6.81 (d, 8.4 Hz); H2’ and H6’, 7.36 (d, 8.4 Hz); H2, 8.31 (s); C4’-OH, 9.56 (s); C7-OH, 10.85 (s); C5-OH, 12.93 (s).

Daidzein (700 MHz, DMSO- d_6): H3’ and H5’, 6.81 (d, 8.4 Hz); H8, 6.85 (s); H6, 6.93 (d, 8.9 Hz); H2’ and H6’, 7.38 (d, 8.4 Hz); H5, 7.96 (d, 8.7 Hz); H2, 8.28 (s); C4’-OH, 9.53 (s); C7-OH, 10.78 (s).

Deuterated daidzein (700 MHz, DMSO- d_6): H3' and H5', 6.80 (d, 8.4 Hz); H6, 6.93 (d, 8.9 Hz); H2' and H6', 7.38 (d, 8.4 Hz); H5, 7.96 (d, 8.7 Hz); H2, 8.28 (s); C4'-OH, 9.53 (s); C7-OH, 10.78 (s).

4.3.7. Preparation of genistein and daidzein deuterated standards

Genistein and daidzein were individually dissolved in 5% (v/v) aqueous deuterated methanol containing 0.1% deuterated formic acid (25 mg/L). Genistein solution was incubated for three days, while daidzein solution was incubated for five days in a heating block maintained at 90°C. After incubation, deuterated isoflavones were separated from the reaction volume using Sep-PakTM C_{18} reverse-phase cartridges (Water's Associates, Milford, MA, USA). Before sample loading, Sep-PakTM C_{18} cartridges were primed with 2 mL of methanol, followed by conditioning with same volume of DDW. The sample was then loaded onto the cartridge and the deuterated formic acid was subsequently washed with 3 mL DDW. The deuterated isoflavones were recovered with 1.2 mL of methanol, which aids in reinstating the protic hydroxyl groups via H/D back exchange. Methanol was subsequently evaporated using a speed-vac (Savant, DNA110), and the residue was re-dissolved in dimethylsulfoxide (DMSO)-d_6 and immediately analyzed by NMR. Based on NMR data (Data submitted for publication elsewhere), the structures of the deuterated standards of genistein and daidzein were deduced to be 6,8-dideutero-5,7-dihydroxy-3-(4-hydroxyphenyl) chromen-4-one (genistein-d_2) and 8-monodeutero-7-hydroxy-3-(4-hydroxyphenyl) chromen-4-one (daidzein-d_1), respectively. The isotopic purity of the deuterated standards was ~ 98%.

4.3.8. Animal study design

Charles River male Wistar rats (24 in total) aged 4 weeks (75-100 g) were divided into four treatment groups (6 rats per treatment). Based on power analysis, the variability within each treatment group was expected to be between 10% and 50%. Assuming the larger variability, with 6 rats per treatment, we anticipated a detection of 45% difference with

80% power and a significance level of 0.05, using a one-way ANOVA with Tukey-HSD correction for multiple comparisons. Analysis was performed on the log2 scale, where a variability of 50% is a range of 1 unit, so the within group standard deviation was estimated to be 2.25 μmol/L based on plasma genistein concentrations at 2 h after an oral dose(32). All animals were housed and cared for in the Research Animal Resources (RAR) facility by trained personnel. All protocols were approved by the Institutional animal Care and Use Committee (IACUC). The animals were subjected to an adjustment period of 10 days to remove any traces of isoflavones from their system. During the adjustment period the rats were fed a casein-based diet following the formulation described by the American Institute of Nutrition (AIN – 93M). The non-fasted rats were housed individually in stainless steel mesh cages in a temperature-controlled room (22–23 °C) with a 12 h light–dark cycle and feed and water ad libitum. Rats in each treatment group were gavaged with one of the four isoflavones (malonylgenistin, genistin, malonyldaidzin or daidzin) at a dose of 100 μmole/kg body weight. Isoflavones were suspended in water (500 μL) and vortexed prior to gavaging. The isoflavone dosage amount was calculated based on the human energy equivalent intake of 12.50 mg, which falls within the range of daily average human intake of isoflavones (2-50 mg/day). Blood (100 μL) from the saphenous vein of each rat was collected into lithium heparin microtainers at 0, 2, 4, 6, 8, 12 and 24 h for daidzin; 0, 3, 6, 9, 12, 15, 24, 30 and 48 h for malonyldaidzin; 0, 2, 4, 6, 8 and 12 h for genistin and 0, 2, 3, 6, 9 and 12 h for malonylgenistin. Blood collected at 0 h before the oral administration of the assigned treatment was used as the control. Collected blood was centrifuged for 3 min at 4°C, 6000 × g, and plasma was collected and stored at -80°C until analysis. Urine was also collected at 0, 6, 12, 24, 36 and 48 h and stored at -80°C until analysis. At the end of the study, the rats were euthanized with carbon dioxide and donated to the raptor center at the University of Minnesota.

4.3.9. Stable isotope dilution liquid chromatography mass spectrometry (SID-LC/MS) analysis

SID-LC/MS analysis was conducted on an ultra-high pressure LC system (Shimadzu UFLC XR) online with a triple stage quadrupole mass spectrometer (5500 QTRAP, AB Sciex, Washington, D.C., USA) equipped with a 50 × 2.1 mm inner diameter, 5 µm, YMC C18 column. The column temperature was maintained at 25°C. An injection volume of 5 µL was chosen. A linear binary gradient at a flow rate of 0.4 mL/min with water and acetonitrile as solvents were used, with each containing 0.1% formic acid. The initial gradient concentration was 20% acetonitrile, which was kept constant for one min, linearly increased to 95% in 4.50 min, kept constant for one min, followed by column equilibration steps. The LC column eluate entered the electrospray ionization (ESI) interface of the mass spectrometer operating in the positive ion mode. The MS parameters were: sheath gas (N_2, 99.99%, flow rate = 20 units); vaporization temperature 150°C; collision cell exit potential 17 V; spray voltage 4.5 kV; entrance potential 10 V; declustering potential 55 V; collision energy 28 units. Acquisition was carried out in multiple reaction monitoring (MRM) mode, so as to achieve maximal sensitivity and reliable quantitation over several orders of magnitude of compound abundance (Sawada et al., 2009; Bhat et al., 2011). The MRM transitions of the analytes of interest are summarized in Table 8. Concentrations of isoflavones were calculated based on peak areas integrated by MultiQuant™ (version 2.0.2).

4.4.10. Calibration

An aliquot (10 µL) of each of six working standards containing genistein, daidzein and equol (20 µg/L, 1 mg/L, 2mg/L, 6mg/L, 12mg/L and 18 mg/L) and an aliquot (10 µL) of the cocktail containing their respective deuteriated standards (6 mg/L) were added, in triplicate, to 20 µL of control rat plasma, which was then subjected to the extraction procedure described above. The final concentrations of the isoflavones in the standard extracts were 1, 50, 100, 300, 600 and 900 µg/L, and the final concentration of their respective deuterated standards in each standard extract was 300 µg/L. All standards were analyzed following the SID-LC/MS method described above. Calibration curves were obtained by plotting the response ratio of the variable analyte to that of the constant

internal standard against the analyte concentration. Analyte response was measured in the MRM mode. An additional step was included to correct for the isotopic overlap between genistein/daidzein and their respective deuterated standards. Daidzein and genistein were run separately in the absence of their respective deuterated standards, and the MRM transitions of their natural isotopic peaks, which can interfere with their respective deuterated standards, were monitored. Subsequently, the obtained responses were subtracted from that obtained from the calibration.

Table 8. Multiple reaction monitoring (MRM) transitions of all the compounds used in the present study.

Analyte	MRM transitions	
	Q1* mass	Q3^ mass
Genistein	271	153
Genistein-d_2	273	155
Daidzein	255	199
Daidzein-d_1	256	200
Equol	243	105
Equol-d_4	247	108

* first quadrupole; ^ third quadrupole

4.3.11. Calculation of pharmokinetic parameters

Areas under the curves (AUC) were calculated using the software Prism (Version 6, GraphPad Software, Inc.) that employs trapezoidal rule to calculate AUC. Absorption rates and elimination rates were calculated as the slope of the concentration vs. time curves between two consecutive time points. For instance initial absorption rate was calculated as the slope of the concentration vs. time curve from 0 h to the subsequent time point which is 2 h in case of daidzin, malonlgenistin and genistin and 3 h in case of malonyldaidzin.

4.3.12. Statistical analysis

Analysis of variance (ANOVA) was carried out utilizing SPSS 20 for Windows (Version 11.5). When a factor effect or an interaction was found significant, indicated by a significant F test ($P \leq 0.05$), differences between the respective means (if more than 2 means) were determined using Tukey-Kramer multiple means comparison test.

4.4. Results

4.4.1. Plasma and urinary pharmokinetics of daidzein post the oral administration of daidzin and malonyldaidzin

Post the oral administration of the daidzin and malonyldaidzin isoflavone, daizein was detected in the plasma and urine extracts; however, marked differences were noted in the pharmokinetic parameters (Figure 36, A and B). Based on the plasma data, the initial rate of absorption of daidzein calculated between 0-2 h post the administration of daidzin was 2.5 μM/h, while that of daidzein calculated between 0-3 h post the administration of malonyldaidzin was ~ 3 times lower (0.85 μM/h). After 2 h of the administration of daidzin, the rate of absorption decreased to 0.58 μM/h, as calculated between 2-4 h. Plasma concentration of daidzein post the administration of daidzin reached its peak (C_{max} = 6.09 ± 1.24 μM) after 4 h (t_{max}). The C_{max} of daidzein post the administration of malonyldaidzin (2.84 ± 0.67 μM) was significantly ($P \leq 0.05$, ANOVA Table 12, Appendix D) lower than that post the administration of daidzin (Table 9, ANOVA Table 12, Appendix D). After 4 h of the administration of daidzin and malonyldaidzin, the rate of elimination of daidzein was 1.41 μM/h and 0.25 μM/h, respectively. Daidzein concentrations dropped to insignificant levels after 12 h of the oral dosage (Figure 36 A).

Upon administration of daidzin, urine concentration of daidzein (24.13 ± 0.18 nmoles) reached a maximum between 0 to 6 h, followed by a significant decrease after 12 h, and approached zero after 36 h (Figure 36 B). On the other hand, after administration of malonyldaidzin, urine concentration of daidzein peaked between 0 to 6 h reaching a concentration of only 1.66 ± 0.02 nmoles, followed by a significant decrease, approaching zero after 12 h (Figure 36 B).

The bioavailability of daidzin, in terms of AUC for daidzein in the plasma (84.11 ± 5.17 μM.hr), was significantly higher (~ 2 times, $P \leq 0.05$, ANOVA Table 12, Appendix D) than that of malonyldaidzin (40.63 μM.hr) (Table 9). Urine data demonstrated a complementary trend in the bioavailability of daidzin vs. malonyldaidzin (Table 10). The urinary AUC of daidzein (15.03 ± 2.39 nmoles.hr) post the administration of daidzin was significantly greater ($P \leq 0.05$, ANOVA Table 12, Appendix D) than that post the administration of malonyldaidzin (0.44 ± 0.77 nmoles.hr).

4.4.2. Plasma and urinary pharmokinetics of equol post the oral administration of daidzin and malonyldaidzin

Equol plasma and urine concentrations at various time points post the administration of daidzin were significantly different ($P \leq 0.05$, ANOVA Table 13, Appendix E) than those observed post the administration of malonyldaidzin (Figure 37, A and B). Post the administration of daidzin, plasma equol concentration continued to increase over time, reaching 1.52 ± 0.29 μM at the 24 h time point. Data was not collected beyond the 24 h time point, thus accurate calculation of C_{max} and rate of elimination cannot be achieved. On the other hand, while equol concentration seemed to peak (C_{max} = 0.09 ± 0.09 μM) at 30 h post the administration of malonyldaidzin, no significant differences were observed in equol concentration across the different time points, including the control.

Urine concentration of equol post oral administration of daidzin reached a maximum (11.01 ± 2.33 nmole) between 12 to 24 h, followed by a significant decrease, approaching zero after 36 h (Figure 36 B). A similar trend was observed for daidzein after the administration of malonyldaidzin, however, the maximum diadzein concentration reached was only 5.75 ± 0.84 nmoles, followed by a significant decrease, approaching zero after 36 h. The plasma and urine AUC data of equol complemented that of daidzein post the administration of daidzin and malonyldaidzin (Tables 9 and 10, ANOVA Table 13, Appendix E).

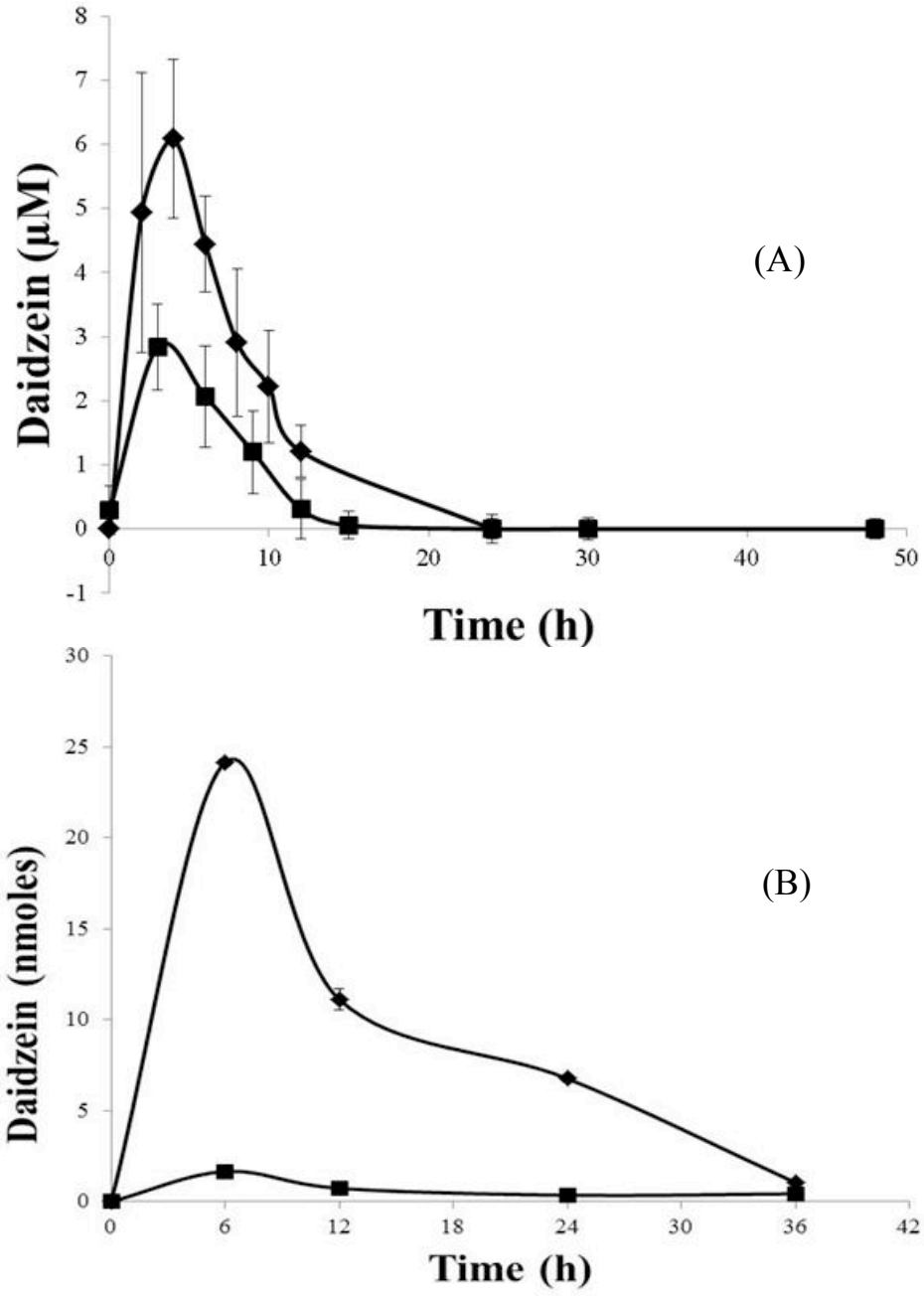

Figure 36**.** (A) Mean (± SD) plasma concentrations (µM) and (B) mean (± SD) urine concentrations (nmoles) of daidzein in 12 rats at 0, 2, 4, 6, 8, 12 and 24 h and 0, 3, 6, 9, 12, 15, 24, 30 and 48 h following a single intake of 100 µmole/kg body weight of daidzin (♦) and malonyldaidzin (■), respectively.

Table 9. Maximum plasma concentrations (C_{max}), mean area under the curves (AUC) of daidzein and equol after the ingestion of daidzin and malonyldaidzin, and of genistein after ingestion of genistin and malonylgenistin.

	Ingested Isoflavone	
Pharmokinetic parameters of daidzein	**Daidzin**	**Malonyldaidzin**
Plasma Data		
C_{max} (μM)	6.09 ± 1.24 a	2.84 ± 0.67 b
AUC (μM.hr)	84.11 ± 5.17 a	40.63 ± 9.45 b

	Ingested Isoflavone	
Pharmokinetic parameters of equol	**Daidzin**	**Malonyldaidzin**
Plasma Data		
C_{max} (μM)	1.52 ± 0.29 a	0.09 ± 0.09 b
AUC (μM.hr)	14.76 ± 2.23 a	2.11 ± 0.68 b

	Ingested Isoflavone	
Pharmokinetic parameters of genistein	**Genistin**	**Malonylgenistin**
Plasma Data		
C_{max} (μM)	7.87 ± 2.83 a	3.94 ± 1.26 b
AUC (μM.hr)	57.04 ± 14.38 a	22.36 ± 4.74 b

Means in each raw, followed by the same letter, are not significantly different according to ANOVA ($P \leq 0.05$).

Table 10. Maximum urine concentrations (C_{max}), mean area under the curves (AUC) of daidzein and equol after the ingestion of daidzin and malonyldaidzin, and of genistein after ingestion of genistin and malonylgenistin.

	Ingested Isoflavone	
Pharmokinetic parameters of daidzein	**Daidzin**	**Malonyldaidzin**
Urine Data		
C_{max} (nmoles)	24.13 ± 0.18 a	1.66 ± 0.02 b
AUC (nmoles.hr)	15.03 ± 2.39 a	0.44 ± 0.77 b
	Ingested Isoflavone	
Pharmokinetic parameters of equol	**Daidzin**	**Malonyldaidzin**
Urine Data		
C_{max} (nmoles)	11.01 ± 2.33 a	5.75 ± 0.84 b
AUC (nmoles.hr)	53.03 ± 15.18 a	13.72 ± 2.92 b
	Ingested Isoflavone	
Pharmokinetic parameters of genistein	**Genistin**	**Malonylgenistin**
Urine Data		
C_{max} (nmoles)	36.62 ± 3.73 a	10.68 ± 2.03 b
AUC (nmoles.hr)	67.22 ± 27.17 a	41.73 ± 26.56 b

Means in each raw, followed by the same letter, are not significantly different according to ANOVA ($P \leq 0.05$).

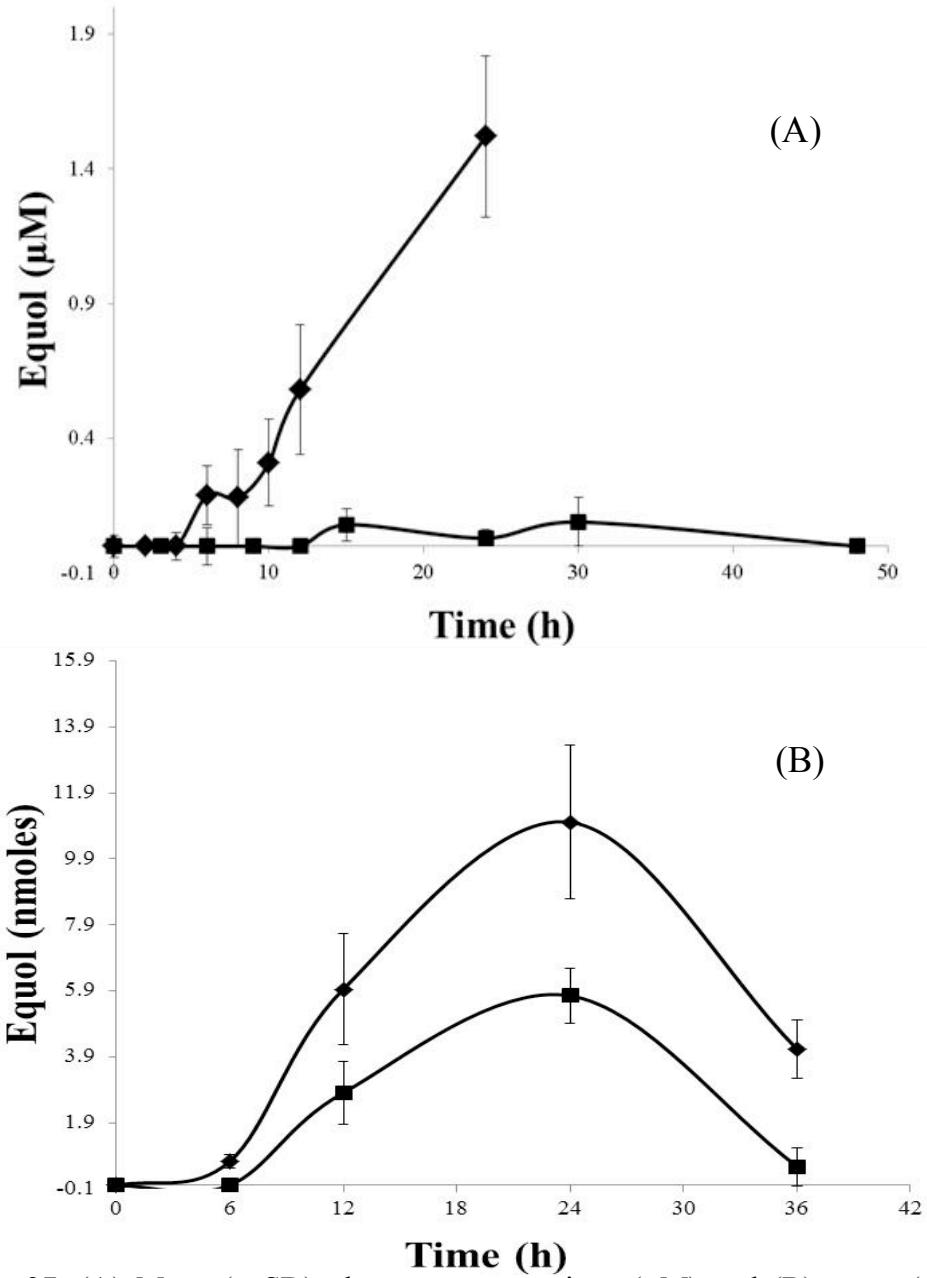

Figure 37. (A) Mean (± SD) plasma concentrations (µM) and (B) mean (± SD) urine concentrations (nmoles) of equol in 12 rats at 0, 2, 4, 6, 8, 12 and 24 h and 0, 3, 6, 9, 12, 15, 24, 30 and 48 h following a single intake of 100 µmole/kg body weight of daidzin (♦) and malonyldaidzin (■), respectively.

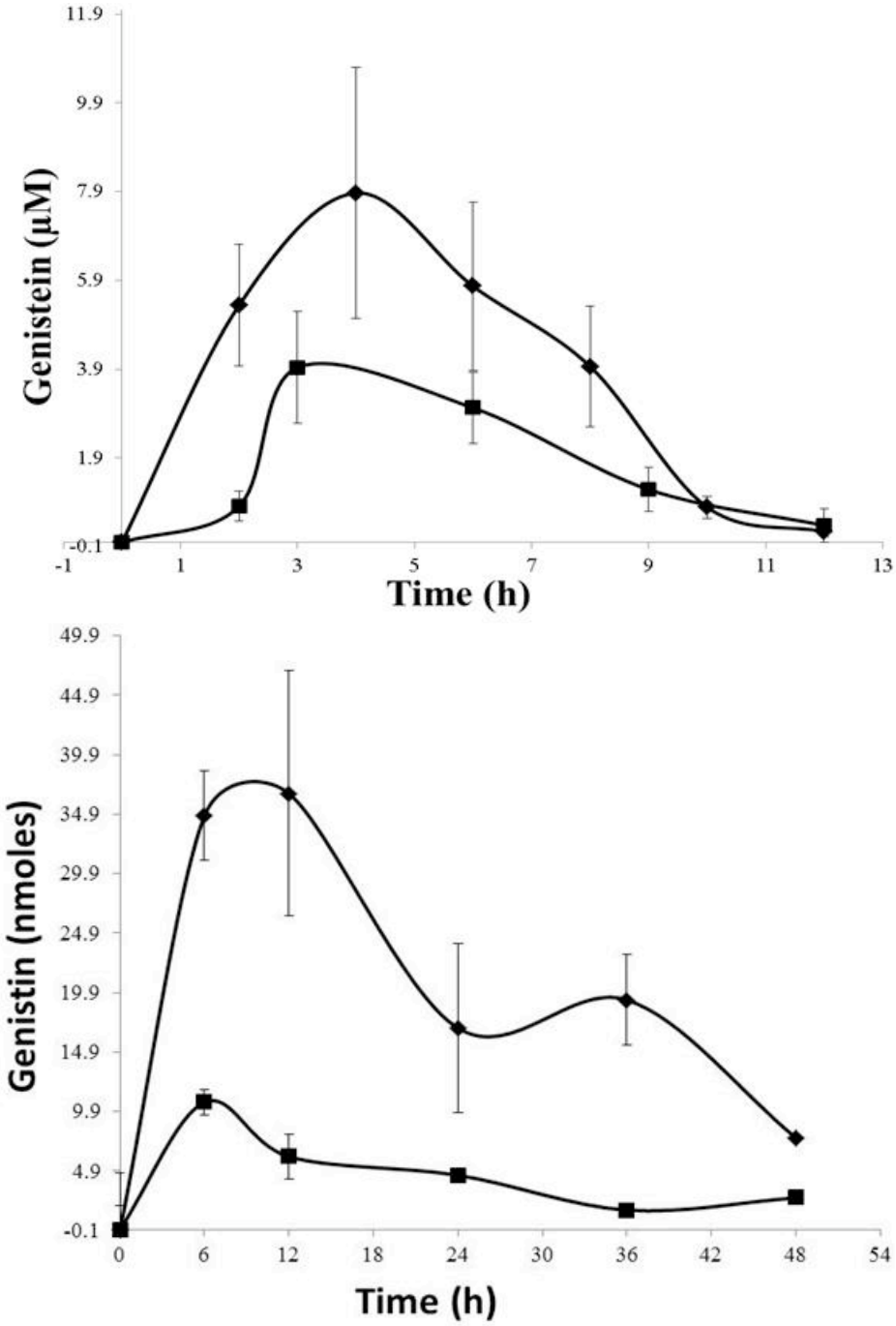

Figure 38. (A) Mean (± SD) plasma concentrations (µM) and (B) mean (± SD) urine concentrations (nmoles) of genistein in 12 rats at 0, 2, 4, 6, 8 and 12 h for genistin and 0, 2, 3, 6, 9 and 12 h, following a single intake of 100 µmole/kg body weight of genistin (♦) and malonylgenistin (■), respectively.

4.4.3. Plasma and urinary pharmokinetics of genistein post the oral administration of genistin and malonylgenistin

Post the oral administration of the genistin and malonylgenistin isoflavone, genistein was detected in the plasma and urine extracts; however, marked differences were noted in the pharmokinetic parameters (Figure 37, A and B). Based on the plasma data, the initial rate of absorption of genistein calculated between 0-2 h post the administration of genistin was 2.67 μM/h, while that of genistein calculated between 0-3 h post the administration of malonylgenistin was ~ 6 times lower (0.41 μM/h). After 2 h of the administration of genistin, the rate of absorption decreased to 1.27 μM/h, as calculated between 2-4 h. The mean plasma concentration of genistin post the administration of genistin reached its peak (C_{max} = 7.87 ± 2.83 μM) after 4 h (t_{max}). The mean C_{max} of genistein post the administration malonylgenistin (3.94 ± 1.26 μM) was significantly ($P \leq 0.05$, ANOVA Table 14, Appendix F) lower than that post the administration of genistin (Table 9). After 4 h of the administration of genistin and malonylgenistin, the rate of elimination of genistein was 1.84 μM/h, and 0.31 μM/h, respectively. Genistein concentrations dropped significantly ($P \leq 0.05$) after 12 h of the oral dosage (Figure 37 A).

Urine concentrations of genistein post the administration of genistin reached a maximum between 6 to 12 h (Figure 37 B), while that post oral administration of malonylgenistin peaked between 0 to 6 h (Figure 37 B). However, C_{max} of genistein for the administration of genisting was three times greater than that post the administration of malonylgenistin (Table 10).

The bioavailability of genistin, in terms of AUC for genistein in the plasma (57.04 ± 14.38 μM.hr), was significantly higher (~ 3 times, $P \leq 0.05$, ANOVA Table 14, Appendix F) than that of malonylgenistin (22.36 ± 4.74 μM.hr) (Table 9). Urine data demonstrated a complementary trend in the bioavailability of genistin vs. malonylgenistin (Table 10).

4.5. Discussion

The non-conjugated β-glucosides, daidzin and genistin were absorbed relatively quickly, as was observed by other researchers (Kwon et al., 1998; Sepehr et al., 2009). Based on the AUC values, the bioavailability of daidzin was significantly ($P \leq 0.05$) greater than that of genistin. The pharmokinetic data is in excellent agreement with previous results, and fall within the range of reported values (Izumi et al., 2002; Sepehr et al., 2009; Cassidy et al., 2006).

The data confirms that non-conjugated β-glucosides undergo hydrolysis into aglycones by gut β-glucosidases. Setchell et al. (2001) reported no active transport of non-conjugated β-glucosides via the intestinal epithelium, and found no glucosides in the plasma. However, they reported active transport of aglycones through the intestinal epithelium, which was attributed to their hydrophobic nature and low molecular weight.

Our study, for the first time, provided conclusive *in-vivo* pharmokinetic data of the most abundant malonylglucosides, malonyldaidzin and malonylgenistin, when ingested in their pure forms. The study was conducted in a model rat system following a design that complements the study design employed by numerous other studies found in the literature, thus making comparison of the data conducive and appropriate (Xu et al., 1994; King and Bursill, 1998; Setchell et al., 2001; Liu and Hu, 2002). Further, we made critical improvements to our study design by taking into account the highlighted NIH recommendations pertaining to accurate isoflavone profiling, bioavailability, reliable analytical techniques and relevant dosage (Klein et al., 2010). We believe these critical improvements will help streamline the experimental approach undertaken by various researchers to achieve consistent clinical conclusions.

Pharmokinetic parameters obtained for malonylglucosides differed significantly from their respective non-conjugated β-glucosides. The AUC values of the metabolites in the plasma and urine obtained after the administration of non-conjugated β-glucosides were 2-6 times greater than those of their respective malonylglucosides. The lower initial absorption rates of malonylglucosides when compared to non-conjugated glucosides indicated that the malonyl group hinders the extent and rate of malonylglucoside hydrolysis by β-glucosidases to their respective aglycones. This data demonstrates that non-conjugated β-glucosides are relatively more bioavailable than their respective

malonylglucosides. The lower bioavailability of malonylglucosides can be partially attributed to the inefficacy of gut β-glucosidases in hydrolyzing them into aglycones at the same rate as hydrolyzing non-conjugated β-glucosides (Ismail and Hayes, 2005). Structural differences between malonylglucosides and their respective non-conjugated β-glucosides are the primary reason behind the lower hydrolysis rates. Since enzyme activity is structure specific, malonyl conjugation on the sixth carbon of the glucose moiety will result in stearic hindrance that reduces drastically the rate at which β-glucosidases can hydrolyze malonylglucosides. As a consequence, the bioavailability of these forms becomes limited. It is suggested that malonlyglucosides might get hydrolyzed in the distant regions of the gut where the bacterial concentrations and hence enzyme activity is high (Barnes et al., 1996). In distant region of the gut hydrolysis might be aided by microbial de-esterases that can cleave the malonyl group off thus facilitating the hydrolysis into aglycones by glucosidases. This assumption is yet to be confirmed by future *in vivo* studies. Given that in this study aglycones were found in the plasma post the ingestion of malonylglucosides, it is thus concluded that partial hydrolysis did in fact occur.

In their seminal work on the bioavailability of isoflavones, Setchell et al. (2001) found that non-conjugated β-glucosides have greater bioavailability than aglycones (Setchell et al., 2001). However, other researchers confirmed the opposite (Izumi et al., 2002; Cassidy et al., 2006) or found no difference (Zubik and Meydani, 2003). The reason behind these discrepancies is attributed to the difference in the isoflavone profile that was ingested. While Setchell et al. (2001) used pure forms of both aglycones and non-conjugated β-glucosides, Izumi et al. (2002) and other researchers who confirmed the opposite, used an isoflavone dose that constituted of all major forms of glucosides (non-conjugated β-glucosides and conjugated glucosides), containing specifically a significant amount of malonylglucosides. Based on our findings, the low bioavailability of malonylglucosides must have contributed to a reduced overall bioavailability of the mixed glucoside dose used by the researchers compared to that of a dose constituting only pure non-conjugated β-glucosides.

Results of this study can also explain the discrepancies observed in several bioactivity studies. For instance, isoflavones in the aglycone forms were shown to have a beneficial role in ameliorating inflammation and reducing insulin resistance by down regulating cytokines gene expression and inflammatory factors (Pinent et al., 2011), and have caused significant reduction in hot flushes in post-menopausal women (Crisafulli et al., 2004; D'Anna et al., 2007). Contradictory findings, however, have been reported. Soymilk supplementation did not affect plasma markers of inflammation, such as IL-6, T-NFα, and COX I in postmenopausal women (Beavers et al., 2009), and no significant difference in the reduction of weekly hot flushes were observed (Campagnoli et al., 2005). While former researchers used pure aglycones in their study designs, the latter researchers used a diet that constituted a mixture of aglycones and glucosides (both non-conjugated and malonyl- conjugated forms). Because malonylglucosides are less bioavailable than non-conjugated glucosides, less physiological contributions are expected when consuming an isoflavone dosage rich in malonylglycosides.

Considering the fact that malonylglucosides are abundant in many soy-based products, it is of prime importance to determine their bioavailability in order to understand the overall physiological relevance of isoflavones. Results of this study will help streamline the experimental approach undertaken by various researchers to achieve consistent clinical conclusions. Providing consistent data will encourage funding organizations to allocate money for new isoflavone research, thus aiding in better and more in-depth understanding of the physiological contributions of isoflavones. These results combined with inspired future studies will contribute significantly to both nutrition as well as food science fields and will narrow the gap between them. Food science researchers will use the outcome of these studies as a guide to develop processing technologies that will result in an optimized isoflavone profile with maximum health benefits.

5. OVERALL CONCLUSIONS, IMPLICATIONS, AND RECOMMENDATIONS

Isoflavones are extensively researched both in the food science and nutrition fields owing to their potential health benefits. From a nutritional standpoint, the research on isoflavones has been largely confined to understand which isoflavone form (in what dose) induces maximum health benefits. On the other side, food science related isoflavone research concentrated more on the storage and processing effects on isoflavones stability. It is important to understand that there exists a symbiosis between nutrition and food science research conducted on isoflavones and that they complement each other. This work served as a bridge linking nutrition and food science research to better characterize the biological relevance of the different isoflavone forms and the effects of processing on these forms.

While the existence of isomers in soy matrices was reported earlier, the present work provided complete structural characterization of the malonylglucoside isomers. We demonstrated for the first time that the formation of the soy malonyl isomers is governed by thermal processing time in a soymilk system. Further, a clear distinction was observed between the rates of interconversions between malonylgenistin and its isomer when compared between buffered and soymilk systems. Results highlighted the role of isoflavone-protein interactions in the determination of isomer stability in complex systems that are subjected to processing. Due to the close structural similarity of the identified isomers to known isoflavone forms and the fact that they convert to biologically relevant forms, it is crucial to include the isomers in the calculation of total isoflavone content, profile and loss. Disregarding the isomer formation upon heating can result in overestimation of loss in total isoflavone content and misinterpretation of the biological contributions and will result in obtaining consistent conclusions about the processing effect on isoflavones.

Present literature lacks a clear understanding of the health benefit of isoflavones due to inconsistent conclusions. The National Institute of Health (NIH) conducted a scientific workshop and concluded that inadequate profiling of isoflavones, lack of standardization of the source of isoflavones (different soy matrices and supplements), and lack of

standard analytical techniques are the main reasons behind the inconsistent conclusions. In this work, we have addressed these limitations in the current isoflavone research.

This work provided a validated analytical SID-LC/MS method to detect isoflavones in biological fluids. The produced SIL analogues of daidzin and genistin, mono- and dideutero substituted at the ortho positions, exhibited minimal deuterium isotopic effect, and were stable under the employed sample preparation protocol and MS analysis. A strategy to eliminate errors due to the isotopic overlap between the synthesized SIL analogues of isoflavones and their respective analytes of interest was developed in the MRM mode, thereby improving the accuracy of the proposed analytical method. Such analytical method would be invaluable for the research focused on determining accurately the bioavailability of the different forms of isoflavones.

Finally, this work differentiated, for the first time, the bioavailability of malonylglucosides as compared to their non-conjugated counterparts. The collected data demonstrated that non-conjugated β-glucosides are relatively more bioavailable than their respective malonylglucosides. These results highlighted the importance of considering structural differences among isoflavone glucosides in evaluating their bioavailability. The observed differences explained to a significant extent the controversy in isoflavone research. Considering the fact that malonylglucosides are abundant in many soy-based products, it is of prime importance to determine their bioavailability in order to understand the overall physiological relevance of isoflavones. We believe that the results of this work will help streamline the experimental approach undertaken by various researchers to achieve consistent clinical conclusions and to optimize the processing parameters that result in the most bioavailable isoflavone profile, thus maximizing their health benefits.

This work serves to be an impetus for designing future studies that can provide consistent and accurate results pertaining to isolfavone bioavailability and bioactivity. We believe that there is a need to conduct an extensive *in vivo* study to elucidate the influence of the gut microflora on the metabolism of malonylglucosides. While malonylglucosides were less bioavailable, aglycones were found in the plasma post the ingestion of malonylglucosides, it is thus concluded that partial hydrolysis did in fact

occur at some distant region of the intestine. Additionally, isoflavones should be administered in both pure forms and soy extracts, to elucidate the effect of soy matrix on isoflavone bioavailability. Studies focused on the bioactivity of the different isoflavones as influenced by their chemical structure and relative bioavailability will also need to be conducted. Finally, since malonyl-isomeric forms were found in relevant amounts in complex soy systems, studies focused on determining their bioavailability are needed. The recommended future studies will provide data that can lead to a resumption of funding and thus progress in understanding the physiological effects of isoflavones.

COMPREHENSIVE BIBLIOGRAPHY

Achouri, A.; Boye, I. J; Belanger, C. Soybean isoflavones: efficacy of extraction conditions and effect of food type on extractability. *Food Res Intl.* **2005**, *38*, 1199-1204.

Adlercreutz, H.; Honjo. H.; Higashi, A.; Fotsis, T.; Hamalainen, E.; Hasegawa, T.; Okada, H. Urinary excretion of lignans and isoflavonoid phytoestrogens in Japanese men and women consuming a traditional Japanese diet. *Am J of Clin Nutr*. **1991**, *54*, 1093–1100.

Adlercreutz, H.; Fotsis, T. Kurzer, M. S.; Wahala, K.; Makela, T.; Hase, T. Isotope dilution gas chromatographic-mass spectrometric method for the determination of unconjugated lignans and isoflavonoids in human feces, with preliminary results in omnivorous and vegetarian women. *Anal. Biochem.* **1995**, *225*, 101-108.

Adlercreutz, C. H. T.; Goldin, B. R.; Gorbach, S. L. Soybean phytoestrogen intake and cancer risk. *J. Nutr*. **1995**, *125*, 757S–770S.

Albertazzi, P.; Pansini, F.; Bonaccorsi, G.; Zanotti, L.; Forini, D.; Aloysio, D. The effect of soy supplementation on hot flashes. **1998**, *Obstet Gynecol. 91*, 6–11.

Alekel, D. L.; Van Loan, M. D.; Koehler, K. J.; Hanson, L. N.; Stewart, J. W.; Hanson, K. B.; Kurzer, M. S.; Peterson, C. T. The soy isoflavones for reducing bone loss (SIRBL)

study: a 3-y randomized controlled trial in postmenopausal women. *Am. J. Clin. Nutr.* **2010**, *91*, 218–230.

Angela C. D.; Anne, M.; David, A. D.; Andrew, S. C.; Bernard J. C.; Gresshoff, P. M. Regulation of the Soybean-Rhizobium Nodule Symbiosis by Shoot and Root Factors. *Plant Physiol.* **1986**, *82*, 588-590.

Antignac, J. P.; Isabelle, G. H.; Naegeli, H.; Carioua, R.; Elliott, C.; Bizec, B. L. Multi-functional sample preparation procedure for measuring phytoestrogens in milk, cereals, and baby-food by liquid-chromatography tandem mass spectrometry with subsequent determination of their estrogenic activity using transcriptomic assay. *Analytica Chimica Acta.* **2009**, *637,* 55-63.

Arjmandi, B. H.; Alekel, L.; Hollis, S. W.; Amin, D.; Stacewics-Sapuntzakis, M.; Guo, P.; Kureja, S. C. Dietary soy protein prevents bone loss in an ovariectomized rat model of osteoporosis. *J. Nutr.* **1996**, *42*, 2466-2474.

Arjmandi, B. H.; Smith, B. J. Soy isoflavones' osteoprotective role in postmenopausal women: mechanism of action. *Journal of Nutritional Biochemistry*. **2002**, *13*, 130-137.

Arora, A.; Nair, M.; Strasburg, G. Antioxidant activities of isoflavones and their biological metabolites in a liposomal system. *Archives of Biochemistry and Biophysics*. **1998**, *356,* 133–141.

Barnes, S.; Kirk, M.; Coward, L. Isoflavones and their conjugates in soy foods: Extraction conditions and analysis by HPLC-Mass spectrometry. *J. Agric. Food Chem.* **1994**, *42*, 2466-2474.

Barnes, S.; Sfakianos, J.; Coward, L.; Kirk, M. Soy isoflavonoids and cancer prevention. In Dietary phytochemicals in cancer prevention and treatment. American Institute for Cancer Research; Plenum Press: New York, **1996**, 87-100.

Barnes, S.; Coward, L.; Kirk, M.; Sfakianos, J. HPLC-mass spectrometry analysis of isoflavones. *Proc. Soc. Exp. Biol. Med.* **1998**, *217*, 254-262.

Barnes, S.; Wang, C. C.; Smith-Johnson, M.; Kirk, M. Liquid chromatography: mass spectrometry of isoflavones. *J. Med. Food*. **1999**, 2, 111-117.

Becka, V.; Rohrb, U.; Jungbauera, U. Phytoestrogens derived from red clover: An alternative to estrogen replacement therapy? *Journal of Steroid Biochemistry & Molecular Biology*. **2005**, *94,* 499–518.

Beavers, K. M.; Serra, M.; Beavers, D. P.; Cooke, M. B.; Willoughby, D. S. Soymilk supplementation does not alter plasma markers of inflammation and ozidative stress in postmenopausal women. *Nutr. Res*. **2009**, *29*, 616-622.

Beavers, K. M.; Serra, M.; Beavers, D. P.; Cooke, M. B.; Willoughby, D. S. Soy and the exercise-induced inflammatory response in postmenopausal women. *Appl. Physiol. Nutr. Metab*. **2010**, *35*, 261-269.

Berk, Z. Isolate soybean protein. In *technology of production of edible flours and protein products from soybeans*, Berk, Z.; Technicon: Haifa, Israel. 1992, 83-96.1.

Bhat, S. H.; Gelhaus, S. L.; Mesaros, C.; Vachani, A.; Blair, I. A. A new liquid chromatography/mass spectrometry method for 4-(methylnitrosamino)-1-(3-pyridyl)-1-butanol (NNAL) in urine. *Rapid Comunn. Mass Spectrom.* **2011**, *25*, 115-121.

Boersma, B. J.; Barnes, S.; Kirk, M. Soy isoflavonoids and cancer metabolism at the target site. *Mutat Res.* **2001**, *480,* 121–127.

Bonner, W. A. $C_1 - C_2$ acteyl migration on methylation of the anomeric 1,3,4,6-tertra-*O*-acetyl-$_D$-glucopyranoses. *J. Org. Chem.* **1959**, *24*, 1388-1390.

Brezezinski, A.; Debi, A. Phytoestrogens: the "natural" selective estrogen receptor modulators? *European J Obstetrics Gynecol Reprod Biol*. **1999**, *85*, 47-51.

Burke, G. L.; Legault, C.; Anthony, M.; Bland, D. R.; Morgan, T. M.; Naughton, M. J.; Leggett, K.; Washburn, S. A.; Vitolins, M. Z. Soy protein and isoflavone effects on

vasomotor symptoms in peri- and postmenopausal women: The soy estrogen alternative study. *Menopause*. **2000**, *10*, 147 –153.

Cassidy, A.; Brown, J. E.; Hawdon, A.; Faughnan, M. S.; King, L. J.; Millward, J.; Zimmer-Nechemias, L.; Wolfe, B.; Setchell, K. D. R. Factors affecting the bioavailability of soy isoflavones in humans after ingestion of physiologically relevant levels from different soy foods. *The J. Nutr.* **2006**, *136*, 45-51.

Campagnoli, C.; Abba, C.; Ambroggio, S.; Peris, C.; Perona, M.; Sanseverino, P. Polyunsaturated fatty acids (PUFAs) might reduce hot flushes: An indication from two controlled trials on soy isoflavones alone and with a PUFA supplement. *Maturitas*. **2005**, *51*, 127–134.

Cavaliere, C.; Cucci, F.; Foglia, P.; Guarino, C.; Samperi, R.; Lagana, A. Flavanoid profile in soybeans by high-performance liquid chromatography/tandem mass spectrometry. *Rapid Commun. Mass Spectrom*. **2007**, *21*, 2177-2187.

Centers for Disease Control and Prevention. National Center for Health Statistics. Health Data Interactive. www.cdc.gov/nchs/hdi.htm. Accessed on 01/26/2011. (2006).

Cesare, R. S.; Anna, A.; Stuart, K. J. Phytoestrogens: End of a tale? *Annals of Medicine*. **2005**, *37*, 423–438.

Chang, Y-C; Nair, M.G.; Santell, R.C.; Helferich, W.G. Microwave-mediated synthesis of anticarcinogenic isoflavones from soybeans. *J. Agric. Food Chem.*, **1994**, *42*, 1869 - 1871.

Chen, J.; Halls, S. C.; Alfaro, J. F.; Zhou, Z.; Hu, M. Potential beneficial metabolic interactions between tamoxifen and isoflavones via cytochrome P450-mediated pathways in female rat liver microsomes. *Pharmaceutical Research.* **2004**, *21*, 2095-2104.

Chiechi, L.; Secreto, G.; D'Amore, M.; Fanelli, M.; Venturelli, E.; Cantatore, F. Efficacy of a soy rich diet in preventing post-menopausal osteoporosis: the Menfis randomized trial. *Maturitas*. **2002**, *42*, 295–300.

Chien, J. T.; Hsieh, H. C.; Kao, T. H.; Chen. B. H. Kinetic model for studying the conversion and degradation of isoflavones during heating. *Food Chemistry*. **2005**, *91*, 425-434.

Christiansen, C.; Christensen, M. S.; Transbol, I. Bone mass in postmenopausal women after withdrawal of oestrogen/gestagen replacement therapy. *Lancet.* **1981**, *1*, 459-461.

Chun, O. K.; Chung, S. J.; Song, W. O. Urinary isoflavones and their metabolites validate the dietary isoflavone intakes in US Adults. *J Am Diet Assoc.* **2009**, *109,* 245-254.

Clarke, D. B.; Lloyd, A. S.; Botting, N. P.; Oldfield, M. F.; Needs, P. S.; Wisemand, H. Measurement of intact sulfate and glucuronide phytoestrogen conjugates in human urine

using isotope dilution liquid chromatography-tandem mass spectrometry with [$^{13}C_3$] isoflavone internal standards. *Analytical Biochemistry*. **2002**, *309*, 158–172.

Cohen, J. D.; Baldi, B. G.; Slovin, J. P. $^{13}C_6$-[Benzene Ring]-Indole-3-Acetic Acid: A new internal standard for quantitative mass spectral analysis of Indole-3-Acetic acid in plants. *Plant Physiol*. **1986,** *80*, 14-19.

Cohen, L. A.; Zhou, Z.; Pittman, B.; Scimeca, J. A. Effect of intact and isoflavones-depleted soy protein on NMU-induced rat mammary tumorigenesis. *Carcinogenesis*. **2000**, *21*, 929–935.

Coward, L.; Barnes, N.; Setchell, K.; Barnes, S. Genistein, daidzein, and their beta-glycoside conjugates: antitumor isoflavones in soybean food from American and Asian diets. *J. Agric. Food Chem.* **1993**, *41,* 1961–1967.

Coward, L.; Smith, M.; Kirk, M.; Barnes, S. Chemical modifications of isoflavones in soyfoods during cooking and processing. *Am J Clin Nutr.* **1998**, *68*, 1486S-1491S.

Crisafulli, A.; Marini, H.; Bitto, A.; Altavilla, D.; Squadrito, G.; Romeo, A.; Adamo, E. B.; Marini, R.; D'Anna, R.; Corrado, F.; Bartolone, S.; Frisina, N.; Squadrito, F. Effects of genistein on hot flushes in early postmenopausal women: A randomized, double-blind EPT- and placebo-controlled study. *Menopause*. **2004**, *11*, 400–404.

Crouse, J. R.; Morgan, T.; Terry, J. G.; Ellis, J.; Vitolins, M.; Burke, G. L. A randomized trial comparing the effect of casein with that of soy protein containing varying amounts of isoflavones on plasma concentrations of lipids and lipoproteins. *Arch. Intern. Med.* **1999**. *159*, 2070–2076.

D'Anna, R.; Cannata, M. L.; Atteritano, M.; Cancellieri, F.; Corrado, F.; Baviera, G.; Triolo, O.; Antico, F.; Gaudio, A.; Frisina, N.; Bitto, A.; Polito, F.; Minutoli, L.; Altavilla, D.; Marini, H.; Squadrito, F. Effects of the phytoestrogen genistein on hot flushes, endometrium, and vaginal epithelium in postmenopausal women: a 1-year randomized, double-blind, placebo-controlled study. *Menopause*. **2007**, *14*, 648-655.

Davies, C. G. A.; Netto, F. M.; Glassenap, N.; Gallaher, C. M.; Labuza, T. P.; Gallaher, D. D. Indication of maillard reaction during storage of protein isolates. *J. Agric. Food Chem*. **1998**. *46*, 2485-2489.

Delmas, P. D.; Bjarnason, N. H.; Mitlak, B. H.; Ravoux, A. C.; Shah, A. S.; Huster, W. J.; Draper, M.; Christiansen, C. Effects of Raloxifene on Bone Mineral Density, Serum Cholesterol Concentrations, and Uterine Endometrium in Postmenopausal Women. *N Engl J Med.* **1997**, *337*, 1641-1647.

Dijsselbloem, N.; Vanden Berghe, W.; De Naeyer, A; Haegeman, G. Soy isoflavone phyto-pharmaceuticals in interleukin-6 affections. Multi-purpose nutraceuticals at the

crossroad of hormone replacement, anti-cancer and anti-inflammatory therapy. *Biochem Pharmacol*. **2004**, *68*, 1171-1185.

Dixon, A. R.; Harrison, M. J.; Paiva, N. L. The isoflavonoid phytoalexin pathway: from enzymes to genes to transcription factors. *Physiologia Plantarum*. **1995**, *93,* 385-392.

Doerschuk, A. P. Acyl migrations in partially acylated, polyhydroxylic systems. *J. Am. Chem. Soc.* **1952**, *74*, 4202-4203.

Dong, Z. M.; Chapman, S. M.; Brown, A . A.; Frenette, P. S.; Hynes, R. O.; Wagner, D. D. The combined role of P- and E-selectins in atherosclerosis. *J Clin Invest.* **1998**, *102*, 145-152.

Duncan, A. M.; Phipps, W. R.; Kurzer, M. S. Phyto-oestrogens: *Best Practice Res Clin Endocrinol Metab.* **2003**, *17*, 253–271.

Ebbing, D. D.; Gammon, S. D. Quantum theory of atom. In *General Chemistry*, ninth edition no.; Charles Hatford: Belmont, CA, 2007; 263.

Edwards, R.; Tiller, S. A.; Parry, A. D. The effect of plant age and nodulation on the isoflavonoid content of red clover *(Trifolium pretense). J Plant Physiol*. **1997**, *150*, 603-610.

Ejsing, C. S.; Duchoslav, E.; Sampaio, J.; Simons, K.; Bonner, R.; Thiele, C.; Ekroos, K.; Shevchenko, A. Automated Identification and Quantification of Glycerophospholipid Molecular Species by Multiple Precursor Ion Scanning. *Anal. Chem*. **2006**, *78*, 6202-6214.

Faizi, S.; Siddiqi, H.; Naz, A.; Bano, S.; Lubna. Specific Deuteration in patuletin and related flavonoids via keto-enol tautomerism: solvent- and temperature-dependent 1H-NMR studies. *Helvetica Chimica Acta.* **2010**, *93*, 466-481.

Farmakalidis, E.; Murphy, P. A. Semi-preparative high-performance liquid chromatographic isolation of soybean isoflavones. *J Chromatogr. A.* **1984**, *295*, 510-514.

Faughnan, M. S.; Hawdon, A.; Ah-Singh, E.; Brown, J.; Milward, D. J.; Cassidy, A. Urinary isoflavone kinetics: the effect of age, gender, food matrix and chemical composition. Br. *J. Nutr*. **2004**, *91*, 567-574.

Fenn, J. B.; Mann, M.; Meng, C.; Wong, S. K.; Whitehouse, C. Electrospray ionization for mass spectrometry of large biomolecules. *Science*. **1989**. *246,* 64-71.

Ferlay, J.; Shin, H. R.; Bray, F.; Forman, D.; Mathers, C.; Parkin, D. M. Estimates of worldwide burden of cancer in 2008: GLOBOCAN 2008. Available from: http://globocan.iarc.fr, accessed on 01/26/2011. (2008).

Ferrer, I.; Barberb, L. B.; Thurmana, E. M.; J. Chromatogr. A. Gas chromatographic–mass spectrometric fragmentation study of phytoestrogens as their trimethylsilyl derivatives: Identification in soy milk and wastewater samples. **2009**, *1216*, 6024-6032.

Franke, A.; Yu, M.; Maskarinec, G.; Fant, P.; Zheng, W.; Custer, L. Phytoestrogens in human biomatrices including breast milk. *Biochem. Soc. Trans.* **1999**, *27*, 308–318.

Gaussian 03, Revision C.02, Frisch, M. J.; Trucks, G. W.; Schlegel, H. B.; Scuseria, G. E.; Rob, M. A.; Cheeseman, J. R.; Montgomery Jr., J. A.; Vreven, T.; Kudin, N. R.; Burant, J. C.; Millam, J. M.; Iyengar, S. S.; Tomasi, J.; Barone, V.; Mennucci, B.; Cossi, M.; Scalmani, G.; Rega, N.; Petersson, G. A.; Nakatsuji, H.; Hada, M.; Ehara, M.; Toyota, K.; Fukuda, R.; Hasegawa, J.; Ishida, M.; Nakajima, T.; Honda, Y.; Kitao, O.; Nakai, H.; Klene, M.; Li, X.; Knox, J. E.; Hratchian, H..P. Cross, J. B.; Bakken, V.; Adamo, C.; Jaramillo, J.; Gomperts, R.; Stratmann, R. E.; Yazyev, O.; Austin, A. J.; Cammi, R.; Pomelli, C.; Ochterski, J. W.; Ayala, P. Y.; Morokuma, K.; Voth, G. A.; Salvador, P.; Dannenberg, J. J.; Zakrzewski, V. G.; Dapprich, S.; Daniels, A. D.; Strain, M. C.; Farkas, O.; Malick, D. K.; Rabuck, A. D.; Raghavachari, K.; Foresman, J. B.; Ortiz, J. V.; Cui, Q.; Baboul, A. G.; Clifford.; Cioslowski, J.; Stefanov, B. B.; Liu, G.; Liashenko, A.; Piskorz, P.; Komaromi, I.; Martin, R. L.; Fox, D. J.; Keith, T.; Al-Laham, M. A.; Peng, C. Y.; Nanayakkara, A.; Challacombe, M.; Gill, P. M. W.; Johnson, B.; Chen, W.; Wong, M. W.; Gonzalez, C.; Pople, J. A.; Gaussian, Inc., Wallingford, CT, 2004.

Gottlieb, H. E.; Kotlyar, V.; Nudelman, A. NMR chemical shifts of common laboratory solvents as trace impurities. *J. Org. Chem.* **1997**, *62,* 7512-7515.

Griffith, A. P.; Collision, M. W. Improved methods for the extraction and analysis of isoflavones from soy-containing foods and nutritional supplements by reversed-phase high-performance liquid chromatography and liquid-chromatography-mass spectrometry. *J Chromatogr. A.* **2001**. 913, 397-413.

Grubisha, D. S.; Lipert, R. J.; Park, H-Y.; Driskell, J.; Porter, M. D. Femtomolar detection of prostate-specific antigen: an immunoassay based on surface-enhanced Raman scattering and immunogold labels. *Anal. Chem*. **2003**, *75*, 5936-5943.

Grun, I. U.; Adhikari, K.; Li, C.; Li, Y.; Lin, B.; Zhang, J.; Fernando, L. N. Changes in the profile of genistein, daidzein, and their conjugates during thermal processing of tofu. *J. Agric. Food Chem*. **2001**. *49*, 2839-2843.

Gu, L.; Gu, W. Characterization of soy isoflavones and screening for novel malonyl glycosides using high-performance liquid chromatography–electrospray ionization-mass spectrometry. *Phytochem. Anal*. **2001**, *12,* 377-382.

Gurst, J. E. NMR and the structure of D-glucose. *J. Chem. Educ.* **1991**, *68*, 1003-1004.

Haimi, P.; Chaithanya, K.; Kainu, V.; Hermansson, M.; Somerharju, P. Instrument-independent software tools for the analysis of MS–MS and LC–MS lipidomics data methods. *Mol. Biol*. **2009**, *580*, 285-294.

Hanai, T.; Koizumi, K.; Kinoshita, T.; Arora, R.; Ahmed, F. *J Chromatogr. A*. **1997**, *762*, 55-61.

Hakamatsuka, T.; Noguchi, H.; Ebizuka, Y.; Sankawa, U. Isoflavone synthase from cell suspension cultures of *Pueraria lobata. Chemical and Pharmaceutical Bulletin.* **1990**, *38,* 1942-1945.

Hashim, M. F.; Hakamatsuka, T.; Ebizuka, Y.; Sankawa, U. Reaction mechamism of oxidative rearrangement of flavanone in isoflavone biosynthesis. *FEBS letters.* **1991**, *271*, 219-222.

Heinonen, S.; Wahala, K.; Adlercreutz, H. Identification of isoflavone metabolites dihydrodaidzein, dihydrogenistein, 6′-OH-O-dma, and cis-4-OH-equol in human urine by gas chromatography–mass spectroscopy using authentic reference compounds. *Anal. Biochem*. **1999**, *274*, 211-219.

Heinonen, S. M.; Hoikkala, A.; Wahala, K.; Adlercreutz, H. Metabolism of the soy isoflavones daidzein, genistein and glycitein in human subjects.: Identification of new

metabolites having an intact isoflavonoid skeleton. *J. Steroid Biochem. Mol. Biol.* **2003**, 87, 285-299.

Henderson, B. E.; Paganini-Hill, A.; Ross, R. K. Decreased mortality in users of estrogen replacement therapy. *Arch Intern Med*. **1991**, *151*, 75-78.

Hendrich, S.; Murphy, P. A. Isoflavones: source and metabolism. In *handbook of nutraceuticals and functional foods*, Wildman R. E. C.; CRC Press: Boca Raton, Florida, 2001, 55-75.

Ho, S. C.; Chan, S. G.; Yi, Q.; Wong, E.; Leung, P. C. Soy intake and the maintenance of peak bone mass in Hong Kong Chinese women. *J. Bone Miner. Res*. **2001**, *16*, 1363–1369.

Hodgson, J. M; Puddey, I. B.; Croft, K. D.; Mori, T. A.; Rivera, J.; Beilin, L. J. Isoflavonoids do not inhibit in vivo lipid peroxidation in subjects with high-normal blood pressure. *Atherosclerosis*. **1999**, *145*, 167–172.

Hohenberg, P.; Kohn, W. Inhomogeneous electron gas. *Physical Review.* **1964**, *136*, B864–B871.

Horn-Ross, P. L.; John, E. M.; Lee, M.; Stewart, S. L.; Koo, J.; Sakoda, L. C. Phytoestrogen consumption and breast cancer risk in a multiethnic population: the Bay Area Breast Cancer Study. *Am J Epidemiol*. **2001**, *154*, 434–41

Hsiao, K.-F.; Lin, H.-J.; Leu, D.-L.; Wu, S.-H; Wang, K.-T. Kinetic study of deacetylation and acetyl migration of peracetylated l-methyl α,β-D-glycopyranosides by *Candida* lipase-catalyzed hydrolysis. *Bioorg. Med. Chem. Lett.* **1994**, *4*, 1629-1632.

Ingram, D.; Sanders, K.; Kolybaba, M.; Lopez, D. Casecontrol study of phyto-oestrogens and breast cancer. *Lancet*. **1997**, *350*, 990–994.

Ismail, B.; Hayes, K. Glycosidase activity toward different glycosidic forms of isoflavones. *J. Agric. Food Chem*. **2005**, *53*, 4918-4924.

Izumi, T.; Piskula, M. K.; Osawa, S.; Obata, A.; Tobe, K.; Saito, M.; Kataoka, S.; Kubota, Y.; Kikuchi, M. Soy isoflavone aglycones are absorbed faster and in higher amounts than their glucosides in humans. *J. Nutr*. **2000,** *130*, 1695-1699.

Jackson, C. J. C.; Dini, J. P.; Lavandier, C.; Rupasinghe, H. P. V.; Faulkner, H.; Poysa, V.; Buzzell, D.; Degransi, S. Effects of processing on the content and composition of isoflavones during manufacturing of soy beverage and tofu. *Process Biochemistry*. **2002**, *37*, 1117-1123.

Jacobs, A.; Wegewitz, U.; Sommerfeld, C.; Grossklaus, R.; Lampen, A. Efficacy of isoflavones in relieving vasomotor menopausal symptoms: a systematic review. *Mol. Nutr. Food Res.* **2009**, *53*, 1084–1097.

Jandera, P.; Novotna, K. Characterization of High-Performance Liquid Chromatography Columns by Chromatographic Methods, *Anal Lett*. **2006**, *39*, 2095-2152.

Jeanmaire, D. L.; Van Duyne, R. P. Surface raman spectroelectrochemistry: Part I. Heterocyclic, aromatic, and aliphatic amines adsorbed on the anodized silver electrode. *J. Electroanal. Chem.* **1977**, *84,* 1-20.

Jenkins, D. J., C.; Kendall, W.; Garsetti, M. Effect of soy protein foods on low-density lipoprotein oxidation and ex vivo sex hormone receptor activity: a controlled crossover trial. *Metabolism*. **2002**, *49*, 537–543.

Johannes T. P. D.; Cuperus, F. P.; Peter, K. Paints and coatings from renewable resources. *Industrial Crops and Products*. **1995**. *3*, 225-236.

M. Jones, Jr. Substitution reactions of aromatic compounds, In Organic chemistry, third edition.; W. W. Norton and Company, Inc.: New York, NY, 2004, 708.

M. Jones, Jr. Substitution reactions of aromatic compounds, In Organic chemistry, third edition.; W. W. Norton and Company, Inc.: New York, NY, 2004, 898.

Kang, J.; Hick, L. A.; Price, W. E. A fragmentation study of isoflavones in negative electrospray ionization by MS_n ion trap mass spectrometry and triple quadrapole mass spectrometry, *Rapid Commun. Mass Spectrom*. **2007**, *21*, 857-868.

Kerry, N and Abby, M. The isoflavone genistein inhibits copper and peroxyl radical mediated low density lipoprotein oxidation in vitro. *Atherosclerosis.* **1998**, *140*, 341-347.

Khaodhiar, L.; Ricciotti, H. A.; Li, L.; Pan, W.; Schickel, M.; Zhou, J.; Blackburn, G. L. Daidzein-rich isoflavone aglycones are potentially effective in reducing hot flashes in menopausal women. *Menopause*. **2008**, *15*, 125–132.

King, R.; Bursill, D. Plasma and urinary kinetics of the isoflavones daidzein and genistein after a single soy meal in humans. *Am J Clin Nutr*. **1998**, *67*, 867–872.

King, R. Daidzein conjugates are more bioavailable than genistein conjugates in rats. *Am. J. Clin. Nutr*. **1998**, *68*, 1496S-1499S.

Kinney, A. J. Development of genetically engineered soybean oils for food applications. *Journal of Food Lipids*. **2007**, *4*, 273-292.

Klein, M. A.; Nahin, R. L.; Messina, M. J.; Rader, J. I.; Thompson, L. U.; Badger, T. M.; Dwyer, J. T.; Kim, Y. S.; Pontzer, C. H.; Starke-Reed, P. E.; Weaver, C. M. Guidance from an NIH workshop on Designing, implementing, and reporting clinical studies of soy interventions. *J. Nutr.* **2010**, *140*, 1192S-1204S.

Klejdus, B.; Vacek, J.; Benesova, L.; Kopecky, J.; Lapcik, O.; Kuban, V. Rapid-resolution HPLC with spectrometric detection for the determination and identification of

isoflavones in soy preparations and plant extracts. *Anal Bioanal Chem*. **2007**, *389*, 2277-2285.

Klump, S. P.; Allred, J. L.; MacDonald, J. M.; Ballam, J. Determination of isoflavones in soy and selected foods containing soy by extraction, saponification, and liquid chromatography: collaborative study. J. *Assoc. Off. Anal. Chem*. *Int*. **2000**, *84*, 1865-1883.

Kreiger, M. The other side of scavenger receptors: pattern recognition for host defence. *Curr Opin Lipidol.* **1997**, *8*, 275-280.

Krishnakumar, V.; Keresztury, G.; Sundius, T.; Ramasamy, R. Simulation of IR and Raman spectra based on scaled DFT force fields: a case study of 2-(methylthio)benzonitrile, with emphasis on band assignment. *Journal of Molecular Structure*. **2004**, *702*, 9-21.

Kuduo, S.; Fleury, Y.; Welti, D.; Magnolato, D.; Uchida, T.; Kitamru, K.; Okubo, K. Malonyl isoflavone glycosides in soybean seeds (*Glycine max* MERRILL). *Agric. Biol. Chem.* **1991**, *55*, 2227-2233.

Kurzer, M. S. J. Nutr. Phytoestrogen supplement use by women. **2003**, *133,* 1983S-1986S

Kurzer, M. S. Hormonal effects of soy isoflavones: Studies in premenopausal and postmeopausal women. *J. Nutr.* **2000**, *130*, 660S-661S.

Kyle, E.; Neckers, L.; Takimoto, C.; Curt, G.; Bergan, R. Genistein-induced apoptosis of prostate cancer cells is preceded by a specific decrease in focal adhesion kinase activity. *Mol Pharmacol.* **1997**, *51*, 193–200.

Kwon, T. W.; Song, S. Y.; Kim, J. S.; Moon, G. S.; Kim, J. I.; Honh, J. H. Current research on the bioactive functions of soyfoods in Korea. *J. Korean Soybean Dig*. **1998**, *15*, 1–12.

Lamartiniere, C. A.; Moore, B. J.; Brown, N. M.; Thomson, R.; Harden, M. J.; Barnes, S. Genistein suppresses mammary cancer in rats. *Carcinogenesis.* **1995**, *16*, 2833-2840.

Larkin, T.; William, E. P.; Astheimer, L. The Key Importance of Soy Isoflavone Bioavailability to Understanding Health Benefits. *Critical Reviews in Food Science and Nutrition*. **2000**, *48,* 538–552.

Lee, M. M.; Gomez, S. L.; Chang, J. S.; Wey, M.; Wang, R. T.; Hsing, A. W. Soy and isoflavone consumption in relation to prostate cancer risk in China. *Cancer Epidemiol*. **2003**, *12*, 665-668.

Lee, H. P.; Gourley, L.; Duffy, S. W.; Esteve, J.; Lee, J.; Day, N. E. Dietary effects on breast cancer risk in Singapore. *Lancet.* **1991**, *337*, 1197-1200.

Lethaby, A. E.; Brown, J.; Marjoribanks, J.; Kronenberg, F.; Roberts, H.; Eden, J. Phytoestrogens for vasomotor menopausal symptoms. *Cochrane Database Syst. Rev*. **2007**, CD001395.

Libby P. Inflammation in atherosclerosis. *Nature*, **2002**, *420,* 868–874.

Liebisch, G.; Lieser, B.; Rathenberg, J.; Drobnik, W.; Schmitz, G. High-throughput quantification of phosphatidylcholine and sphingomyelin by electrospray ionization tandem mass spectrometry coupled with isotope correction algorithm. Biochimica et Biophysica Acta. **2004**, *1686*, 108-117.

Lijuan, C.; Xia, Z.; Linyu, F.; Games, D. E. Quantitative determination of acetylglucosides isoflavones and their metabolites in human urine suing combined liquid chromatography – mass spectrometry. *J. Chromatogr. A*. **2007**, *1154*, 103-110.

Lin, F.; Giusti, M. Effects of solvent polarity and acidity on the extraction efficiency of isoflavones from soybeans. (*Glycine max). J. Agric. Food Chem*. **2005**. *53*, 3795-3800.

Liu,Y.; Hu, M. Absorption and metabolism of flavonoids in the Caco-2 cell culture model and a perused rat intestinal model. *Drug Metabolism and Disposition*. **2002**, *30*, 370–377.

Lockley, J. S. W. Regiochemical differences in the isotopic fractionation of deuterated benzoic acid isotopomers by reversed-phase high-performance liquid chromatography. *J Chromatogr. A*, **1989**, 483, 413-418.

Lori, C.; Neil, C. B.; Setchell, K. D. R.; Barnes, S. Genistein, daidzein, and their glycoside conjugates: antitumor isoflavones in soybean foods from American and Asian diets. *J. Agric. Food Chem*. **1993**, *41*, 1961-1967

Mahungu, S. M.; Diaz-Mercado, S.; Li, J.; Schwenk, M.; Singletary, K.; Faller, J. Stability of isoflavones during extrusion processing of corn/soy matrix. *J. Agric. Food Chem*. **2002**, *47,* 279-284.

Malaypally, S. P.; Ismail, B. Effect of protein content and denaturation on the extractability and stability of isoflavones in different soy systems. *J. Agric. Food Chem. 2010*, **58**, 8958-8965.

Mathias, K.; Ismail, B.; Corvalan, C.; Hayes, K. Heat and pH effects on the conjugated forms of genistin and daidzin isoflavones. *J. Agric Food Chem*. **2006**, *54*, 7495-7502.

Matsuura, M.; Obata, A. β-Glucosidase from soybeans hydrolyze daidzin and genistein. *Journal of Food Science*. **1993**, *58,* 144-147.

May, M. J.; Wheeler-Jones, C. P.; Pearson, J. D. Effects of protein tyrosine kinase inhibitors on cytokine-induced adhesion molecule expression of ICAM-1 and VCAM-1 on human umbilical vein endothelial cells. *Scand J Immunol*. **1997**, *45*, 385-392.

Mazor, W.; Fotsis, T.; Wahala, K.; Ojala, S.; Salakka, A.; Adlercreutz, H. Isotope Dilution Gas Chromatographic–Mass Spectrometric Method for the Determination of Isoflavonoids, Coumestrol, and Lignans in Food Samples. *Anal. Biochem.* **1996**, *233*, 169-180.

Medjakovic, S.; Mueller, M; Jungbauer, A. Potential health-modulating modulating effects of isoflavones and metabolite via activation of PPAR and AhR. *Nutrients*. **2010**, *2*, 241-279.

Mei, J.; Yeung, S. S.; Kung, A. W. High dietary phytoestrogen intake is associated with higher bone mineral density in postmenopausal but not premenopausal women. *J. Clin. Endocrinol. Metab*. **2001**, *86*, 5217–5221.

Merz-Demlow, B. E.; Duncan, A. M.; Wangen, K. E.; Xu, X.; Carr, T. P.; Phipps, W. R.; Kurzer, M. S. Soy isoflavones improve plasma lipids in normocholesterolemic, premenopausal women. *Am J Clin Nutr*. **2000**, *71*, 1462–1469.

Messina, M. Legumes and soybeans: overview of their nutritional profiles and health effects. *Am J Clin Nutr*. **1999**, *70*, 439S–450S.

Messina, M.; Nagata, C.; Wu, A. H. Estimated Asian adult soy protein and isoflavone intakes. *Nutr Cancer*. **2006**, *55*, 1–12.

Messina, M. A brief historical overview of the past two decades of soy and isoflavone research. *The Journal of Nutrition*. **2010**, *14*, 1350S-1354S.

Mitchell, J.; Gardner, P.; McPhail, D.; Morrice, P.; Collins, A.; Duthie, G. Antioxidant efficacy of phytoestrogens in chemical and biological model systems. *Archives of Biochemistry and Biophysics*. **1998**, *360,* 142–148.

Mortensen, A.; Kulling, S. E.; Schwartz, H.; Rowland, I.; Ruefer, C. E.; Rimbach, G.; Cassidy, A.; Magee, P.; Millar, J.; Hall, W. L.; Kramer Birkved, F.; Sorensen, I. K.; Sontag, G. Analytical and compositional aspects of isoflavones in food and their biological effects. *Mol. Nutr. Food Res*. **2009**, *53 (Suppl. 2)*, S266–S309.

Morton, M. S.; Chan, P. S. F.; Cheng, C. Lignans and isoflavonoids in plasma and prostatic fluid in men: samples from Portugal, Hong Kong, and the United Kingdom. *Prostate*. **1997**, *32*, 122–128.

Mousavi, Y.; Adlercreutz, H. Genistein is an effective stimulator of sex hormone binding globulin production in hepatocarcinoma human liver cells and suppresses proliferation of theses cells in culture. *Steroids*. **1993**, *132*, 1956-1961.

Murakami, H.; Asakawa, T.; Terao, J.; Matsushita, S. Antioxidant stability of tempeh and liberation of isoflavones by ferementation. *Agric. Boil. Chem*. **1984**, *48*, 2971-2975.

Murkies, A. L.; Lombard, C.; Strauss, B. J. G.; Wilcox, G.; Burger, H. G.; Morton, M. S. Dietary flour supplementation decreases postmenopausal hot flushes: effect of soy and wheat. *Maturitas*. **1995**, *21*, 189–195.

Murphy, P.; Song, T.; Buseman, G.; Barua, K.; Beecher, G.; Trainer, D.; Holden, J. Isoflavones in retail and institutional soy foods. *J. Agric. Food Chem*. **1999**, *47*, 2697–2704.

Murphy, P. A.; Barua, K.; Hauck, C. C. Solvent extraction selection in the determination of isoflavones in soy foods. *J.Chromatogr. B*. **2002**, *777*, 129-138.

Nagata, C.; Takatsuka, N.; Kawakami, N.; Shimizu, H. Soy product intake and hot flashes in Japanese women: results from a community-based prospective study. *Am J Epidemiol.* **2001**, *153*, 790–793.

Nagata, C.; Iwasa, S.; Shiraki, M.; Ueno, T.; Uchiyama, S.; Urata, K.; Sahashi, Y.; Shimizu, H. Associations among maternal soy intake, isoflavone levels in urine and blood samples, and maternal and umbilical hormone concentrations (Japan). *Cancer Causes Control*. **2006**, *17*, 1107–1113.

Nagarajan, S.; Stewart, B. W.; Badger, T. M. Soy isoflavones attenuate human

monocyte adhesion to endothelial cell-specific CD54 by inhibiting monocyte CD11a. *J Nutr*. **2006**, *136,* 2384-2390.

Nagarajan, S.; Burris, R. L.; Stewart, B. W.; Wilkerson, J. E.; Badger, T. M. Dietary soy protein isolate ameliorates atherosclerotic lesions in apolipoprotein E-deficient mice potentially by inhibiting monocyte chemoattractant protein-1 expression. *J. Nutr.* **2008**, *138,* 332-337.

Nestel, P. J; Yamashita, T.; Sasahara, T. Soy isoflavones improve systemic arterial compliance but not plasma lipids in menopausal and perimenopausal women. *Arterioscler Thromb Vasc Biol.* **1997**, *17*, 3392–3398.

Newton, K. M.; Buist, D. S.; Keenan, N. L.; Anderson, L. A.; LaCroix, A. Z. Use of alternative therapies for menopause symptoms: results of a population-based survey. *Obstet. Gynecol*. **2002**,*100*, 18-25.

Nufer, K. R.; Ismail, B.; Hayes, K. D. Effects of processing and extraction conditions on content, profile, and stability of isoflavones in a soymilk system. *J. Agric Food Chem*. **2009**, *57*, 1213-1218.

Oseni, T.; Patel, R.; Pyle, J.; Jordan, V. C. Selective estrogen receptor modulators and phytoestrogens. *Planta Med*. **2008**, *74*, 1656-1665.

Paganini-Hill, A. Estrogen replacement therapy and stroke. *Progress in Cardiovascular Diseases*. **1995**, *38*, 223-242.

Pahk, A. H; DeLong, M. J. Vitamin D3 and genistein induce detoxification enzymes in MCF-7 human breast cancer cells [abstract]. *Toxicologist.* **1993**, *42*, 317.

Panay, N. Integrating phytoestrogens with prescription medicines-A conservative clinical approach to vasomotor symptom management. *Maturitas*. **2007**, *57*, 90-94.

Park, Y. K.; Aguiar, C. L.; Alencar, S. M.; Mascrenhas, H. A.; Scamparini, A. R. P. Conversion of malonyl β-glycosides isoflavones into glycoside isoflavones found in some cultivars of Brazilian soybeans. *Cienc. Tecnol. Aliment*. **2002**, *22*, 130-135.

Parr, A.; Bolwell, G. Review. Phenols in the plant and in man. The potential for possible nutritional enhancement of the diet by modifying the phenols content or profile. *J Sci Food Agric*. **2000**, *80*, 985–1012.

Patisaul, H. B; Jefferson, W. The pros and cons of phytoestrogens. *Frontiers in Neuroendocrinology*. **2010**, *31*, 400-419.

Penavlo, J. L.; Nurmi, T.; Adlercreutz, H. A simplified HPLC method for total isoflavones in soy products. *Food Chemistry*. **2004**, *87*, 297-305.

Peterson, G.; Barnes, S. Genistein and biochanin A inhibit the growth of human prostate cancer cells but not epidermal growth factor receptor tyrosine autophosphorylation. *Prostate*. **1993**, *22*, 335–345.

Peterson, T. G.; Coward, L.; Marion, K.; Charles, N. F.; Barnes, S. The role of metabolism in mammary epithelial cell growth inhibition by the isoflavones genistein and biochanin A. *Carcinogenesis*. **1996**, *17,* 1861-1869.

Pinent, M.; Espinel, A. E.; Delgado, M. A.; Baifes, I.; Blade, C.; Arola, L. Isoflavones reduce inflammation in 3T3-L1 adipocites. *Food Chem*. **2011**, *125*, 513-520.

Potter, S. M.; Baum, J. A.; Teng, H.; Stillman, R. J.; Shay, N. F.; Erdman, J. W. Soy protein and isoflavone: their effects on blood lipids ad bone density in postmenopausal women. *Am J Clin Nutr*. **1998**, *68*, 1375S-1379S.

Prasain, J. K.; Jones, K.; Kirk, M.; Wilson, L.; Johnson, M. S.; Weaver, C.; Barnes, S. Profiling and Quantification of Isoflavanoids in Kudzu Dietary Supplements by High-Performance Liquid Chromatography and Electrospray Ionization Mass Spectrometry. *J. Agric Food Chem*. **2003**, *51*, 4213-4218.

Price, K.; Fenwick, G. Naturally occurring oestrogens in foods – A review. *Food Additives and Contaminants.* **1985**, *2*, 73–106.

Quella S. K.; Leprinzi, C. L.; Barton, D. L. Evaluation of soy phytoestrogens for the treatment of hot flashes in breast cancer survivors: a north central cancer treatment group trial. *J Clin Oncol.* **2000**, *18*, 1068–1074.

Raman, C. V.; Krishnan, K. S. A new type of secondary radiation. *Nature*, **1928**, *121*, 501-502; Raman, C. V.; Krishnan, K. S. A new type of secondary radiation. *Nature*, **1928**, *121*, 711-712.

Huo, Y.; Jung, U.; Ghosh, S.; Manka, D. R.; Sarembock, I. J.; et al. Direct demonstration of P-selectin- and VCAM-1-dependent mononuclear cell rolling in early atherosclerosis lesions of apolipoprotein E-deficient mice. *Circ Res.* **1999**, *84,* 1237-1244.

Richelle, M.; Pridmore-merten, S.; Bodenstab, S.; Enslen, M.; Offord, E. Hydrolysis of isoflavone glycosides to aglycones by β-glycosidase does not alter plasma and urine isoflavone pharmacokinetics in postmenopausal women. *J. Nutr.* **2002**, *132*, 2587–2592.

Rickert, D. A.; Meyer, M. A.; Hu, J.; Murphy, P. A. Effect of extraction pH and temperature on isoflavone and saponin partitioning and profile during soy protein isolate production. *Journal of Food Science*. **2004**, *69*, C623-C631.

Rijke, E. D.; Kanter, F. D.; Ariese, F.; Brinkman, A. U.; Gooijer, C. Liquid chromatography coupled to nuclear magnetic resonance spectroscopy for the

identification of isoflavone glucoside malonates in T. pratense L. leaves. *J. Sep. Sci.* **2004**, *27*, 1061-1070.

Ronald, K. R.; Annlia, P. H.; Peggy, C. W.; Malcolm, C. P. Effect of Hormone Replacement Therapy on Breast Cancer Risk: Estrogen Versus Estrogen Plus Progestin. *Journal of the National Cancer Institute*, **2000**, *92*, 328-332.

Ross R. Atherosclerosis-an inflammatory disease. *N Engl J Med,* **1999**, *340*, 115–126.

Rostagno, M. A.; Palma, M.; Barroso, C. G. Short-term stability of soy isoflavones extracts: sample conservation aspects. *Food Chemistry*. **2005**, *93*, 557-564.

Rowland, I.; Faughnan, M.; Hoey, L.; Wahala, K.; Williamson, G.; Cassidy, A. Bioavailability of phyto-oestrogens. *British Journal of Nutrition*. **2003**, *89*, S45–S58.

Rufer, C. E.; Bub, A.; Moseneder, J.; Winterhalter, P.; Sturtz, M.; Kulling, S. E. Pharmokinetics of the soybean isoflavone daidzein in its aglycones and glucoside form: A randomized, double-blind, crossover study. *Am. J. Clin. Nutr*. **2008**, 87, 1314-1323.

Uzzan, M.; Labuza, T. P. Critical issues in R&D of soy isoflavones-enriched foods and dietary supplements. *J. Agric. Food Chem*. **2004**, *69*, 8958-8965.

Sawada, Y.; Akiyama, K.; Sakata, A.; Kuwahara, A.; Otsuki, H.; Sakurai, T.; Saito, K.; Hira, M. Y. Widely targeted metabolomics based on large-scale MS/MS data for

elucidating metabolite accumulation patterns in plants. *Plant Cell Physiol.* **2009**, *50*, 37-47.

Sathyamoorthy, N.; Wang, T. Differential effects of dietary phytooestrogens daidzein and equol on human breast cancer MCF-7 cells. *European Journal of Cancer*. **1997**, *33*, 2384–2389.

Scalbert, A.; Williamson, G. Dietary intake and bioavailability of polyphenols. *J. Nutr.* **2000**, *130*, S2073–S2085.

Scherer, M.; Leuthauser-Jachinski, K.; Ecker, J.; Schmitz, G.; Liebisch, G. A rapid and quantitative LC-MS/MS method to profile sphingolipids. *Journal of Lipid Research*. **2010**, *51*, 2001-2011.

Seigel, R.; Ward, E.; Brawley, O.; Jemal, A. Cancer statistics. *CA: Cancer J Clin*. **2011**, *61*, 212.

Sepeher, E.; Cooke, m. G.; Robertson, P.; Gilani, S. G. Effect of glycosidation of isoflavones on their bioavailability and pharmacokinetics in aged male rats. *Mol. Nutr. Food res.* **2009**, *53*, S16-S26.

Setchell, K. D. R.; Zimmer-Nechemias, L.; Cai, J.; Heubi, J. E. Exposure of infants to phyto-oestrogens from soy-based infant formula. *Lancet*. **1997**, *350*, 23-27.

Setchell, K. D. R. Phytoestrogens: the biochemistry, physiology, and implications for human health of soy isoflavones. *Am J Clin Nutr*. **1998**, *68(suppl)*, 1333S-1346S.

Setchell, K.; Brown, N.; Desai, P.; Zimmer-Nechimias, L.; Wolfe, B.; Brashear, W.; Kirschner, A.; Cassidy, A.; Heubi, J. Bioavailability of pure isoflavones in healthy humans and analysis of commercial soy isoflavone supplements. *J. Nutr*. **2001**, *131*, S1362–S1375.

Setchell, K.; Maynard, N. B.; Desai, P.; Zimmer-Nechimias, L.; Wolfe, B.; Jakate, A.; Creutzinger, V.; Heubi, J. Bioavailability, disposition, and dose-response effects of soy isoflavones when consumed by healthy women at physiologically typical dietary intakes. *J. Nutr*. **2003**, *133*, 1027–1035.

Setchell, K. D. R.; Brown, N. M.; Zimmer-Nechemias, L.; Brashear, W. T.; Wolfe, B. E.; Kirshner A. S.; Heubi, J. E. Evidence for lack of absorption of soy isoflavone glycosides in humans, supporting the crucial role of intestinal metabolism for bioavailability. *Am J Clin Nutr.* **2004**, *69*, C623-C631.

Severson, R. K.; Nomura, A. Y. M.; Grove, J. S.; Stemmerman, G. N. A propective study of demographics and prostate cancer among men of Japanese ancestry in Hawaii. *Cancer Res*. **1989**, *49*, 1857-1860.

Smekel, A. Zur quantentherie der dispersion. *Naturwissenschaften.* **1923**, *11,* 873-875.

Singletary, K.; Faller, J.; Li, Y. J.; Mahungu, S. Effect of extrusion on isoflavone content and antiproliferative bioactivity of soy/corn mixtures. *J. Agric Food Chem*. **2000**, *48*, 3566-3571.

Shabir, A. Development and validation of a liquid chromatography-mass spectrometry method for the determination of 4,5-Diazafluoren-9-one. *J Chromatogr Sci.* **2008**, *46*, 643-648.

Shang, Y.; Brown, M. Molecular determinants for the tissue specificity of SERMs. *Science*. **2002**, *295*, 2465-2468.

Shin, S. C.; Choi, J. S.; Li, X. Enhanced bioavailability of tamoxifen after oral administration of tamoxifen with quercetin in rats. *International Journal of Pharmaceutics*. **2006**, *313*, 144-149.

Shu, X. O.; Jin, F.; Dai, Q. Soyfood intake during adolescence and subsequent risk of breast cancer among Chinese women. *Cancer Epidemiol Biomarkers Prev*. **2001**, *10*, 483-488.

Shurtleff, W.; Aoyagi, A. "History of world soybean production and trade", Pts. 1 and 2. http://www.soyinfocenter.com/HSS/production_and _trade.php, 2007.

Somekawa, Y.; Chiguchi, M.; Ishibashi, T.; Takeshi, A. Soy intake related to menopausal symptoms, serum lipids, and bone mineral density in postmenopausal Japanese women. *Obstet. Gynecol*. **2001**, *97*, 109–115.

Song, T. T.; Hendrich, S.; Murphy, P. A. Estrogenic activity of glycitein, a soy isoflavone. *J. Agric Food Chem.* **1999**, *47*, 1607–1610.

Song. T.; Barua, K.; Buseman, G.; Murphy, P. Soy isoflavone analysis: quality control and a new internal standard. *Am J Clin Nutr.* **1998**, *68*, 1474S-1479S.

Spence, L. A.; Lipscomb, E. R.; Cadogan, J.; Martin, B.; Wastney, M. E.; Peacocock, M. The effect of soy protein and soy isoflavones on calcium metabolism in postmenopausal women: a randomized crossover study. *Am J Clin Nutr*. **2005**, *81*, 916–922.

Stuertz, M.; Lander, V.; Schmid, W.; Winterhalter, P. Preparative isolation of isoflavones from soy and red clover. *Mol. Nutr. Food Res.* **2006**, *50*, 356-361.

Stintzing, F. C.; Hoffman, M.; Carle, R. Thermal degradation kinetics of isoflavone aglycones from soy and red clover. *Mol. Nutr. Food Res*. **2006**, *50*, 373-377.

Teede, H. J.; Dalais, F. S.; Kotsopoulos, D.; Liang, Y. L.; Davis, S.; McGrath, B. P. Dietary soy has both beneficial and potentially adverse cardiovascular effects: a placebo-controlled study in men and postmenopausal women. *J Clin Endocrinol Metab*. **2001**, *86*, 3053–3060.

Teunissena, S. F.; Rosinga, H.; Koornstrab, R. H.; Linnb, S. C.; Schellensc, J. H. M.; Schinkelc, A. H.; Beijnena, J. H. Development and validation of a quantitative assay for the analysis of tamoxifen with its four main metabolites and the flavonoids daidzein, genistein and glycitein in human serum using liquid chromatography coupled with tandem mass spectrometry. *J. Chromatogr. B*. **2009**, *877*, 2519-2529.

Trdan, T.; Roškar, R.; Trontelj, J.; Ravnikar, M.; Mrhar, A. Determination of raloxifene and its glucuronides in human urine by liquid chromatography–tandem mass spectrometry assay. **2011**, *879*, 2323–2331.

Tsuda, Y.; Yoshimoto, K. General path of O-acyl migration in $_D$-glucose derivatives. *Carbohydr. Res.* **2004**, *339*, 1353-1360.

Turner, N. J.; Thomson, B. M.; Shaw, I. C. Bioactive isoflavones in functional foods: the importance of gut microflora on bioavailability. *Nutrition Reviews*. **2003**, *61*, 204-213.

Twaddle, N. C.; Churchwell, M. I.; Doerge, D. R. High-throughput quantification of soy isoflavones in human and rodent blood using liquid chromatography with electrospray mass spectrometry and tandem mass spectrometry detection. *J. Chromatogr. B*. **2002**, *777,* 139-145.

Ungar, Y.; Osundahunsi, O.; Shimoni, E. Thermal stability of genistin and daidzin and its effect on their antioxidant activity. *J. Agric. Food Chem*. **2003**, *51*, 4394-4399.

Uzzan, M.; Labuza, T. P. L. Critical Issues in R&D of Soy Isoflavone-enriched Foods and Dietary Supplements. *Journal of Food Science,* **2006**, *69,* CRH77 - CRH86.

Upmalis, D. H.; Lobo, R.; Bradley, L.; Warren, M.; Cone, F. L.; Lamia, C. A. Vasomotor symptom relief by soy isoflavone extract tablets in postmenopausal women: a multicenter, double-blind, randomized, placebocontrolled study. *Menopause*. **2000**, *7*, 236–242.

Vaidya, N. A.; Mathias, K.; Ismail, B.; Hayes, K. D.; Corvalan, C. M. The Effects of Processing and Extraction Conditions on Content, Profile, and Stability of Isoflavones in a Soymilk System. *J. Agric Food Chem*. **2007**, *55*, 3408-3413.

Vega-Lopez, S.; Yeum, K. J.; Lecker, J. L.; Ausman, L. M.; Johnson, E. J.; Devaraj, S.; et al. Plasma antioxidant capacity in response to diets high in soy or animal protein with or without isoflavones. *Am J Clin Nutr.* **2005**, *81,* 43-49.

Vincent, A.; Fitzpatrick, A. L. Soy Isoflavones: Are They Useful in Menopause? *Mayo Clin Proc*. **2000**, *75*, 1174-1184.

Wahala, K.; Rasku, S.; Parikka, K. Deuterated phytoestrogen flavonoids and isoflavonoids for quantitation. *J. Chromatogr. B*. **2002**, *777*, 111-122.

Wakai, K.; Egami, I.; Kato, K.; Kawamura, T.; Tamakoshi, A.; Lin, Y.; Nakayama, T.; Wada, M.; Ohno, Y. Dietary intake and sources of isoflavones among Japanese. *Nutr Cancer*. **1999**, *33,* 139-145.

Walle, T.; Browning, A. M.; Steed, L. L.; Reed, S. G.; Walle, U. K. Flavonoid glucosides are hydrolyzed and thus activated in the oral cavity in humans. *J. Nutr*. **2005**, 135, 48-32.

Wang, H.; Murphy, P. Isoflavone composition of American and Japanese soybeans in Iowa: effects of variety, crop year, and location. *J. Agric. Food Chem*. **1994**, *42*, 1674–1677.

Wang, H.; Murphy, P. Isoflavone content in commercial soybean foods. *J. Agric. Food Chem*. **1994**, *42*, 1666–1673.

Wang, H.; Murphy, P. Mass balance study of isoflavones during soybean processing. *J. Agric. Food Chem*. **1996**. *44*, 2377–2383.

Wang, J.; Sporns, P. MALDI-TOF MS analysis of isoflavones is soy products. *J. Agric. Food Chem.* **2000**, 48, 5887-5892.

Wang, S.; Cyronak, M.; Yang, E. Does a stable isotopically labeled internal standard always correct analyte response?: A matrix effect study on a LC/MS/MS method for the determination of carvedilol enantiomers in human plasma. *Journal of Pharmaceutical and Biomedical Analysis*. **2007**, *43*, 701-707.

Wangen, K. E.; Duncan, A. M.; Xu, X.; Kurzer, M. S. Soy isoflavones improve plasma lipids in normocholesterolemic and mildly hypercholesterolemic postmenopausal women. *Am. J. Clin Nutr.* **2001**, *73*, 225–231.

Washburn, S.; Burke, G. L.; Morgan, T.; Anthony, M. Effect of soy protein supplementation on serum lipoproteins, blood pressure, and menopausal symptoms in perimenopausal women. *Menopause*. **1999**, *6*, 7–13.

Watanabe, S.; Koessel, S. Colon cancer: an approach from molecular epidemiology. *J. Epidemiol.* **1993**, *3*, 47-61.

Watanabe, S.; Yamaguchi, M.; Sobue, T.; Takahashi, T.; Miura, T.; Arai, Y.; Mazur, W.; Wahala, K.; Adlercreutz, H. Pharmacokinetics of soybean isoflavones in plasma, urine, and feces of men after ingestion of 60 g baked soybean powder (Kinako). *J. Nutr*. **1998**, *128*, 1710–1715.

Weaver, C. M.; Cheong, J. M. K. Soy isoflavones and bone health: The relationship is still unclear. *J. Nutr.* **2005**, *135*, 1243-1247.

Weaver, C. M.; Martin, B.; Jackson, G. S.; McCabe, G. P.; Nolan, J. R.; McCabe, L. D.; Barnes, S.; Reinwald, S.; Boris, M. E. Antiresorptive effects of phytoestrogen supplements compared with estradiol or risedronate in postmenopausal women using (41) Ca methodology. *J. Clin. Endocrinol. Metab*, **2009**, *94,* 3798–805.

Weber, C.; Negrescu, E.; Erl, W.; Pietsch, A.; Franenberger, M.; Ziegler-Heitbrock, H. W.; et al. Inhibitors of protein tyrosine kinase suppress TNF-stimulated induction of endothelial cell adhesion molecules. *J Immunol.* **1995**, *155*, 445-451.

Wei, H.; Bowen, R.; Cai, Q.; Barnes, S.; Wang, Y. Antioxidant and antipromotional effects of the soybean isoflavone genistein. *Proceedings of the Society for Experimental Biology and Medicine.* **1995**, *208*, 124–130.

Wilkinson, A. P.; Wahala, K.; Williamson, G. Identification and Quantification of polyphenol estrogens in foods and human biological fluids. *J. Chromtogr. B*. **2002**, *777*, 93-109.

Winter, J.; Bokkenheuser, V. Bacterial metabolism of natural and synthetic sex hormones undergoing enterohepatic circulation. *Journal of Steroid Biochemistry*. **1987**, *27*, 1145–1149.

Wiseman H.; O'Reilly, J. D.; Adlercreutz, H.; Mallet, A. I.; Bowey, E. A.; Rowland, I. R. Isoflavone phytoestrogens consumed in soy decrease F2-isoprostane concentrations and increase resistance of low-density lipoprotein to oxidation in humans. *Am J Clin Nutr*. **2000**, *72,* 395–400.

Writing Group for the Women's Health Initiative Investigators. Risks and benefits of estrogen plus progestin in healthy postmenopausal women: principal results from the Women's Health Initiative randomized controlled trial. *JAMA*. **2002**, *288*, 321-333.

Wu, N. J.; Thompson, R. Fast and Efficient Separations Using Reversed Phase Liquid Chromatography, *J Liq Chromatogr RT*. **2006**, *29*, 949-988.

Wu, Q.; Wang, M.; Sciarappa, W. J.; Simon, J. E. LC/UV/ESI-MS Analysis of Isoflavones in Edamame and Tofu Soybeans. *J. Agric. Food Chem*. **2004**, *52*, 2763-2769.

Wu, Q.; Wang, M.; Simon, J. E. Analytical methods to determine phytoestrogenic compounds. *J. Chromatogr*. *B*. **2004**, *812*, 325-355.

Wu, A. H.; Ziegler, R. G.; Horn-Ross, P. L. Tofu and risk of breast cancer in Asian-Americans. *Cancer Epidemiol Biomarkers Prev*. **1996**, *5*, 901–906.

Wu, A. H.; Yang, D.; Pike, M. C. A meta-analysis of soyfoods and risk of stomach cancer: the problem of potential confounders. *Cancer Epidemiol Biomarkers Prev.* **2000**, *9*, 1051–1058.

Wybraniec, S. Chromatographic investigation on acyl migration in betacyanincs and their decarboxylated derivatives. *J. Chromatogr. B.: Anal. Technol. Biomed. Life Sci.* **2008**, *861*, 40-47.

Xu, X.; Wang, H.; Murphy, P.; Cook, L.; Hendrich, S. Daidzein is a more bioavailable soymilk isoflavone than is genistein in adult women. *J. Nutr.* **1994**, *124*, 825–832.

Xu, X.; Harris, K.; Wang, H.; Murphy, P. Bioavailability of soybean isoflavones depends upon gut microflora in women. *J. Nutr.* **1995**, *125*, 2307–2315.

Xu, X.; Wang, H.; Murphy, P.; Hendrich, S. Neither background diet nor type of soy food affects short-term isoflavone bioavailability in women. *J. Nutr*. **2000**, *130,* 798–801.

Xu. Z.; Wu, Q.; Godber, J. S. Stabilities of daidzin, glycitin, genistin, and generation of derivatives during heating. *J. Agric. Food Chem*. **2002**, *50*, 7402–7406.

Yerramsetty, V.; Mathias, K.; Bunzel, K.; Ismail, B. Detection and structural characterization of thermally generated isoflavone malonylglucoside glucosides. *J. Agric Food Chem*. **2011**, *59*, 174-183.

Yu-Chen, C.; Muraleedharan, G. N.; Ross, C. S.; William, G. H. Microwave-mediated synthesis of anticarcinogenic isoflavones from soybeans. *J. Agric. Food Chem.* **1994**, *42*, 1869-1871.

Yu, O.; Jung, W.; Shi, J.; Croes, R.; Fader, R. G.; McGonigle, B.; Odell, J. Production of the isoflavones genistein and dadizein in non-negume dicot and monocot tissues. *Plant Physiol*. **2000**, *124,* 781–793.

Zhang, Y.; Wang, G. J.; Song, T. T.; Murphy, P. A.; Hendrich, S. Urinary Disposition of the Soybean Isoflavones Daidzein, Genistein and Glycitein Differs among Humans with Moderate Fecal Isoflavone Degradation Activity. *J. Nutr*. **1999**, *129*, 957-962.

Zhang, X.; Young, M. A.; Lyandres, O.; Van Duyne, R. P. Rapid Detection of an Anthrax Biomarker by Surface-Enhanced Raman Spectroscopy. *J. Am. Chem. Soc.* **2005**, *127*, 4484–4489.

Ziegler, R. G.; Hoover, R. N.; Pike, M. C.; Hildesheim, A.; Nomura, A. M.; West, D. W. Migration patterns and breast cancer risk in Asian-American women. *J Nat Cancer Inst.* **1993**, *85*, 1819–1827.

Zubik, L.; Meydani, M. Bioavailability of soybean isoflavones from aglycone and glucoside forms in American women. *Am J Clin Nutr*. **2003**, *77*, 1459-1465

Appendix A: Calibration Curves for the 11 isoflavone standards

The figures shown in this appendix are the calibration curves which were used determine the line equations that relate response area of each isoflavone standard from HPLC with their respective known concentrations. These line equations can be used to determine the unknown concentrations of isoflavones.

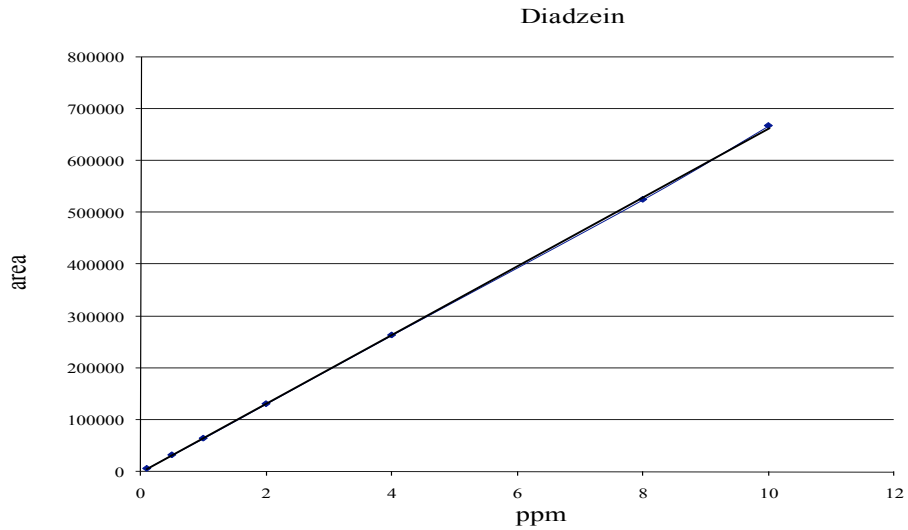

Figure 39. Calibration curve for daidzein with area (of the peak from HPLC analysis) on y-axis and concentration (in ppm) on x-axis. The line equation obtained after performing simple linear regression analysis of the data was: $y = 66457x - 1182.5$ with R^2 value of 0.99.

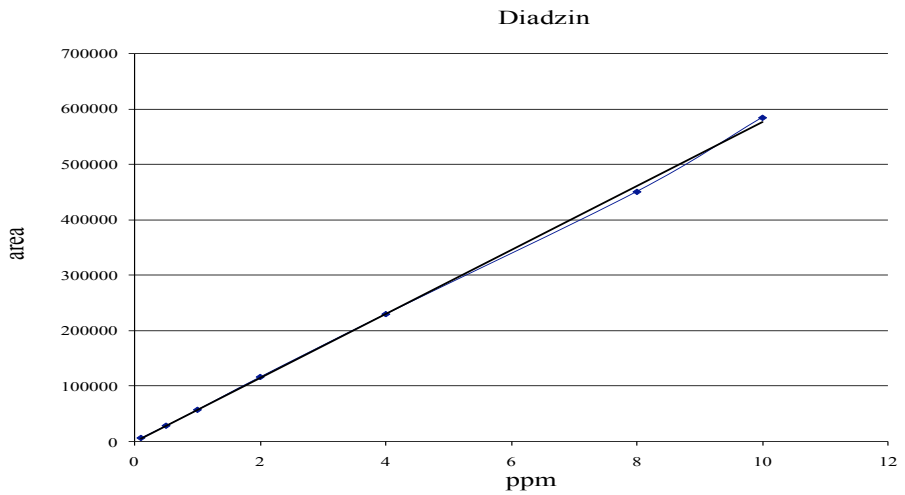

Figure 40. Calibration curve for daidzin with area (of the peak from HPLC analysis) on y-axis and concentration (in ppm) on x-axis. The line equation obtained after performing simple linear regression analysis of the data was: y = 57693x – 1238.8 with R^2 value of 0.99.

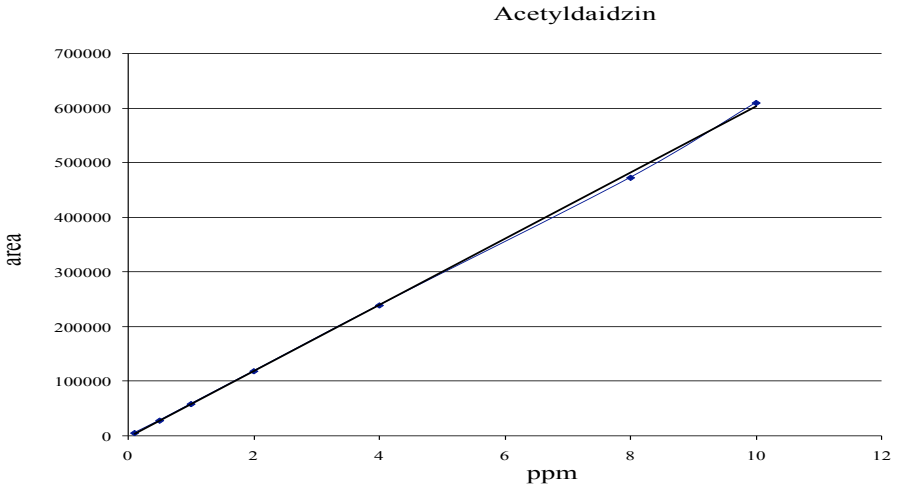

Figure 41. Calibration curve for acetyldaidzin with area (of the peak from HPLC analysis) on y-axis and concentration (in ppm) on x-axis. The line equation obtained after performing simple linear regression analysis of the data was: y = 60457x – 1866.4 with R^2 value of 0.99.

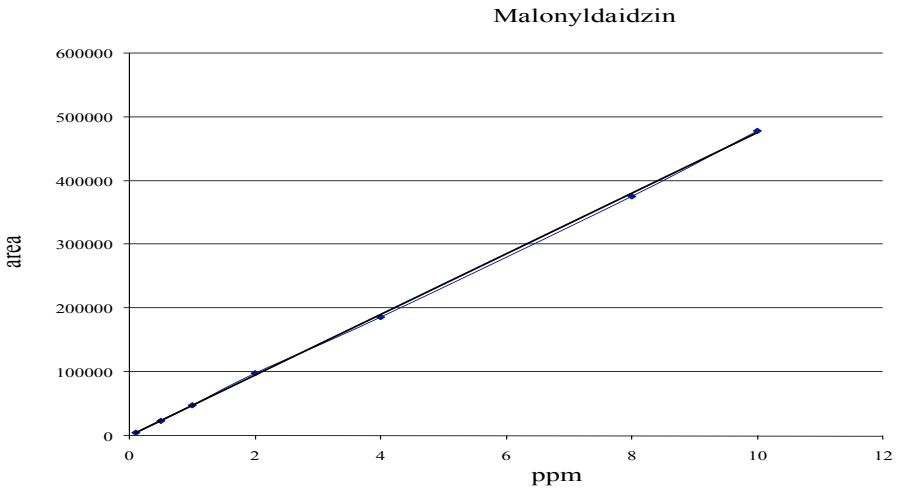

Figure 42. Calibration curve for malonyldaidzin with area (of the peak from HPLC analysis) on y-axis and concentration (in ppm) on x-axis. The line equation obtained after performing simple linear regression analysis of the data was: y = 47502x – 107.47 with R^2 value of 0.99.

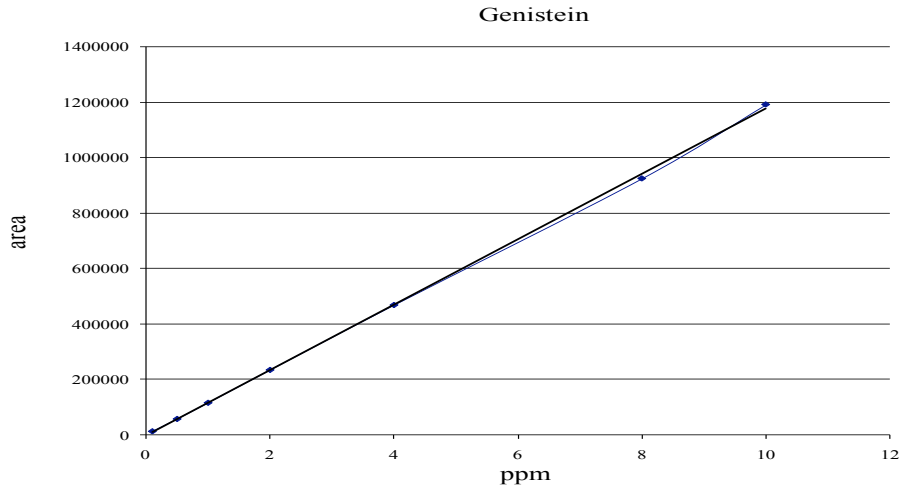

Figure 43. Calibration curve for Genistein with area (of the peak from HPLC analysis) on x-axis and concentration (in ppm) on y-axis. The line equation obtained after performing simple linear regression analysis of the data was: y = 118005x – 3306.6 with R^2 value of 0.99.

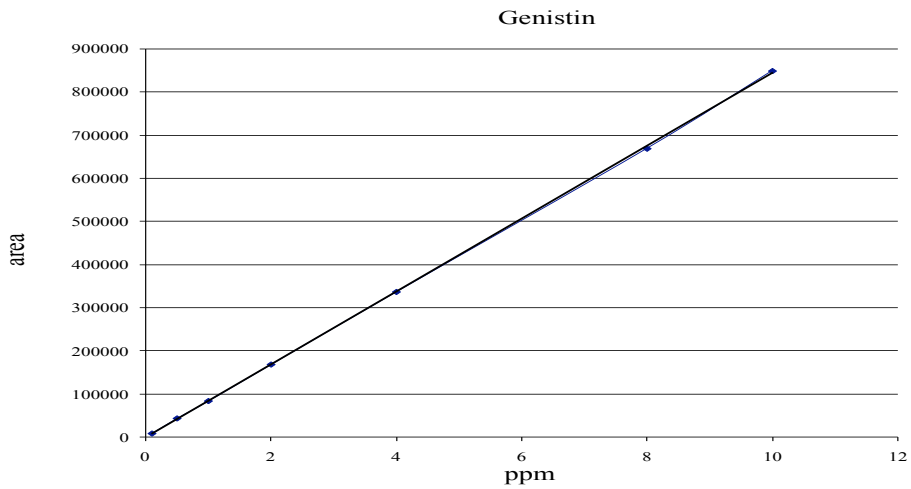

Figure 44. Calibration curve for Genistin with area (of the peak from HPLC analysis) on x-axis and concentration (in ppm) on y-axis. The line equation obtained after performing simple linear regression analysis of the data was: y = 84460x – 769.51 with R^2 value of 0.99.

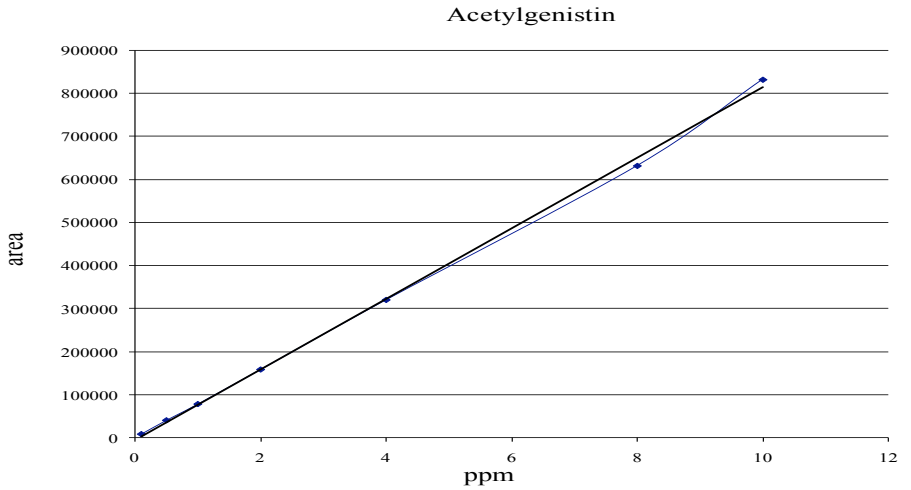

Figure 45. Calibration curve for Acetylgenistin with area (of the peak from HPLC analysis) on x-axis and concentration (in ppm) on y-axis. The line equation obtained after performing simple linear regression analysis of the data was: y = 81966x – 4484.7 with R^2 value of 0.99.

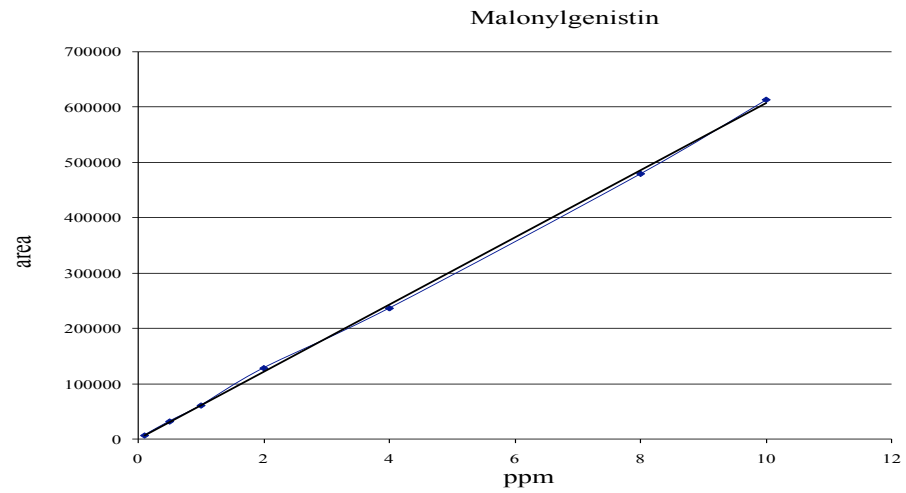

Figure 46. Calibration curve for Malonylgenistin with area (of the peak from HPLC analysis) on x-axis and concentration (in ppm) on y-axis. The line equation obtained after performing simple linear regression analysis of the data was: y = 60552x + 748.21 with R^2 value of 0.99.

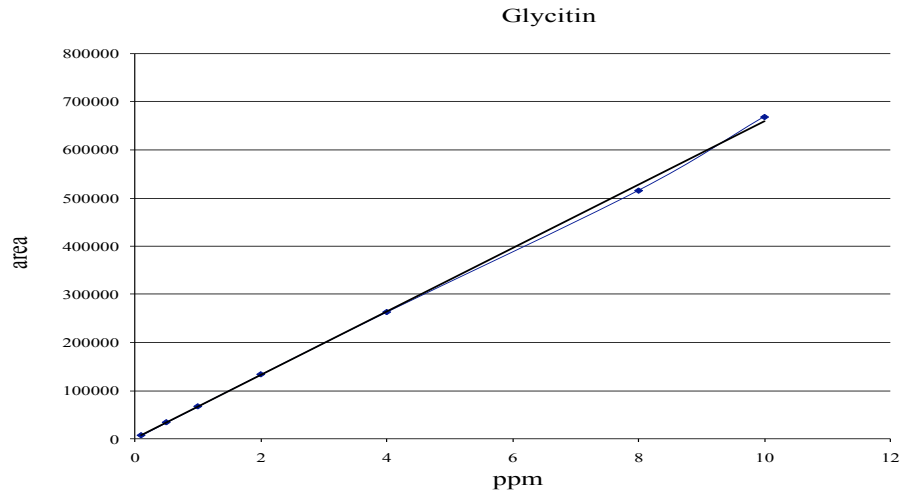

Figure 47. Calibration curve for glycitin with area (of the peak from HPLC analysis) on x-axis and concentration (in ppm) on y-axis. The line equation obtained after performing simple linear regression analysis of the data was: y = 65928x – 340.59 with R^2 value of 0.99.

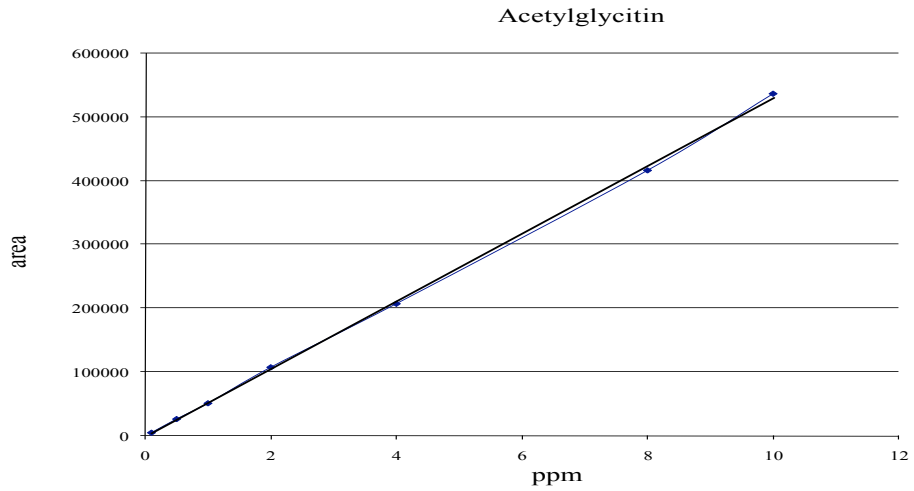

Figure 48. Calibration curve for acetylglycitin with area (of the peak from HPLC analysis) on x-axis and concentration (in ppm) on y-axis. The line equation obtained after performing simple linear regression analysis of the data was: y = 53175x – 1178.1 with R^2 value of 0.99.

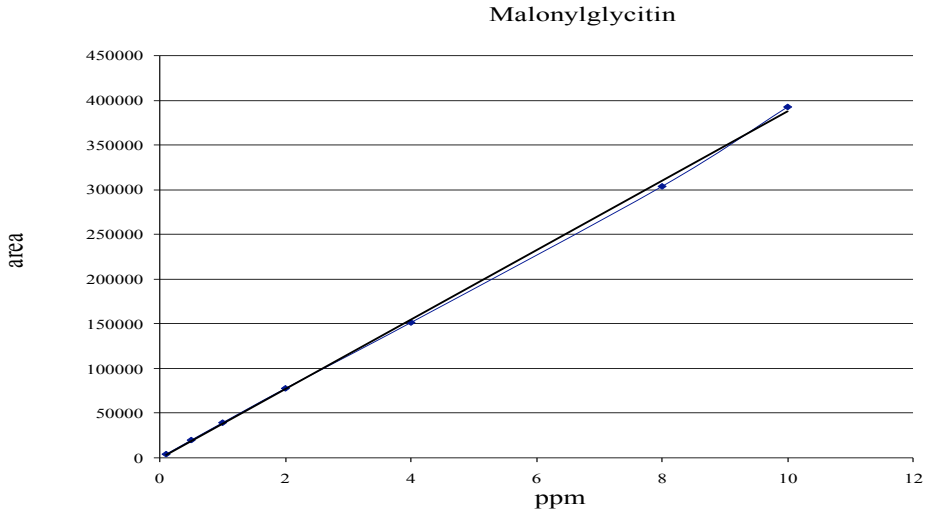

Figure 49. Calibration curve for malonylglycitin with area (of the peak from HPLC analysis) on x-axis and concentration (in ppm) on y-axis. The line equation obtained after performing simple linear regression analysis of the data was: y = 38776x – 549.5 with R^2 value of 0.99.

Appendix B: Heteronuclear single quantum coherence spectra of 6”-*O* malonyldaidzin and its isomeric 4”-*O*-malonyldaidzin

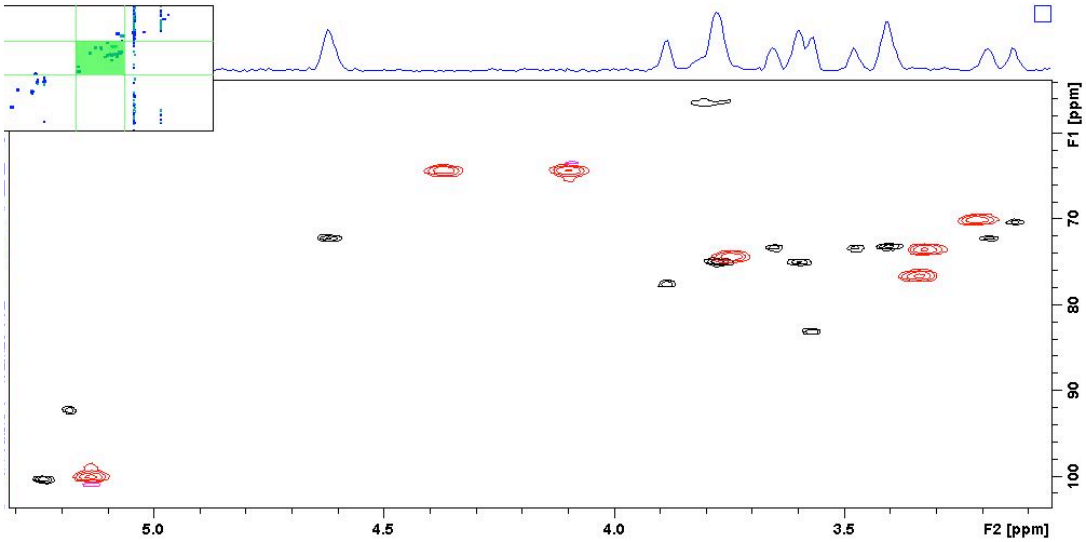

Figure 50. Overlay of the HSQC spectra (carbohydrate region) of malonyldaidzin (6”-*O*-malonyl-daidzin) (black cross peaks) and the malonyldaidzin isomer (4”-*O*-malonyl-daidzin) (red cross peaks). The 1D proton spectrum represents 6”-*O*-malonyl-daidzin

Appendix C: Analysis of Variance Table for the effect of processing time on interconversions of isoflavones in a soymilk system

Table 11. ANOVA of the mean amounts (nmol/g dry weight) of MGin isomer, MGin, Gin, AGin, and total detected genistein derivatives in soymilk samples subjected to thermal treatment at 100°C for several intervals of time ranging from 0-60 min.

Isoflavone	Dependent Variable	Source of Variation	DF^	Means Square	F-Value	Significance ($P \leq 0.05$)
Isomer	Concentration	Time	5	44468	379.6	0.000
		Error	12	177.1		
MGin	Concentration	Time	5	6093764	1055	0.000
		Error	12	5774		
Gin	Concentration	Time	5	3830125	738.8	0.000
		Error	12	5184.1		
AGin	Concentration	Time	5	7886.9	324.7	0.000
		Error	12	129.7		
Gein	Concentration	Time	5	10.7	12.1	0.000
		Error	12	8.061		
Total Gin	Concentration	Time	5	457922	22.5	0.000
		Error	12	20268		

*Isomer, malonylgenisting isomer; Gin, genistin; MGin, malonylgenistin; AGin, acetylgenistin; Gein, genistein. ^Total detected genistein derivatives (Isomer + Gin + Mgin + Agin + Gein).

Appendix D: Analysis of Variance Table for the plasma and urinary pharmokinetics of daidzein post the oral administration of daidzin and malonyldaidzin

Table 12. ANOVA of the maximum mean plasma concentration (μM), plasma and urinary area under the curves (μM.hr) of daidzein post oral administration of daidzin and malonyldaidzin.

	Dependent Variable	Source of Variation	DF^	Means Square	F-Value	Significance ($P \leq 0.05$)
C_{max} (Daidzin vs. Malonyldaidzin)	Concentration	Rat	1	25.31	15.71	0.004
		Error	8	1.61		
AUC plasma (Daidzin vs. Malonyldaidzin)	AUC	Rat	1	5142	23.55	0.001
		Error	9	218.1		
AUC urine (Daidzin vs. Malonyldaidzin)	AUC	Rat	1	580.97	45.43	0.000
		Error	9	12.78		

*C_{max}, maximum mean plasma concentration; AUC, area under curve

Appendix E: Analysis of Variance Table for the plasma and urinary pharmokinetics of equol post the oral administration of daidzin and malonyldaidzin

Table 13. ANOVA of the maximum mean plasma concentration (μM), plasma and urinary area under the curves (μM.hr) of equol post oral administration of daidzin and malonyldaidzin.

	Dependent Variable	Source of Variation	DF^	Means Square	F-Value	Significance ($P \leq 0.05$)
C_{max} (Daidzin vs. Malonyldaidzin)	Concentration	Rat	1	4.65	21.11	0.002
		Error	8	0.22		
AUC plasma (Daidzin vs. Malonyldaidzin)	AUC	Rat	1	436.1	36.15	0.000
		Error	9	11.94		
AUC urine (Daidzin vs. Malonyldaidzin)	AUC	Rat	1	4214	7.99	0.020
		Error	9	527.4		

*C_{max}, maximum mean plasma concentration; AUC, area under curve

Appendix F: Analysis of Variance Table for the plasma and urinary pharmokinetics of genistein post the oral administration of genistin and malonylgenistin

Table 14. ANOVA of the maximum mean plasma concentration (μM), plasma and urinary area under the curves (μM.hr) of genistein post oral administration of genistin and malonylgenistin.

	Dependent Variable	Source of Variation	DF^	Means Square	F-Value	Significance ($P \leq 0.05$)
C_{max} (Genistin vs Malonylgenistin)	Concentration	Rat	1	66.74	3.76	0.025
		Error	9	17.74		
AUC plasma (Genistin vs Malonylgenistin)	AUC	Rat	1	772.9	1.02	0.001
		Error	10	756.5		
AUC urine (Genistin vs Malonylgenistin)	AUC	Rat	1	3187.4	4.57	0.036
		Error	9	696.5		

*C_{max}, maximum mean plasma concentration; AUC, area under curve